12-1-2019

Construction of a Flow-based ATR-FTIR system: Decarboxylation Reactions Rates

Ashley Campanella
University of Northern Colorado

UNIVERSITY OF NORTHERN COLORADO

Greeley, Colorado

The Graduate School

CONSTRUCTION OF A FLOW-BASED ATR-FTIR SYSTEM: DECARBOXYLATION REACTION RATES

A Thesis Submitted in Partial Fulfillment
of the Requirements for the Degree of
Master of Science

Ashley Jordan Campanella

College of Natural and Health Sciences
Department of Chemistry and Biochemistry

December 2019

This Thesis by: Ashley Jordan Campanella

Entitled: *Construction of a Flow-based ATR-FTIR system: Decarboxylation Reaction Rates*

has been approved as meeting the requirement for the Degree of Master of Science in College of Natural and Health Sciences in the Department of Chemistry and Biochemistry

Accepted by the *Thesis Committee:

_____
Michael D. Mosher, Ph.D., Committee Chair

_____
Richard W. Schwenz, Ph.D., Committee Member

_____
Aaron K. Apawu, Ph.D., Committee Member

Accepted by the Graduate School

_____

Cindy K. Wesley
Interim Associate Provost and Dean
The Graduate School and International Admissions
Research and Sponsored Projects

ABSTRACT

Campanella, Ashley. *Construction of a Flow-based ATR-FTIR system: Decarboxylation Reaction Rates.* Unpublished Master of Science Thesis, University of Northern Colorado, 2019.

Diacetyl (2,3-butanedione), a buttery flavored compound made during beer production, is formed from α-acetolactate via oxidative decarboxylation. Current analytical methods to detect diacetyl are time-consuming and expensive; however, measurements of carbon dioxide can be rapid and inexpensive. Attenuated total reflectance–Fourier transform infrared spectroscopy (ATR-FTIR) utilizing a flow cell and mid-range infrared energy (400 cm^{-1} – 4000 cm^{-1}) is capable of measurements for dissolved CO_2. An ATR-FTIR system was constructed using a Ge flow cell, an HPLC pump, and stainless-steel tubing. A method for analyzing a model reaction compared to a natural process in fermentation was developed. Exploring the effects of the different matrices provided a useful analytical tool. The limit of detection for CO_2 was found to be as low as 22.5 ppm and the limit of quantification as low as 74.9 ppm. Concentrations of dissolved CO_2 can be determined using the peak area or height of the asymmetric C=O signal at $\tilde{\upsilon}$ =2349 cm^{-1}. A rate study of the decarboxylation reaction with ethyl acetoacetate revealed that the energy of activation was calculated for a pseudo-first-order decarboxylation of the model reaction was determined to be 54.1 kJ/mol.

THESIS ACKNOWLEDGEMENT

Foremost, I would like to express my sincere gratitude to my advisor Dr. Michael Mosher for the continuous support of my master's degree and research project. His patience, motivation, enthusiasm, and immense knowledge has helped me over the last four years. His guidance assisted me in all the time of research and writing of this thesis. I could not have imagined having a better advisor and mentor.

Besides my advisor, I would like to thank the rest of my thesis committee: Dr. Aaron Apawu and Dr. Richard Schwenz, for their encouragement, insightful comments, and hard questions.

I want to thank my fellow lab mates in the Mosher Research Group, for the stimulating discussions, for the sleepless nights we were working together before deadlines, and for all the fun we have had in the last four years. Also, I would like to thank Dr. Matthew Semak, Michael Nuzum, Quinton Snouffer, Chad Wangeline, Scott Newkirk and Christopher Toe for assisting me with building my instrument and analysis collection.

Last but not the least, I would like to thank my family: my parents Renee and Michael Geha, and Brandon and Natha Campanella, my brother Tyler Campanella, my grandparents Lila and Peter Montez, my great-grandfather William Anderson, and my boyfriend Michael Nuzum for constantly supporting me spiritually throughout my life. I am extremely blessed to have the support system that I have.

God blesses those who patiently endure testing and temptation. Afterward they will receive the crown of life that God has promised to those who love him. (James 1:12, New Living Translation)

TABLE OF CONTENTS:

CHAPTER I - INTRODUCTION 1

CHAPTER II - LITERATURE REVIEW 4

Analysis of Diacetyl 5

Formation of Diacetyl During Fermentation 11

Measuring Carbon Dioxide in Solution 13

Raman Spectroscopic Methods 20

CHAPTER III - METHODOLOGY 24

CHAPTER IV - RESULTS AND DISCUSSION 43

Carbon Dioxide as an Analyte 45

Ethanol as an Analyte 54

Interferences with Carbon Dioxide 60

Acetone as an Analyte 67

Other Interferences on the Infrared Spectrum 70

CHAPTER V - CONCLUSION AND FUTURE WORK 74

APPENDIX 86

LIST OF FIGURES

2.1: Proposed reaction for diacetyl analysis based on the Voges-Proskauer test, in ASBC Beer-25 method B, broad-spectrum method 6

2.2: Fe^{2+} binding with dimethyl glyoxime forming a red complex 7

2.3: GC Chromatogram of diacetyl, 2,3-pentanedione, and 2,3-hexanedione using an Ellutia 200 series gas chromatograph with an electron capture detector 8

2.4: Derivatization of VDK's with OPDA 10

2.5: Metabolic Pathway for Diacetyl 12

2.6: Oxidative decarboxylation reaction with α-Acetolactate 13

2.7: Reaction of ethyl acetoacetate undergoing deesterification, producing acetone and carbon dioxide 13

2.8: Schematic of ATR using infrared light 14

2.9: Diagram of Fast Fourier Transforms. Signal of time and frequency domain of sinusoidal oscillations 15

2.10: IR spectra of the dissolved gases at elevated pressures 17

2.11: IR spectrum of the compounds labeled in Table 2.1 for the reaction of CO_2 in aqueous ethanolamine, over a 4-minute period 18

2.12: FTIR spectrum analyzing the saturation process of a 1.35 g/L CO_2 standard. 19

2.13: Energy-level diagram of the different states involved in Raman spectroscopy 20

3.1: The general set-up based on US patent 15/185,844 25

3.2: Image of the 3-D printed mount 26

3.3: Image of the machine welded mount 26

3.4: Photograph of the Lulzbot Tax 6, the 3-D Printer 27

3.5: Image of the final set-up for the Ge flow cell analysis illustrating how the tubing was connected to an HPLC using Swagelok® fittings 28

3.6: Photograph of the Nicolet™ FTIR with the flow cell attachment from Hellma Analytics 29

3.7: Final set-up of the device. Addition of a pressure gauge and a gas release valve 30

3.8: Reaction of Ethyl-acetoacetate in a sodium acetate buffer. 31

3.9: Photograph of the bubble analysis setup 32

3.10: Photograph of the DeltaNu Advantage 200A series Raman spectrometer 34

3.11: Photograph of iD5 SB-FTIR attachment for the iS5 Nicolet™ FTIR 35

3.12: Photograph of iS50 FTIR from Thermo Fisher 36

3.13: Photograph of the Bausch & Lomb ABBE-3L refractometer used to determine the refractive index and ultimately obtain the specific gravity of the wort solutions 38

3.14: Photograph of a Zahm and Nagel CO_2 piercing device 40

3.15: Diagram using pressure and temperature and giving the volumes of CO_2 measured in the bottle of a carbonated aqueous solution 41

4.1: Mechanism for the first of two reactions for the deesterification reaction of ethyl acetoacetate in acidic conditions 44

4.2: Mechanism for the second of two reactions for the decarboxylation reaction of ethyl acetoacetate in acidic conditions 44

4.3: IR spectrum of chilled seltzer water to analyze CO_2 asymmetric stretch at $\tilde{\upsilon}$ = 2342.8 cm^{-1}, corresponding to 2900 ppm of CO_2 45

4.4: Plot showing the results of cooled and heated solutions of wort throughout fermentation using peak height 48

4.5: Arrhenius plot for the decarboxylation reaction obtained from the bubble analysis 50

4.6: CO_2 method diagram for MB-FTIR analysis of reaction with ethyl acetoacetate and the sodium acetate buffer at various temperatures 51

4.7: Diagram of the amount of CO_2 that was produced over a six-hour period at 65 ˚C from the MB-FTIR method using peak height 51

4.8: Diagram of the amount of CO_2 that was produced over a 3-hour period at 80 ˚C taken at $\tilde{\upsilon}$ = 2342.6 cm^{-1} from the MB-FTIR method using peak height 52

4.9: IR spectrum of the ethyl acetoacetate reaction using the iS50 FTIR 54

4.10: Standard curve of ethanol using the SB-FTIR at ῡ = 1045.2 cm^{-1}. 55

4.11: IR spectrum of C-O stretch for ethanol using SB-FTIR 56

4.12: Standard curve of ethanol using the MB-FTIR at ῡ = 1045.1 cm^{-1} for non-alcoholic beer using peak height 57

4.13: Standard curve of ethanol using the MB-FTIR at ῡ = 1045.2 cm^{-1} for full-strength beer using peak height 57

4.14: Standard curve of ethanol using the MB-FTIR at ῡ = 1044.2 cm^{-1} using peak height. 58

4.15: Standard curve of [EtOH] versus absorbance using the Ge flow cell using peak height 59

4.16: Standard curve of [EtOH] versus peak area using the Ge flow cell using peak area 59

4.17: Standard curve of ethanol using the iS50 FTIR using peak height 61

4.18: IR spectrum of ethanol using the iS50 FTIR at various concentrations 62

4.19: Standard curve of ethanol using the Raman spectrometer using peak area 63

4.20: Standard curve of acetone using MB-FTIR using the peak height 68

4.21: Standard curve of acetone using MB-FTIR using peak area 69

4.22: Standard curve of acetone using Ge flow cell at ῡ = 1696.5 cm^{-1} using peak height 69

4.23: Standard curve of acetone using the Ge flow cell utilizing the peak area 70

4.24: Wort spiked with ethanol analysis using MB-FTIR at ῡ ~1044 cm^{-1} using peak height 71

4.27: Plot of [Acetaldehyde] versus absorbance using the MB-FTIR for ῡ ~ 1715 cm^{-1}, corresponding to the C=O stretch using peak height 72

4.28: Acetaldehyde complex in equilibrium with a single acetaldehyde molecule 72

4.29: The two prominent diastereomers contributing to the many ˈH-NMR signals 73

4.28: IR spectrum of diacetyl using the iS50 FTIR 73

LIST OF TABLES:

2.1: Table of infrared peak assignments for a CO_2 injected ethanolamine solution, corresponding the peaks in the spectrum of Figure 2.9 (Jackson et al., 2009) 18

4.1: Seltzer water analysis in the Ge flow cell at 23 ˚C over time..... 46

4.2: Beer styles and their CO_2 concentrations. Belgian style sour was not refrigerated for a 24-hour minimum like the others, $\tilde{\upsilon}$ = 2342.4 cm^{-1}. 49

4.3: Reaction of ethyl acetoacetate with varying solvent, temperature, pH, and reaction times using the Ge flow cell method..... 53

4.4: Raman data for ethanol concentration determination using peak height and peak area 63

4.5: Data for non-alcoholic beer compared to the standard curve 64

4.6: Comparison of 3.2 %ABW beer versus full-strength beer 64

4.7: Beer styles analyzed for ethanol concentration by MB-FTIR 65

4.8: Ethanol determination using average absorbance value by MB-FTIR..... 66

4.9: Ethanol determination (%ABV) by MB-FTIR 66

4.10: Data collected from an American light lager using the Ge flow cell 67

5.1: Comparison of RSD for different methods and analytes……78

CHAPTER I

INTRODUCTION

In 2018, the United States had approximately 7082 craft breweries (Baker, 2018). This number has significantly increased from 4588 breweries in 2015, 5491 breweries in 2016, and 6372 breweries in 2017 (Baker, 2018). Craft brewery growth continues at 13.2% from 2018 to 2019 with experts projecting that growth to continue in the coming years (Baker, 2018). It is clear there is a passion for beer in the United States. Meeting these high demands resulted in the production of almost 200 million barrels in 2018, equivalent to 6.02 billion gallons of beer (Baker, 2018).

For example, Avery Brewing Company based in Boulder, Colorado, is a nationwide brewery. They distribute their beer throughout the U.S. including Alaska and Hawaii, while also distributing internationally to Sweden and Japan. In 2018, they had the capacity to produce 750 hL (~ 640 barrels or 19800 gallons) of wort each day from their brewhouse (Avery, 2018). Because there are many different varieties of beer it can take anywhere from 1 to 4 weeks to complete the process to make beer from its raw materials. Of the many steps in the brewing process, fermentation can be the most time consuming but also the most important. To a national brewery such as Avery Brewing Company, throughput and efficiency increase by knowing when the fermentation step is complete. Storage space is highly dependent on how long fermentation takes and what the brewery would like to do with the product. They can set aside the unfinished beer for a second fermentation step, storage, or aging but they need vessels and space to

accomplish those tasks. When space and equipment are limited and the brewery is in pursuit of increased production, it analyzes unfinished beer while it is still in the fermentation vessels to ensure it is ready to move forward in the brewing process.

In fermentation, there is a chemical indicator that will tell the brewer when the process is complete. Completion occurs when the level of diacetyl drops below minimum brand specifications for diacetyl. The analysis requires specific methods of detection, instruments and trained personnel to run the analysis in a laboratory setting. In fact, one of the most important analyses performed by the quality control lab is the determination of the amount of diacetyl in solution. Small microbreweries often cannot afford a small functional laboratory to detect diacetyl, whether that is in fermentation or another point in the brewing process. However, all breweries need a way to analyze diacetyl, so they can be a more productive and efficient facility.

Diacetyl or 2,3-butanedione is a vicinal diketone (VDK) that is produced during the initial yeast growth stage of the fermentation process. Based on the strain of yeast used and the temperature of fermentation, the level of diacetyl produced can be as high as 3.5 ppm. While this is a relatively low concentration, diacetyl has a large impact on the flavor of the beer. The reported human flavor threshold, for those sensitive to this flavor, is 50 ppb. When present in the final beer, diacetyl imparts an off-flavor of buttered popcorn or butterscotch (Watson, Decloedt, Vanderputten, & Van Landschoot, 2018).

Fortunately, once the concentration of fermentable sugars has been reduced to minimal levels, the yeast cells begin to take in diacetyl. Once inside the yeast, diacetyl is reduced to 2,3-butanediol (with a flavor threshold of 4500 ppm it contributes little to the overall flavor of the beer). When the yeast remains active and in contact with the

fermenting solution, it consumes essentially all the diacetyl in the beer. In such cases, the diacetyl concentration drops below the flavor threshold (17 ppb in ales and 61 ppb in lagers) (Landaud, Lieben, & Picque, 1998). This process takes time to complete and is the limiting factor in determining the total quantity of beer produced by a brewery. For example, primary fermentation typically requires 18-64 hours to complete. Warm maturation, the term is given to the time to reduce diacetyl concentrations, can take equally as long or longer depending upon the specific strain of yeast.

Brewers use many different methods to analyze VDK's in solution. These methods involve instruments such as UV-vis spectrophotometers or gas chromatographs; however, each existing American Society of Brewing Chemists (ASBC) method requires significant time (~1-1.5 hours) to complete the analysis from sample collection to diacetyl concentration reporting. In a cellar containing numerous fermentation vessels, it can take multiple hours for the brewer to receive results from the analysis. A twelve-hour delay is not uncommon. As was noted before, delays during production can cost the brewery time and money.

Delays in the production of beer can be remediated by building an affordable instrument to detect diacetyl in a solution using an inline or online system. We envision the preparation of a system to measure diacetyl indirectly by analyzing stoichiometric amounts of carbon dioxide. This is possible because carbon dioxide is produced in the decomposition reaction of α-acetolactate t0 form diacetyl. Having an inline or online system allows real-time analysis, which can tell a brewer exactly when the beer can move to the next step in the brewing process. An instrument capable of this analysis will increase production rates while limiting diacetyl levels in the finished beer.

CHAPTER II

LITERATURE REVIEW

Beer as we know it today consists of four main ingredients; malt, hops, yeast, and water. With a specific recipe, the brewer can produce a style of beer in a one- to two-week process. Analyzing the product as it moves through the brewing process allows the brewer to react to unwanted changes in the beer before it is finished. Optimizing production cost and maximizing product consistency using laboratory analyses is essential to the production of a quality product. The success of this enterprise determines if a brewery can survive in today's highly competitive industry.

In order to grow, breweries strive to increase their production rates. Breweries have accomplished this by fermenting high-gravity wort and decreasing primary fermentation time. Unfortunately, when the brewer decreases fermentation time, there is a huge increase in VDK concentration, and the beer quality suffers. During production, the brewery can perform different types of analyses on the beer being produced to ensure better quality. These analyses begin with the incoming malt and continue to the final packaged beer. As such, there are hundreds of methods of analysis to ensure that the final product is within specifications for that particular brand. American brewers typically use the ASBC Methods of Analysis for information about the evaluations they need to accomplish (American Society of Brewing Chemists, 1964).

Analysis of Diacetyl

Diacetyl analysis is one of the most commonly performed analyses due to the noticeable flavor of diacetyl in the finished beer. The ASBC gives five different methods for the analysis of diacetyl in fermenting wort. The first method is an archived method, the macro dimethyl glyoxime method, BEER-25 method A. The ASBC archives older methods where the accuracy and precision are more difficult to control. The methods are still available but are not recommended for implementation. The second is a broad-spectrum method for VDK's, BEER-25 method B (Figure 2.1) (ASBC, 1964). This method requires the distillation of a sample containing diacetyl to separate the VDK's from other compounds in the matrix of beer and to concentrate the diacetyl prior to the analysis. The collected distillate may be diluted with an appropriate amount of water depending upon the level of diacetyl in the beer. Then, α-naphthol, potassium hydroxide, and creatine are added to each aliquot for color development due to complex formation. The solutions are placed in a spectrophotometer to determine the absorbance at 530 nm. The unknown concentration of diacetyl is calculated from a standard curve. The advantage of this method is that it is simple and if the distillation is successful the results can be very accurate and precise. The disadvantage of this method is that the distillation can be very time consuming because of foaming due to proteins in the matrix. In addition, the limit of quantification is approximately 0.25 ppm. Therefore, the typical distillation is performed to concentrate the diacetyl so that it is greater than the limit of the standard curve. From sample collection to reporting the diacetyl concentration, this method takes approximately 2 hours to complete.

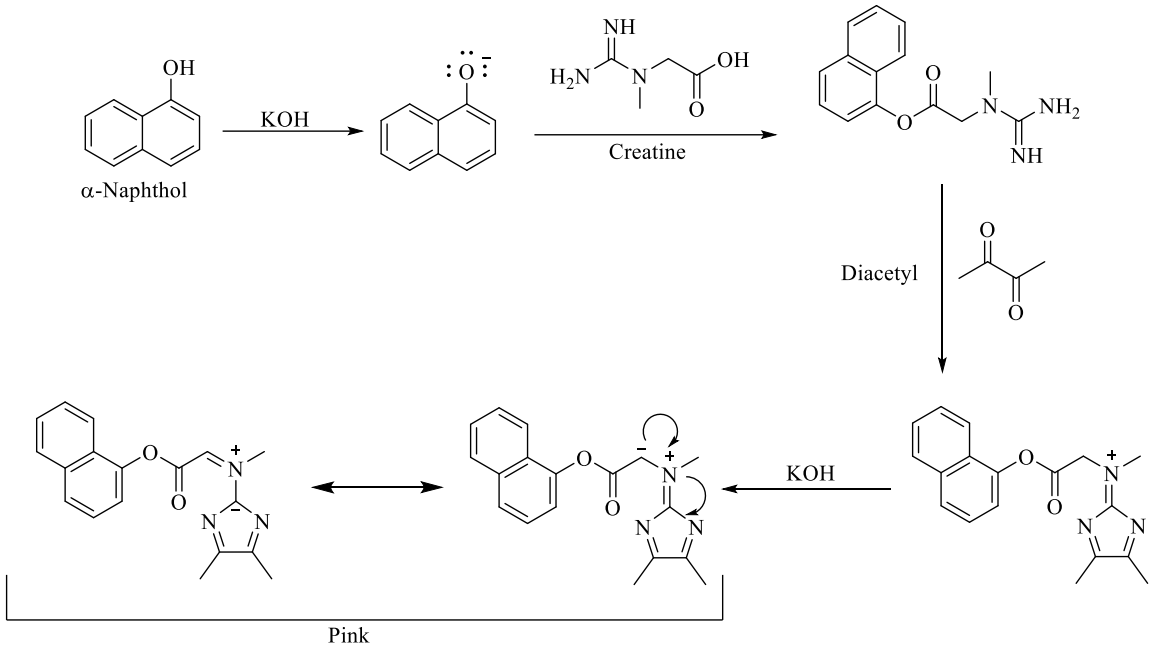

Figure 2.1: Proposed reaction for diacetyl analysis based on the Voges-Proskauer test, in ASBC Beer-25 method B, broad-spectrum method (Bryn, Ulstrup, & Stormer, 1973)

The third ASBC method for the analysis of diacetyl is the micro-dimethylglyoxime, BEER-25 method C (Figure 2.2) (American Society of Brewing Chemists, 1964). As in the first method, this method also requires a working set of diacetyl samples to make a standard curve. Solutions are made from aliquots of the matrix to be analyzed. A separate analysis tube is charged with a hydroxylamine solution and attached to the sample tube with a hose. Carbon dioxide is bubbled through the sample tube for two hours. This carries the diacetyl through the hose and into the analysis tube where it reacts with the hydroxylamine. Iron (II) sulfate is added to develop the color and then the sample is analyzed using a UV-vis spectrophotometer to determine the concentration of diacetyl in solution. The solution turns a pinkish-red color and absorbs at 530 nm. The advantage of this method is that the analysis utilizes an instrument that is relatively easy to use and maintain, the disadvantages include the fact that trace metals

(particularly Fe^{2+}, Ni^{2+}, and Co^{2+}) bind to the product of the color reaction and interfere with the results. From sample collection to reporting, the diacetyl measurements take approximately 3 hours.

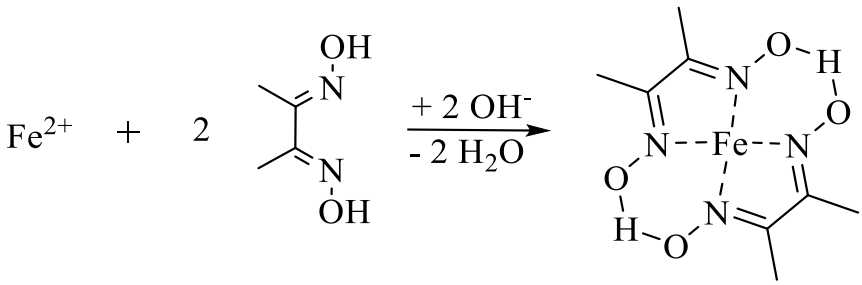

Figure 2.2: Fe^{2+} binding with dimethyl glyoxime forming a red complex

The fourth method, BEER-25 method D, is another archived method and is the UV spectrophotometer method. The fifth ASBC method, BEER-25 method E, for analyzing diacetyl is the gas chromatographic method shown in Figure 2.3 (American Society of Brewing Chemists, 1964). This method requires standard solutions of 2,3-hexanedione, diacetyl, and 2,3-pentanedione to create the standard curve. Beer samples are decarbonated and spiked with a known amount of 2,3-hexanedione (used as the internal standard). The advantage of this method is that it is the only method that identifies each of the specific VDK's. This means diacetyl (2,3-butanedione) is separated from 2,3-pentanedione (another side product of yeast growth during the fermentation step in brewing). The disadvantages of this method are that it is expensive to a) maintain a gas chromatograph (GC), and b) hire a chemist that can perform the analysis efficiently. Potential interactions of the analytes with other compounds in the matrix is also a concern (Dejong, R., Verhagen, L., & Strating, J., 1987). The method is very accurate and precise in measuring VDK concentrations up to 50 ppb. As with the other analyses, it takes time

to provide results; it can take anywhere from 15 minutes to 1 hour to perform this analysis.

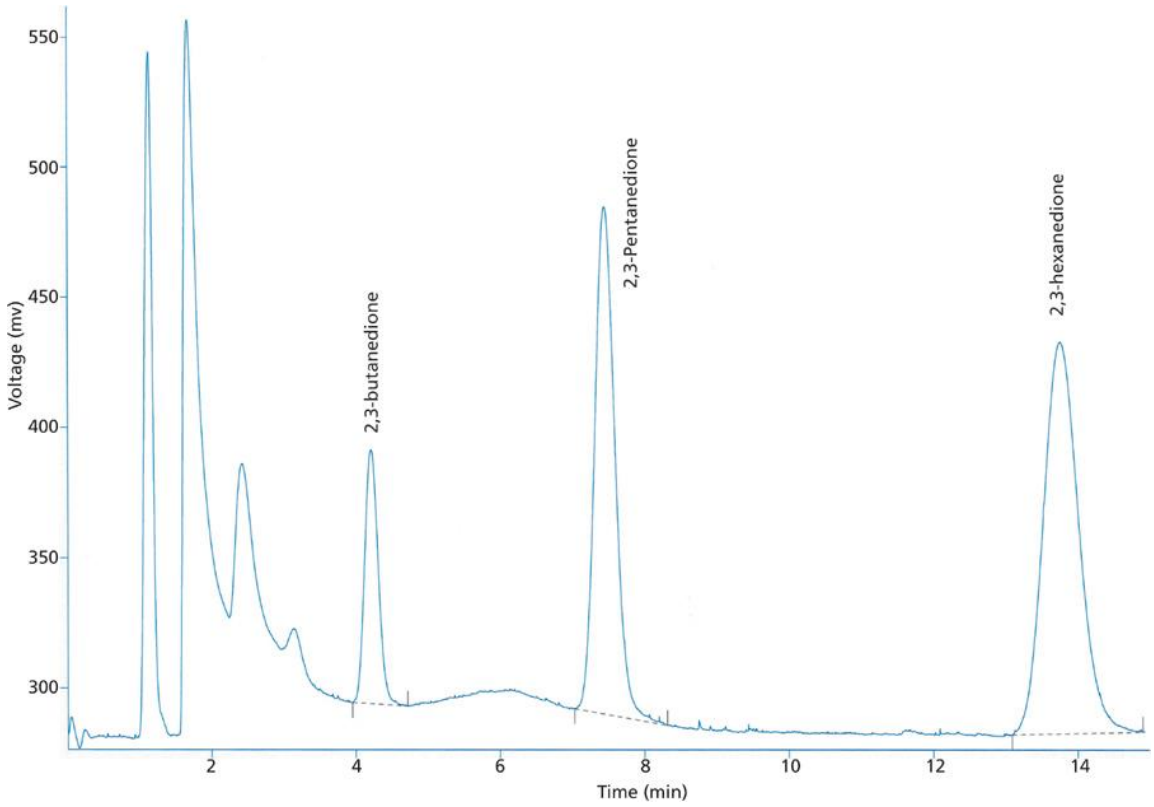

Figure 2.3: GC Chromatogram of diacetyl, 2,3-pentanedione, and 2,3-hexanedione using an Ellutia 200 series gas chromatograph with an electron capture detector

Most brewers in the United States use ASBC methods for analyses that can be performed throughout the brewing process. However, ASBC methods are not the only set of analyses for beer. Another set of standard methods produced by the European Brewery Convention is known as the Analytica-EBC (Analytica-EBC, 1998a). Many of these methods' pre-date ASBC methods. Analytica-EBC suggests two methods that can be used to analyze diacetyl in beer, the first one is entitled 'Vicinal Diketones in Beer: Spectrophotometric Method, 9.24.1'. This method is comparable to the first ASBC

method. The second method is entitled ‘Vicinal Diketones in Beer: Gas Chromatographic method 9.24.2, which is comparable to the third ASBC method, BEER-25 method E (Analytica-EBC, 1998b).

There are many other published methods for the analysis of diacetyl. Most of those methods are confined to either GC or spectrophotometric techniques Spectrophotometric methods typically require that the free diacetyl binds or reacts with colorizing agents. The most common colorizing agents used are creatine and/or naphthol (American Society of Brewing Chemists, 1964), *o*-phenylenediamine (OPDA) (Analytica-EBC, 1998a); (Pejin et al., 2006); (Rodrigues, Barros, Machado-Cruz, & Ferreira 1997); (Rodrigues, Barros, & Rodrigues, 1999); (Rodrigues et al., 2002), and hydroxylamine/ iron (American Society of Brewing Chemists, 1964). GC methods that exist use different detectors such as the electron capture detector (American Society of Brewing Chemists, 1964); (Buckee & Mundy, 1994); (Analytica-EBC, 1998); (Journal of Brewing Chemists, 1999); (Martineau, Acree, & Henick-Kling, 1994); (Harrison, Byrne, & Collins, 1965), mass spectrometer detector (Landaud et al., 1998), voltammetry detector, and pulse polarographic detector (Rodrigues et.al., 1997). Other methods using GC as the instrument for analysis focus on headspace analysis with an electron capture detector (Yunfei, Hao, & Shun, 2012); (Grecsek & Ruppel, 2005).

The reaction of VDK’s with *o*-phenylenediamine produces non-volatile quinoxaline compounds (Rodrigues et.al., 1997, 1999, 2002) (Verhagen et.al., 1987). Specifically, the reaction produces 2,3-dimethylquinoxaline and 2-ethyl-3-methylquinoxaline (Figure 2.4). The conversion of VDK’s to the equivalent quinoxalines is quantitative and fast over a broad pH range from 1-10 (Rodrigues et.al., 1997). The

quinoxaline compounds can then be detected using differential-pulse polarography using a Metrohm multi-mode electrode (MME) as the working electrode, and a platinum wire as a counter electrode and a silver/silver chloride reference electrode. Quinoxalines are polarographically active compounds and an adaptation of a polarographic method was developed for their determination, with a limit of detection is 5 ppb for diacetyl. The proposed method was compared to samples tested on a Hitachi U-2000 model double beam spectrophotometer using a set of 1.01 cm Suprasil quartz cells from Hellma. The more accurate polarographic method has a detection limit approximately ten times lower than the spectrophotometric method.

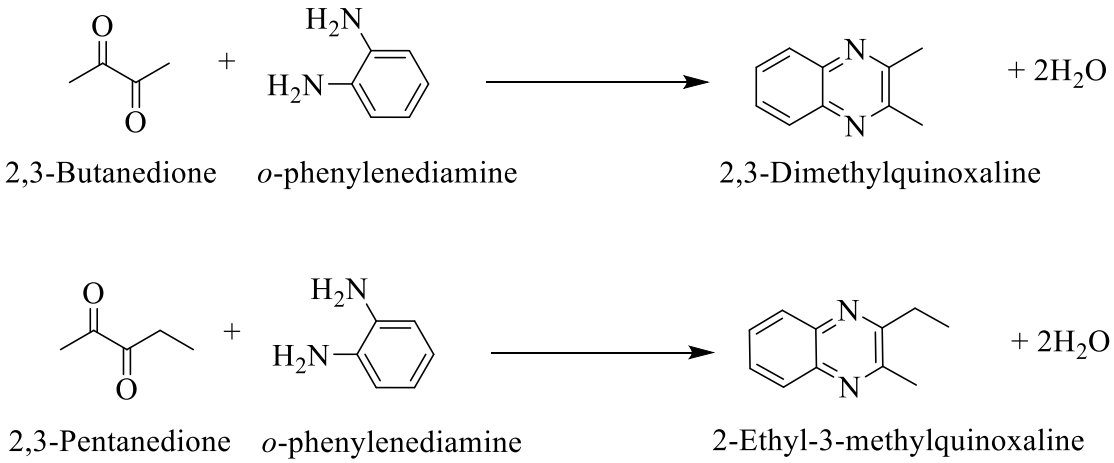

Figure 2.4: Derivatization of VDK's with OPDA

Other methods for the detection of VDK's in beer include HPLC using fluorometric or UV spectrophotometric detection (Li, Duerkop, & Wolfbeis, 2009); (Wang, Wang, Hui, Hua, Li, & Gao, 2017). These methods perform solid-phase extraction (SPE) to reduce interference with other beer ingredients followed by derivatization of the VDK's with 2,3-diaminonaphthalene before HPLC analysis with fluorometric detection (Damiani & Burini, 1998); (McCarthy, 1995). Another method

uses a double SPE (Solid Phase Extraction) sample treatment, derivatized VDK's with OPDA and analyzed with UV spectrophotometric detection (Verhagen, et.al., 1987; Barros, Rodrigues, Almeida, & Oliva-Teles, 1999).

Alternative methods of analysis for diacetyl use UV-vis spectroscopic methods. One such method utilizes an automated distillation method compared to GC analysis (Buijten & Holm, 1979). They used a Technicon AutoAnalyzer II system, coupled to a continuous flow distillation unit. Distilled diacetyl was mixed with OPDA then directed through a 15 mm flow-cell where the product absorbance was measured at 340 nm. Another colorimetric method utilizes an Eppendorf BioSpectrometer to analyze the reaction of VDK's with OPDA to form 2,3-dimethylquinoxaline, which absorbs at 335 nm. The authors calculated VDK concentrations with a standard curve (Geisler & Weiß, 2015).

Formation of Diacetyl During Fermentation

Yeast, during fermentation, uptake maltose as the first step of metabolism. The sugar is cleaved into two glucose units once inside the yeast cell. Glucose is then converted via glycolysis to pyruvate, an important intermediate in metabolism. Pyruvate can go forward through the citric acid cycle when oxygen is present. Pyruvate can also be converted to α-acetolactate, for use in the synthesis of valine; one of the amino acids. Excess α-acetolactate escapes from the yeast cell where it undergoes oxidative decarboxylation to produce diacetyl and carbon dioxide. When the yeast cells do not have enough energy (ATP) they uptake diacetyl from the surrounding solution. Diacetyl is then converted into acetoin and NAD^+. The acetoin can further be converted into 2,3-

butanediol and more NAD^+ (Figure 2.5). The NAD^+ gives the yeast the energy it needs to consume more glucose and produce more energy (Renger, van Hateran & Luyben, 1992).

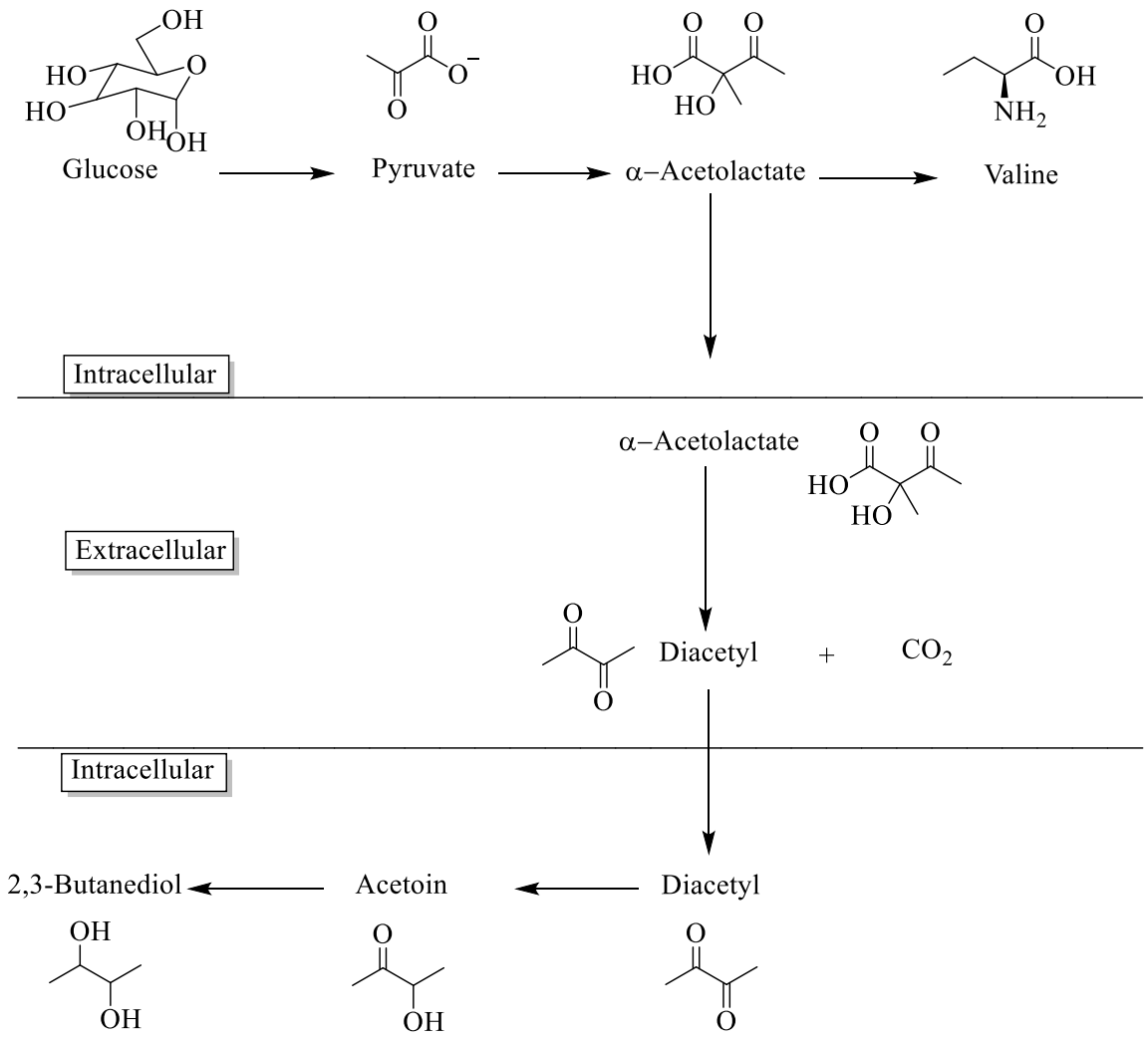

Figure 2.5: Metabolic Pathway for Diacetyl

The carbon dioxide produced by the decarboxylation of α-acetolactate is stoichiometrically related to the concentration of diacetyl (Figure 2.6); therefore, analysis of the concentration of carbon dioxide is a suitable candidate for reporting diacetyl concentrations. α-Acetolactate can be challenging to isolate and/or prepare synthetically

because of its propensity to decarboxylate, therefore another decarboxylation reaction will provide the best option for exploratory analysis.

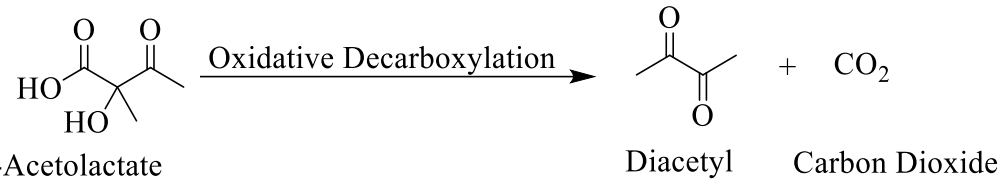

Figure 2.6: Oxidative decarboxylation reaction with α-Acetolactate

For example, ethyl acetoacetate undergoes deesterification under acidic conditions at a known rate (Figure 2.7). The resulting acetoacetic acid, a ß-oxoacid, decarboxylates readily, resulting in carbon dioxide, and acetone. Thus, the concentration of carbon dioxide after the reaction should be equivalent to the initial concentration of ethyl acetoacetate.

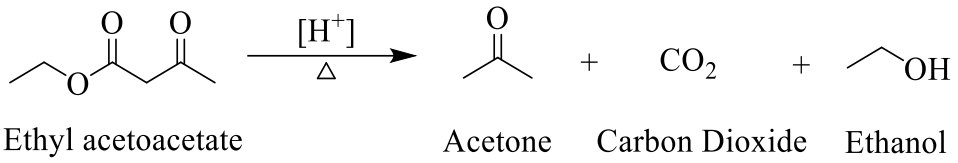

Figure 2.7: Reaction of ethyl acetoacetate undergoing deesterification, producing acetone and carbon dioxide

Measuring Carbon Dioxide in Solution

IR spectroscopy is a nondestructive method for analyzing solids and liquids. IR spectroscopy can provide a real-time inline or online measurement of analytes. Samples for analysis can be in the form of a solid, liquid, or gas when interacting with the infrared radiation. An IR spectrum is produced after this interaction is recorded onto a detector and produces a spectrum of absorbance or percent transmittance versus the frequency or wavelength. ATR or Attenuated Total Reflectance is a technique where the sample is placed in contact with a sensitive element, typically a crystal, and a spectrum is recorded.

Radiation is not transmitted through the sample; the IR radiation is passed through the sample and some of the radiation is absorbed. When the radiation is reflected to the detector, the detector takes the difference in radiation from start to finish to produce an IR spectra (Griffiths & de Haseth, 2007).

ATR utilizes total internal reflectance within a crystal to perform infrared spectroscopic analysis (Mirabella, 1993). Different crystals have different amounts of total internal reflectance based on the material that makes up the crystal and the pathlength of the crystal (Mendelsohn, 2007). The infrared light enters the crystal at a perpendicular angle (Figure 2.8). The light then strikes the face of the crystal upon which the sample is placed. If the angle of incidence on that face is appropriate, the light is completely reflected back into the crystal. That reflectance produces an evanescent wave that is absorbed by the sample on the face of the crystal. The light, minus the component wavelengths that were absorbed from the evanescent wave, then exits the crystal at a perpendicular angle where it strikes the detector.

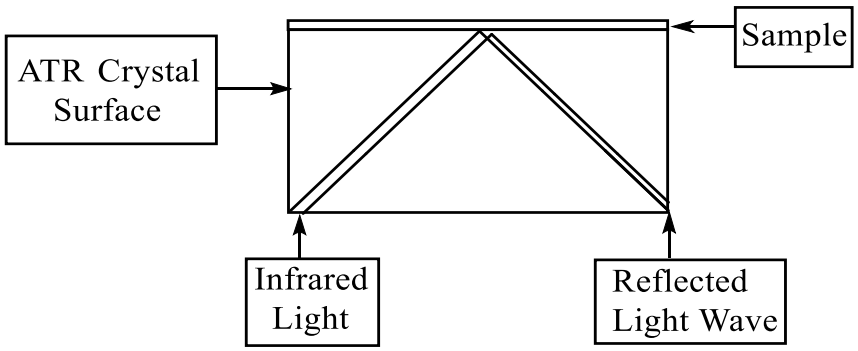

Figure 2.8: Schematic of ATR using infrared light

The detector records the attenuated infrared beam as an interferogram. An interferogram is recorded in time units and organizes incoming constructive and

destructive interferences into continuous signals from the discontinuous signals shown in Figure 2.9. The signals are then Fourier transformed using a computer algorithm (Martín-Ramos, Fernández-Coppel, Ruíz-Potosme, & Martín-Gil, 2018). When ATR and Fast Fourier Transformations are paired with IR spectroscopy, the results of the analysis are obtained almost instantaneously.

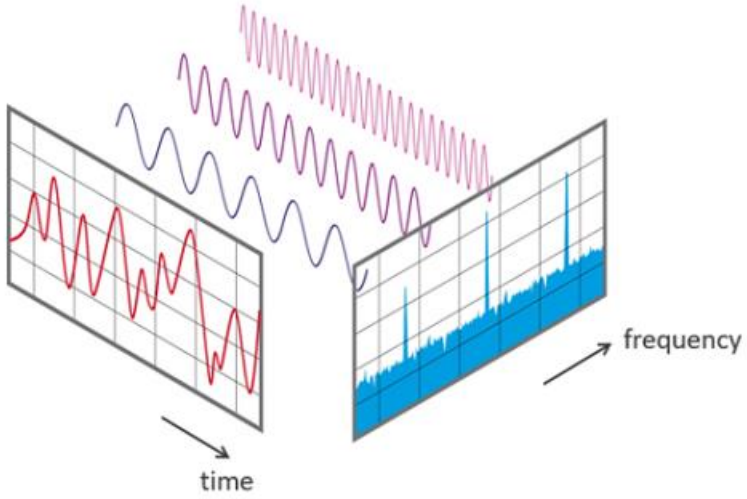

Figure 2.9: Diagram of Fast Fourier Transforms. Signal of time and frequency domain of sinusoidal oscillations

Specific gravity is a measurement is a ratio that can be used for determining the sugar concentration (wort) in an aqueous solution. The ratio is dependent on the temperature and pressure of the sample and water. The pressure in the brewing world is always considered to be 1 atm and the temperature is usually 20 °C for both sample and water, according to ASBC methods. The American Society of Brewing Chemists (ASBC), method for analyzing specific gravity is by using the density measured at 20 °C and reference the density of water at 20 °C which is 0.998203 g/cm^3 (American Society of Brewing Chemists, BEER-2, 1992). The Analytica-EBC, European Brewery Convention method for analyzing specific gravity of the wort, method 8.2, uses a

pycnometer. A liquid pycnometer is an instrument that measures density (Analytica-EBC, 1998). It uses a working liquid with well-known density, such as water. This means the difference between the volume of water that fills the empty pycnometer and the total volume (Heaney, 2012).

Currently, little research has been accomplished for the analysis of dissolved gases by IR spectroscopy. A common laboratory instrument that uses this technique is the Fourier transform infrared (FTIR) spectrometer. An example of this method utilizes an attenuated total reflectance (ATR) flow cell to analyze liquids and gases. Carter and colleagues developed methods using a ReactIR flow cell for micro- and mesofluidic continuous flow chemistry processing applications. They were able to monitor a variety of important functionalities present in organic molecules such as C=O or C=C bonds. Bonds in other analytes, such as C=N, N_3, C-F, and C-O could be visualized as reaction intermediates in real-time, with measured concentrations as low as 0.05 M (Carter et al., 2010). Another study introduced FTIR for the measurement of the equilibrium adsorbed mixture of gases on pellets made from NaX zeolite and γ-alumina (Rege, & Yang, 2001). They created a technique that requires calibration of the infrared absorption peak areas with known adsorbed amounts of the different components using single gases. By measuring the IR peak areas of the adsorbates on the sorbent in contact with the gas mixture, the actual amounts of the sorbate can be determined (Rege &Yang, 2001).

In 2016, Schädle and coworkers described a portable mid-range IR system for monitoring CO_2 and CH_4 in high-pressure situations in the saline aquifer and brine environments (Schädle, Pejcic, Myers, & Mizaikoff, 2016). They demonstrated that FTIR can be used as an analytical tool for online/in-line monitoring systems at varying

environmental conditions. They examined elevated pressures up to 11 MPa across a wide temperature range. The analysis was useful for simultaneous measurements of multiple analytes as they show up in different regions in the infrared spectrum, shown in Figure 2.10 below. Figure 2.10A shows the IR spectra of CO_2 (at 2342 cm^{-1}) across a range of pressures, a plot of the peak area versus pressure, and a plot of the peak area versus the concentration. Figure 2.10B contains similar information for methane (at 1304 cm^{-1}).

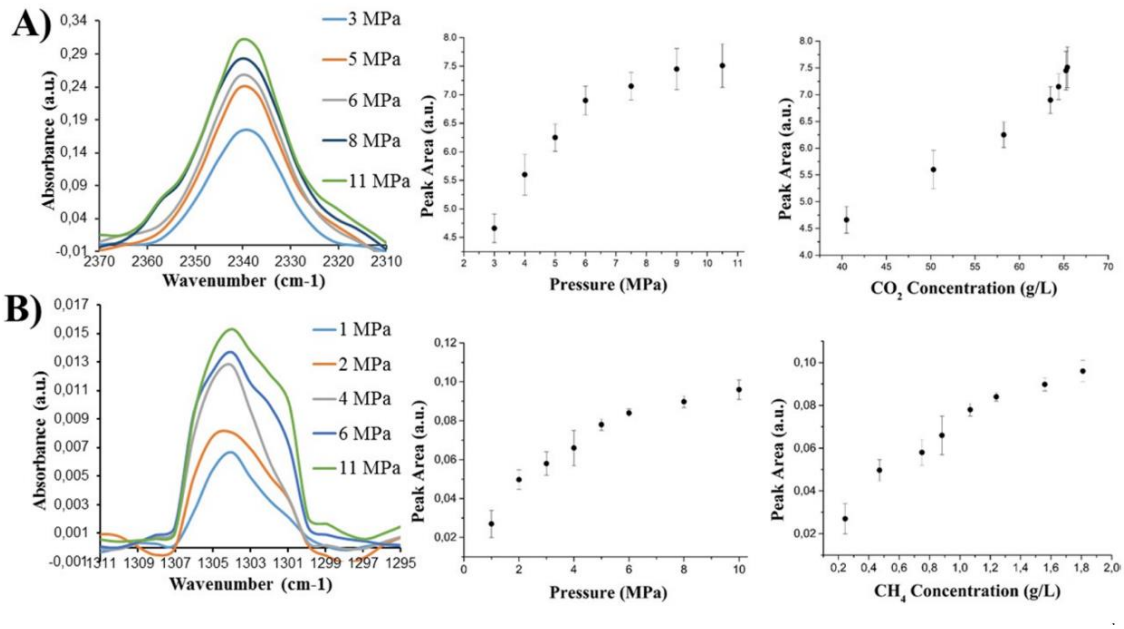

Figure 2.10: IR spectra of the dissolved gases at elevated pressures, (Schädle et al., 2016)

Other research has been published for dissolved gases in solutions utilizing ATR-FTIR. One group used FTIR on the analysis of carbon dioxide absorption and desorption in amine solutions (Jackson, Robinson, Puxty, & Attalla, 2009). The amines that were used to show carbamate and carbonate formation. Table 2.1 and Figure 2.11 show the growth of amine groups and carbamate, carbonate infrared signals were increasing in size during a reaction over a period of four minutes.

Table 2.1: Table of infrared peak assignments for a CO_2 injected ethanolamine solution, corresponding the peaks in the spectrum of Figure 2.9 (Jackson et al., 2009)

Peak	Frequency (cm^{-1})	Assignment	Comment
A, 5	1564	2° amine	Software assignment
B	1491	Possible -HN-C=O	Based on imino-carbonate C-O stretch
C, 6, 7	1464	$-H_2C-NH_2$	Based on experimental observations
D	1385	Carbonate	Based on experimental observations
E	1322	N-C=O(O) in carbamate	Based on phosphate P-O stretch
F	1226	CO-OH	IR correlation chart
G, 8	1156	$-HN-CO_2$ (carbamate)	Based on C-N 2° amine stretch
H, I, 9, 10	1067, 1019	C-N & C-O	Based on experimental observations

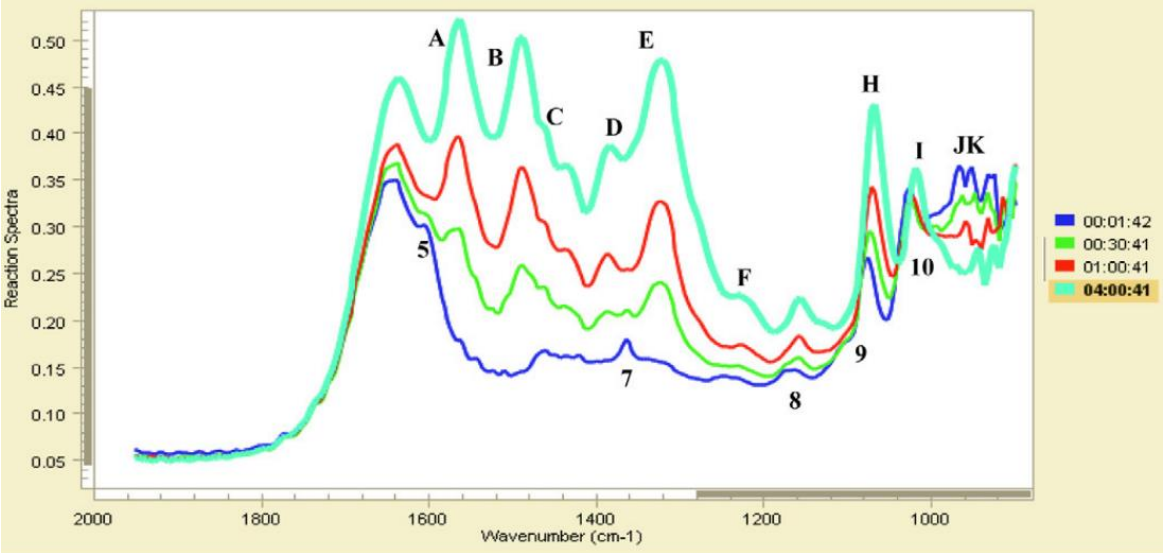

Figure 2.11: IR spectrum of the compounds labeled in Table 2.1 for the reaction of CO_2 in aqueous ethanolamine, over a 4-minute period (Jackson et al., 2009)

A fascinating research study utilizing a quantum cascade laser at 2300 cm^{-1} to determine CO_2 concentrations using a CaF_2 flow-cell in the mid-infrared spectrum (Schaden, Haberkorn, Frank, Baena, & Lendl, 2004). The concentration of dissolved CO_2 was calculated using Henry's law, considering the temperature and the partial pressure of

CO_2. Henry's law is a gas law that states that the amount of dissolved gas in a liquid is proportional to its partial pressure above the liquid (Henry, 1803). They were able to fix the flow cell and the laser beam onto a mercury cadmium telluride (MCT) detector, obtaining a calibration curve of values of 0.338 to 1.350 g/L CO_2 shown in Figure 2.12. Their method had a standard deviation of 19.4 mg/L CO_2 and a limit of detection of 39 mg/L.

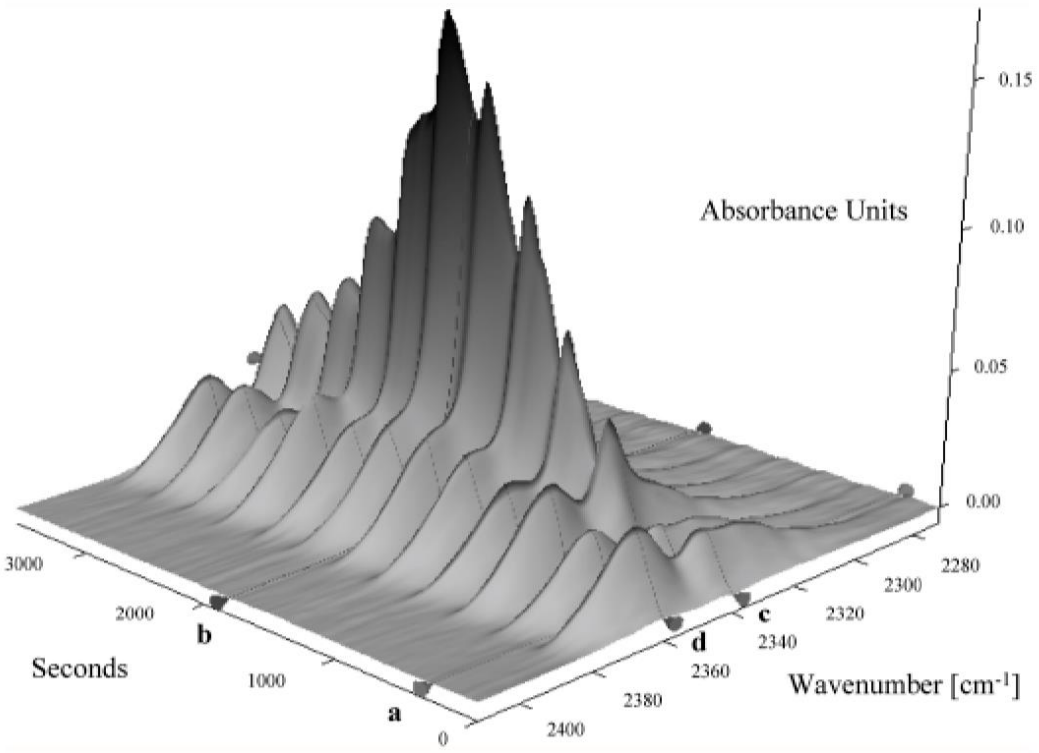

Figure 2.12: FTIR spectrum analyzing the saturation process of a 1.35 g/L CO_2 standard. (a) At 300 s the saturation with CO_2 was started. (b) At 1800 s the solution was purged with N_2 gas. In addition to (c) the analyte characteristic absorption band at 2300 cm^{-1}, (d) gaseous CO_2 absorption bands are also visible (Schaden et al., 2004)

A relevant article was published in 2000, for the analysis of different alcohols in breath using low-resolution FTIR (Laakso et al., 2000). They used a portable FTIR multicomponent analyzer to detect different types of alcohol on a person's breath, mostly

used as a technique for crime scenes. The measured spectra can be saved and analyzed at a different time. They demonstrate that FTIR spectrometry can provide a direct measuring technique that is not dependent on a chemical reaction but the individual molecules themselves.

Raman Spectroscopic Methods

A different type of vibrational spectroscopy that allows researchers to investigate compounds and analytes in the electromagnetic spectrum is Raman spectroscopy. Raman spectroscopy is a spectroscopic technique used to determine vibrational modes of molecules and to provide a structural "fingerprint" unique to each molecule. Raman spectroscopy is considered as a complementary analytical technique with FTIR. It is dependent upon the inelastic scattering of photons, known as Raman scattering by using a monochromatic light source, typically near IR or visible light. This laser light interacts with molecular vibrations, resulting in the energy of the laser photons to be shifted. The shift in energy gives information about the vibrational modes in the system shown in Figure 2.13 (Edinburgh Instruments, 2019).

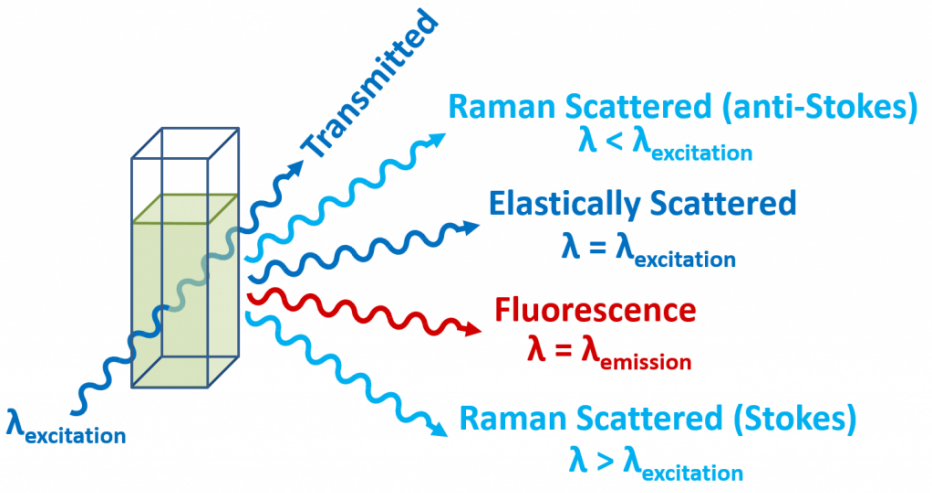

Figure 2.13: Energy-level diagram of the different states involved in Raman spectroscopy (Edinburgh Instruments, 2019)

When photons are scattered, most of them exhibit elastic scattering. This means that the light emitted from the molecules contain the same wavelength as the energy that was absorbed. While they have the same wavelength as the incident photons, they are emitted in a random direction from the orientation of the incident photons. The light waves that are oriented in opposite directions do not hit the detector. The differences between absorption and emission spectra are that absorption lines are where the light has been absorbed by the atom. Emission spectra have spikes in the spectra due to atoms releasing photons at those specific wavelengths (Griffiths & de Haseth, 2007).

When the photons of the laser strike the molecule, the total energy of the system will remain constant even though the molecule moves to a new rovibronic (rotational-vibrational-electronic) state. However, the emitted photon will then come from the new rovibronic state. If the final state is higher in energy than the initial state, the scattered photon will shift to a lower energy level, meaning that the energy remains constant. This shift in energy is defined as a Stokes shift. If the final state is lower in energy, the scattered photon will shift to a higher energy level, this is the opposite of a Stokes shift, it is defined as an anti-Stokes shift (Gardiner, 1989).

The fluorescence interference in Raman spectroscopy typically results from the compound or from fluorescent impurities in the sample. It is an absorption process that causes molecules to be excited to a higher electronic state, which requires high-energy photons (Griffiths & de Haseth, 2007). In order to have this issue ameliorated, near IR lasers can be used to illuminate the sample. Near-IR lasers have longer wavelengths and are long enough that the compound fluorescing does not occur. (Griffiths & de Haseth, 2007).

Raman spectroscopy has been primarily used for qualitative research, however, there is a large interest in the use of Raman spectroscopy as a quantitative analytical technique. Burikov and coworkers, for example, evaluated the hydrogen bonding in water-ethanol systems (Burikov, Dolenko, Patsaeva, Starokurov, & Yuzhakov, 2010). They demonstrated that the maximal strength of H-bonding in water-ethanol mixture corresponds to ethanol concentration between 15–20% w/w. The O-H stretching band in Raman and IR spectra showed that hydrogen bonding in solutions at ethanol concentrations around 15–20% w/w is stronger than water. Davis and Oliver performed a vibrational-spectroscopic study of the species present in the CO_2-H_2O system (Davis, & Oliver, 1972). They determined that at a pressure of 5 atm the solubility of CO_2 in water was 0.17 M. The dissolution of CO_2 in water produced little H_2CO_3, the prominent species being molecular CO_2. They observed that that the vibrational lifetime of CO_2 before a collision occurs, is shorter in H_2O than D_2O. This would imply that the CO_2 molecule is more mobile in H_2O than in D_2O. This was supported by their experimental observations that the self-diffusion rate for H_2O is greater than D_2O. Therefore, in aqueous solutions, the CO_2 molecule is linear and has $D_{\infty h}$ symmetry (Davis, & Oliver, 1972).

A recent article was published by Holzammer and Braeuer on the thermodynamic inhibition effect of different salts on the formation of carbon dioxide gas hydrates using Raman spectroscopy (Holzammer & Braeuer, 2019). Experiments were contained in a high-pressure vessel with an H_2O-rich phase and a CO_2-rich phase. This experiment saw the change in molar reaction enthalpy between strongly and weakly hydrogen-bonded water and the decrease in solubility of carbon dioxide in water. They determined the

number of solid hydrates formed and that there is a reaction constant proving that the molar reaction enthalpy, the solubility of CO_2, and the number of solid hydrates formed are correlated with the effective mole fraction. They showed that a decrease in the molar reaction enthalpy is directly correlated with the equilibrium temperature of the gas hydrates (Holzammer & Braeuer, 2019).

In summary, the craft brewing industry is on the rise and methods to analyze beer and the brewing medium are being developed every day. Published ASBC methods for beer analysis consist of hundreds of analyses with the EBC-Analytica methods on a similar path. There are many methods to analyze beer at all stages of the brewing process, we are focused on fermentation. We have discussed looking into the most unwanted off-flavor, diacetyl, and the methods to analyze this analyte by using standard brewers ASBC and EBC methods. Comparing CO_2 that has a direct relationship with diacetyl makes it a good analyte for FTIR analysis and other types of vibrational spectroscopic techniques.

CHAPTER III

METHODOLOGY

A new method for the determination of carbon dioxide in solution was developed using a flow-cell based ATR-FTIR. This new method allows for fast, real-time determination for in-line analyses. This method can provide researchers with a rapid way to measure decarboxylation reaction rates and evaluate the completion of any decarboxylation reaction if CO_2 is produced in the reaction.

The starting materials and reagents were purchased from Fischer Scientific and/or Sigma Aldrich and were used without further purification. Ethanol (200 proof; 100%) was used in all of the analyses that required ethanol and was diluted with D.I. water as needed. The seltzer water, beer, and liquor were purchased at local grocery and liquor stores and were not purified before use. The instrument used in this analysis was a Thermo Fischer-Nicolet iS5 FTIR, with a microflow cell ATR attachment shown in Figures 3.1 and 3.2. The FTIR contains a KBr/Ge mid-infrared optimized beam splitter, a temperature-controlled solid-state near-IR diode laser, a mid-infrared Ever-Glo IR source, a deuterated triglycine sulfate (DTGS) standard detector, and had vibration, electromagnetic interference, dust, and tilt considered in the design (Nicolet™ iS5, n.d.). The flow cell was purchased from Hellma Analytics, using a germanium crystal (16 reflections) encased in 316 stainless steel. The maximum pressure the flow cell can contain is 20 bar, the maximum temperature the flow cell can handle is 260 °C and the flow cell volume is 40 µL of liquid (Hellma Analytics, n.d.). The liquid is driven through

the system using a Hewlett-Packard Company HPLC pump model 79852-A, obtained as a refurbished unit from Labx.com. All tubing connections between flow cell and the pump to construct the device, are made from Parker A-Lok 4RU1-316-316 stainless steel tubing and Stainless Steel 304L Seamless Round Tubing, 1/4" OD, 0.12" ID, 0.065" Wall, 72" length. The setup for the device is based on the US patent 15/185,844, “In-line detection of chemical compounds in beer” in Figure 3.1.

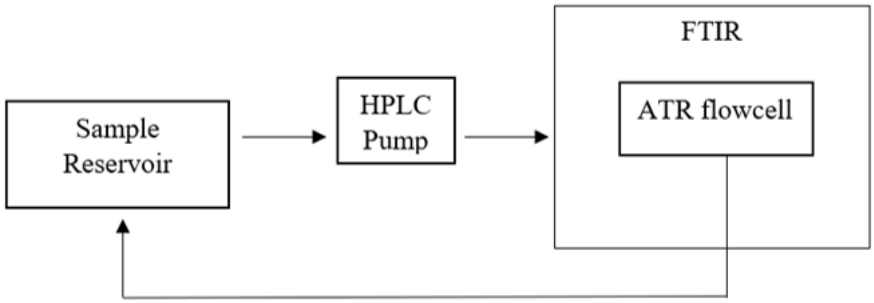

Figure 3.1: The general set-up based on US patent 15/185,844

Stainless steel parts were used as needed in the construction of the device. Beer is corrosive to storage tanks and transportation lines due to its acidity; the pH can be as low as 3. Copper and other metals would react at such low pH values and corrode over time. In addition, beer contains living micro-organisms which can cause corrosion and fouling. The corrosion resistance of stainless steel in the brewery keeps out the unwanted flavors caused by the corrosive electrochemical byproducts of the brewing process.

The first step in the construction of the device was to mount the flow cell to the FTIR housing unit and aligning the instrument laser. A mount was created using two different methods to best fit the flow cell set-up, the first being a 3-D printed mount with two baseplates that allows movement in the Z-direction and tilting of the XY plane. The

second mount was made of stainless steel with a post that allows the Z-direction movement and twisting in the XY plane. Images of the designed mounts can be found in Figure 3.2 and Figure 3.3.

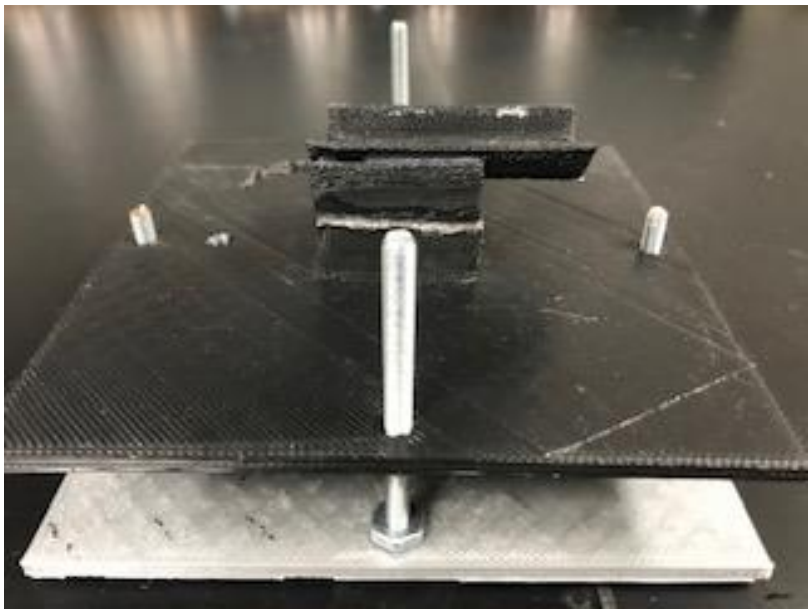

Figure 3.2: Image of the 3-D printed mount

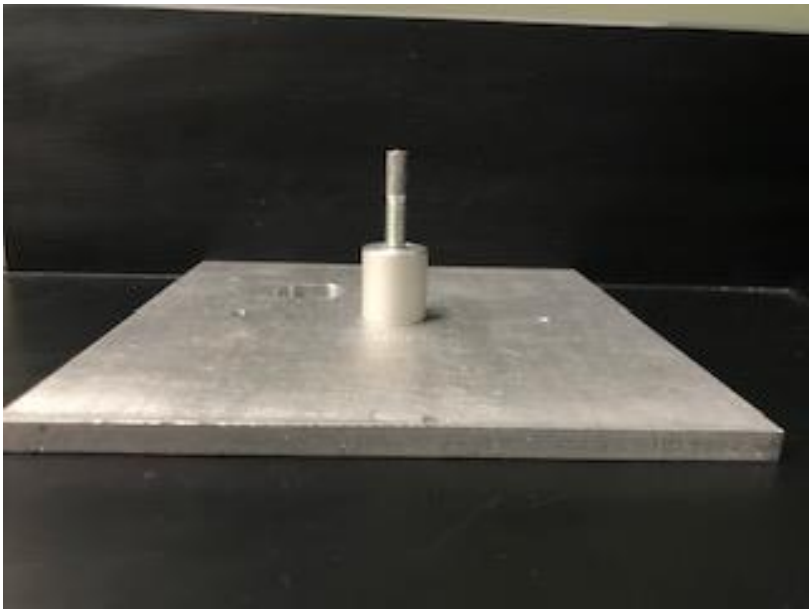

Figure 3.3: Image of the machine welded mount

The 3-D printed mount was assembled with acrylonitrile butadiene styrene filament (ABS) in the University of Northern Colorado's Department of Physics and Astronomy, using 2017 Solidworks software from Dassault Systems for the design. The 3-D printer used was a Taz 6 from Lulzbot with Cura software version 21.08 installed for printing, shown in Figure 3.4. Therefore, the designs created in Solidworks had to be converted to match the printer's formatted Cura software. The second mount was also made at the University of Northern Colorado's campus, utilizing the machine shop. Verification of the proper placement of the flow cell was accomplished by obtaining spectra of water-soluble organic compounds, such as acetone, ethanol, and acetaldehyde, and comparing those results to known IR spectral data.

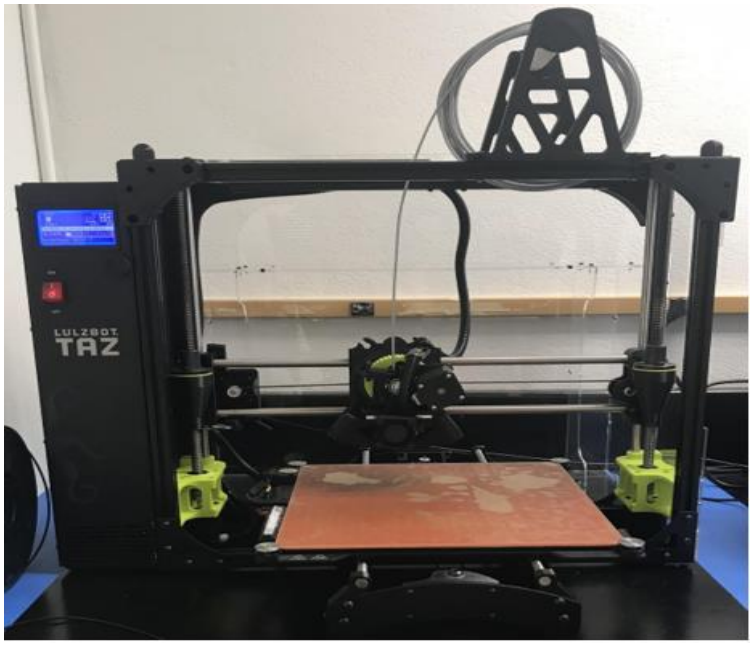

Figure 3.4: Photograph of the Lulzbot Tax 6, the 3-D Printer

After the mounts were built, the flow cell was installed in the IR sample chamber. Stainless-steel tubing was used to attach the HPLC pump to the flow cell. The tubes were clamped in place with Swaglok® fittings. A closeup of the flow cell on the aluminum

mount with attached tubing can be seen in Figure 3.5. The complete setup can be seen in Figure 3.6. In this image, the sample chamber is located on the left-hand side as a glass jar filled with a liquid that has been dyed red. The liquid first enters the HPLC pump and then is passed to the flow cell. The liquid enters the bottom of the flow cell and exits the top of the flow cell. A pressure gauge and needle valve can be seen in the return loop to the sample chamber.

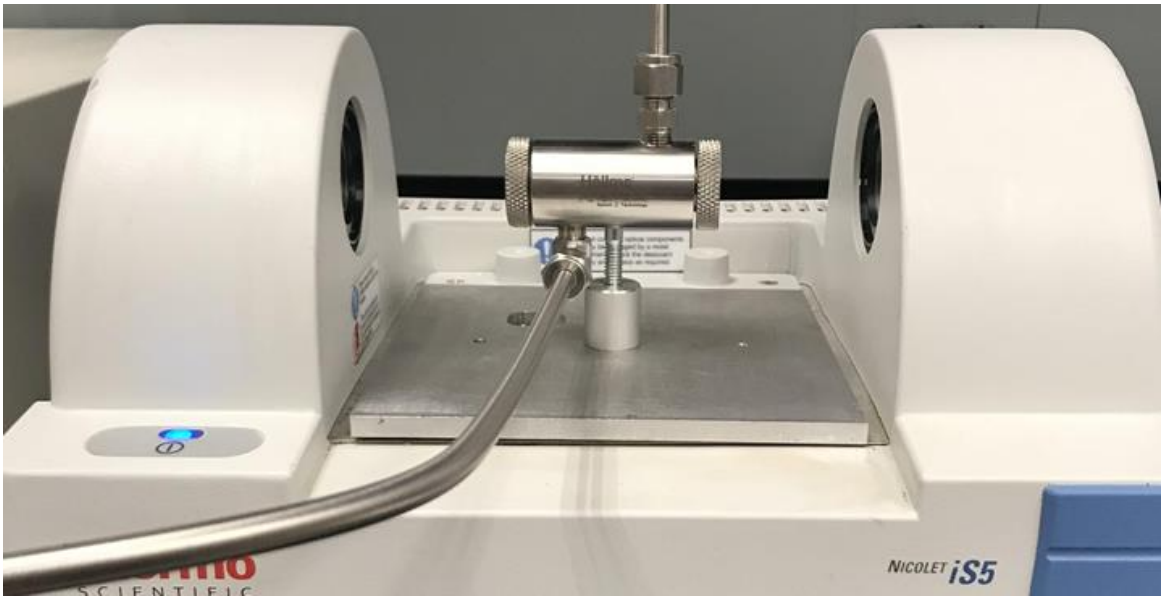

Figure 3.5: Image of the final set-up for the Ge flow cell analysis illustrating how the tubing was connected to an HPLC using Swagelok® fittings

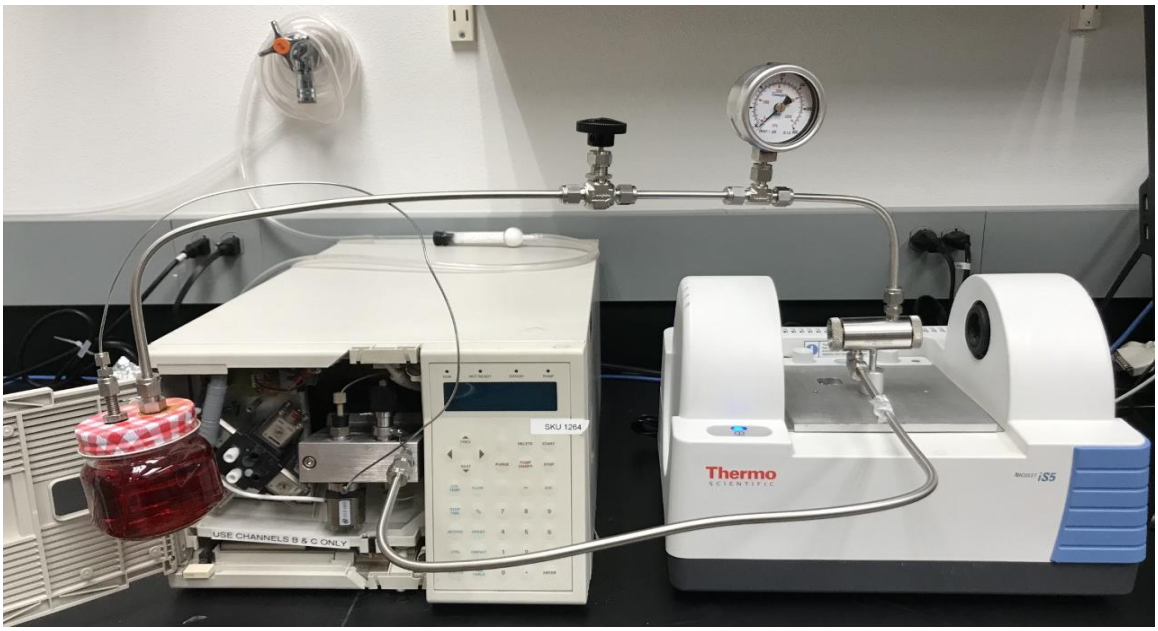

Figure 3.6: Photograph of the Nicolet™ FTIR with the flow cell attachment from Hellma Analytics

Verifying the carbon dioxide signal in the mid-range IR spectrum was vital to this project. Carbon dioxide gas is considerably more soluble in cold water than in warm water (2774 ppm at 5 °C and 1257 ppm at 30 °C); (King & Coan, 1971), so the solution must be chilled to maximize the concentration of carbon dioxide. The pressure of the system also affects the amount of dissolved carbon dioxide (2490 ppm at 1.01 bar and 20 °C versus 2100 ppm at 10.1 bar and 20 °C). Even though the literature values for carbon dioxide solubility are in the water, the trends are similar in other carbonated solutions such as beer and soda. To ensure the appropriate pressure was maintained throughout the flow cell so the samples do not de-gas, a needle valve and pressure gauge were installed to restrict the flow near the outflow into the reservoir, seen in Figure 3.7.

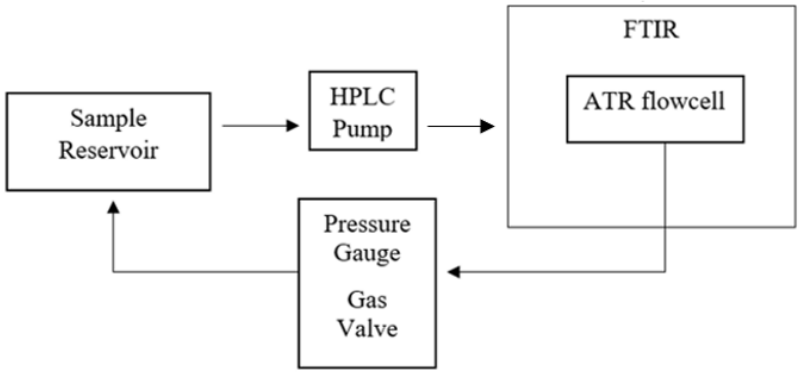

Figure 3.7: Final set-up of the device. Addition of a pressure gauge and a gas release valve

α-Acetolactate is an expensive compound to purchase and is challenging to synthesize; therefore, after the device was constructed a model decarboxylation reaction was studied using an inexpensive compound. This was done to show similarities of product formation between a model reaction and the oxidative decarboxylation reaction with α-acetolactate in fermentation, as both would produce CO_2. This was accomplished to verify that different types of decarboxylation reactions could be analyzed, the system response evaluated, and issues with the flow cell solved before purchasing α-acetolactate. We hypothesized that ethyl acetoacetate would present an appropriate reaction in comparison to the formation of α-acetolactate in the brewing industry, due to the reaction type and its similar product formation. This reaction required ethyl acetoacetate to be suspended in a sodium acetate buffer to control the pH during the analysis. The reaction, whose rate is governed by the temperature of the solution, proceeded slowly to produce acetone, carbon dioxide, and ethanol.

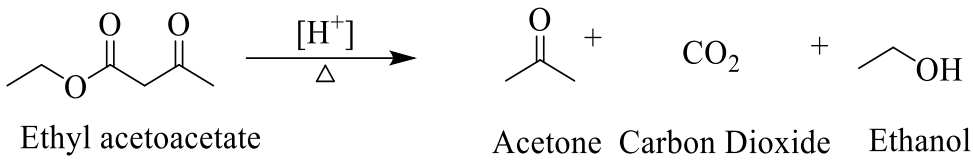

Figure 3.8: Reaction of Ethyl-acetoacetate in a sodium acetate buffer. Acid and heat are added slowly to produce acetone, carbon dioxide, and ethanol and instantly chilled in an ice bath to dissolve the carbon dioxide in solution

To analyze the decarboxylation of ethyl acetoacetate, we explored the IR spectra generated by the iS5 FTIR containing a multibounce iD Foundation adapter from Thermo Scientific ™. This multibounce adapter employed a ZnSe crystal trough where liquid samples could be placed for analysis. The multibounce attachment allows infrared light to reflect approximately ten times before entering the detector. The reaction with ethyl acetoacetate was run through the multi-bounce FTIR (MB-FTIR) for carbon dioxide, acetone, and ethanol detection.

To ensure that carbon dioxide was actually being produced in the reaction we performed a bubble capture analysis shown in Figure 3.9. Performing the bubble analysis in a sodium phosphate buffer (specific pH's ranged from 4 to 6) at various temperatures from 50-80 °C. The volume of gas produced by the reaction was recorded at specific time intervals to obtain a plot of gas produced versus time. We also ran the reaction dissolved in the same amounts of ethanol. The bubble analysis equipment was comprised of a reaction vessel attached to a glass tube that fed into a gas collection tube. The gas collection tube was filled with water, inverted, and placed in a large pool of water. When CO_2 was generated, it would travel through the tube and displace the water in the collection tube. Thus, the volume of CO_2 being produced from the reaction could be easily measured. Because the water was kept slightly above room temperature and the

pressure was ambient, the amount of CO_2 that dissolved in the water was negligible compared to the amount of CO_2 gas collected in the tube.

The bubble analysis reaction was performed at variable pH values and was analyzed at variable temperatures. Collection tubes used for this analysis included a 50 mL gas collection tube and a 10mL graduated cylinder. Because the length of tubing created a large pressure gradient, the smaller 10mL graduated cylinder was preferred for the measurements. However, the size of the tube did not matter as the experiments were only performed to prove the concept that gas was generated in the reaction.

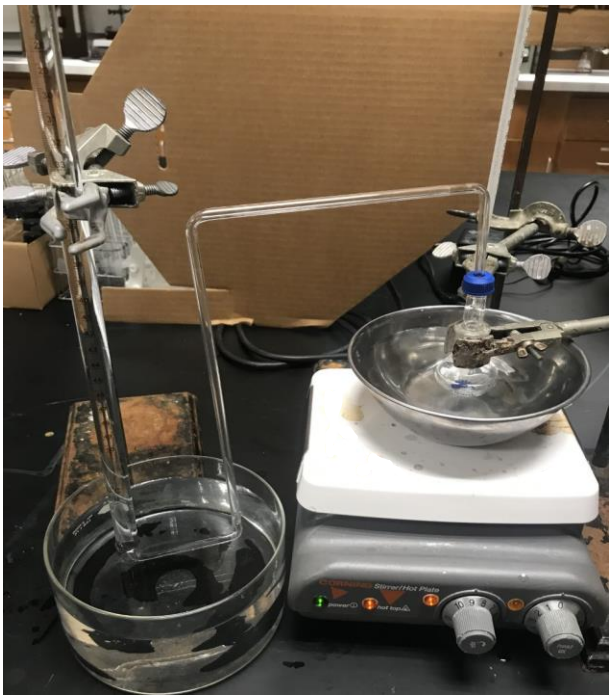

Figure 3.9: Photograph of the bubble analysis setup. The reaction was contained in a round bottom flask set inside a hot water bath. An adapter connecting a glass tube to the reaction vessel was connected to a gas collection tube that was filled with warm water

A germanium crystal Hellma Analytics ATR-flow cell was employed in the evaluation of the decarboxylation of ethyl acetoacetate. The vessel containing the reaction was a glass jar with the lid fitted to the stainless-steel tubes connected to the inlet

and outlet of the flow cell with Swagelok® fittings (as shown in Figure 3.5 above). The vessel containing the reaction was put into a water bath with a hot plate to allow the reaction to be evaluated at multiple temperatures. The reaction was also investigated at multiple pH values over a three to four-hour period.

An analysis of seltzer water was completed by pumping the solution through the MB-FTIR to determine the different peaks that are present with the dissolved carbon dioxide on the infrared spectrum. Seltzer water was chilled in a refrigerator for at least 24 hours before analysis, this was the only sample prep required for this analysis. Raman spectroscopy was also performed for the seltzer water analysis, to see another type of vibrational spectrum for the compound under analysis. The Raman spectrometer used for the various analyses was a Delta Nu Advantage 200A series spectrometer, shown in Figure 3.10. The Raman spectrometer operated with NuSpec™ software. It had a spectral range of 250-3400 cm^{-1}, a resolution of 10 cm^{-1}, and could obtain the data at 70000 counts per second. A low powered 2 mW 633 nm HeNe laser (633 nm) was used to eliminate fluorescence excited by blue/green laser sources (DeltaNu, 2012).

One advantage of using Raman spectroscopy is the ability to use plastic, glass, or capillary melting point tubes to perform analyses. The Raman spectrometer worked by changing the focal length between the sample in the vial and the laser. This difference in space determined the spectral data produced. The IR multibounce requires approximately 1 mL of sample, and the Raman sample cell/container requires approximately 0.1 mL. The amount of seltzer water required for the analysis with the multi-bounce is approximately 1 mL in volume and for Raman spectroscopy one drop of a liquid compound, both requiring no sample preparation.

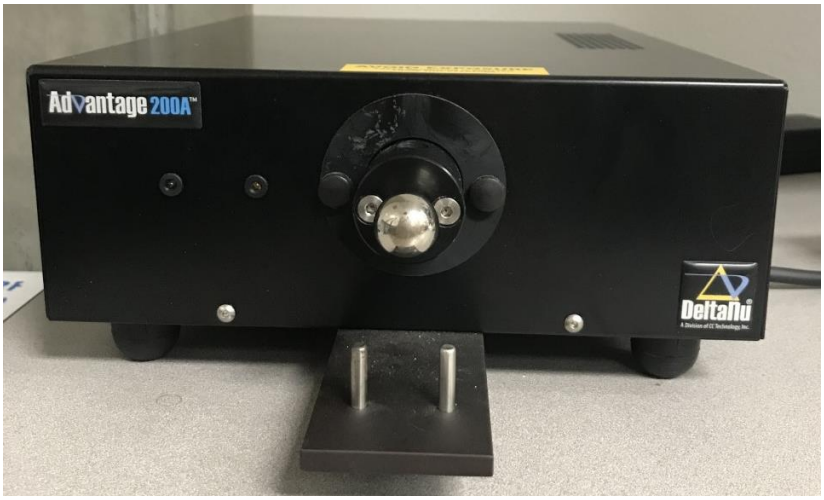

Figure 3.10: Photograph of the DeltaNu Advantage 200A series Raman spectrometer

Ethanol is another product of the reaction with ethyl acetoacetate, so the analysis was performed to ensure the detection of this analyte in the infrared spectrum. Ethanol was first analyzed using the iD5 single bounce FTIR (SB-FTIR). The SB-FTIR reflects IR radiation once off the sample before getting redirected back to the detector. The SB-FTIR is typically used for qualitative analysis. Obtaining quantitative data on the SB-FTIR often requires long acquisition times to increase the signal-to-noise ratio to acceptable levels. The SB-FTIR used in this study contains a single reflection 2 mm crystal made of ZnSe. This allows sample sizes to be as small as a drop.

Quantitative analysis of ethanol was performed using the iD5 attachment (SB-FTIR), as shown in Figure 3.11. Ethanol standards were also analyzed on the MB-FTIR, the Hellma Analytics Ge flow cell, the Raman spectrometer and on a different FTIR (iS50 FTIR) using different quantities of aqueous ethanol solutions. The Nicolet™ iS50 FTIR Spectrometer from Thermo Fisher is shown in Figure 3.12. It contains a liquid nitrogen cooled monothioglycerol (MTG) detector, an automated beam splitter exchanger, an HeNe laser, dual-source capable, a spectral range of 15-27,000 cm^{-1}, the

Polaris™ long-life IR source, a Tungsten-Halogen white light source, a port for collimated or focused emissions, and the ability to add other attachments for modification (Nicolet™ iS50, n.d.).

Figure 3.11: Photograph of iD5 SB-FTIR attachment for the iS5 Nicolet™ FTIR

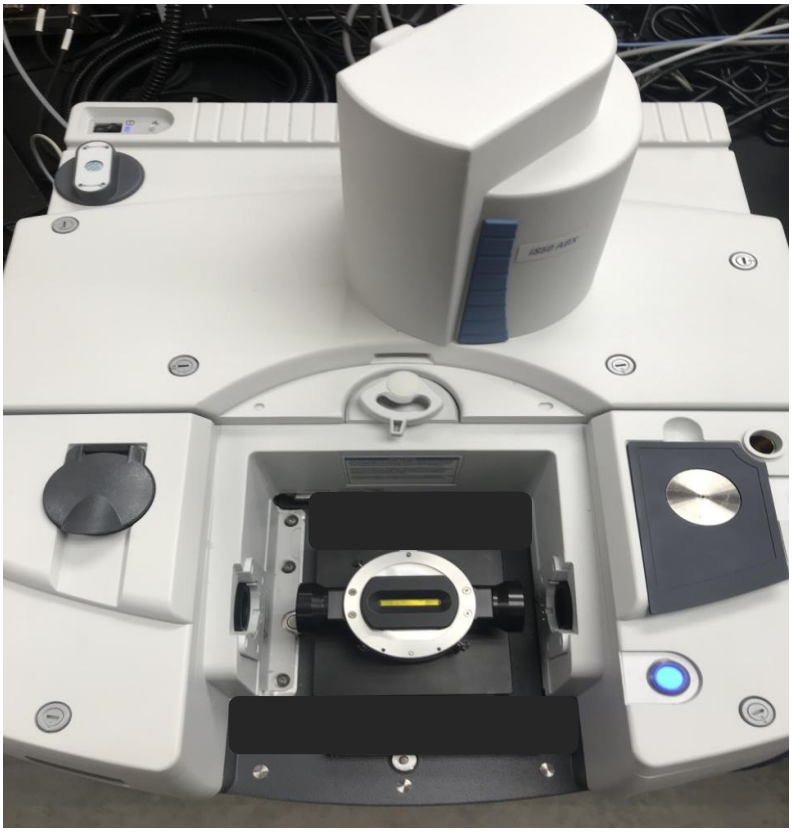

Figure 3.12: Photograph of iS50 FTIR from Thermo Fisher

An IR spectrum of beer was obtained to evaluate the spectrum for analyte detection. An American amber ale, an Oktoberfest/Märzen, a Saison, and a double India pale ale (IPA) were obtained for this analysis. Beer samples were placed on the MB-FTIR trough and compared against a standard ethanol curve obtained on the MB-FTIR. A coffee stout, American lager, a lemon radler, a dry-hopped cider, a rye pale ale, a double IPA, and a nitro milk stout were analyzed using the MB-FTIR to determine their percent alcohol by weight (%ABW). Four beers purchased from a grocery store were analyzed by SB-FTIR using absorbance values to the corresponding wavenumbers. The same four beers were purchased from at a liquor store and were compared with the same four beers purchased at the grocery store. The analysis comparing these eight beers in total was

performed when the Colorado liquor law only allowed grocery stores to sell 3.2 %ABW beer. This law was terminated on January 1, 2019, allowing grocery stores to sell full-strength beer. The absorbance values of the beer samples were then compared to the standard ethanol curve made with the SB-FTIR, on the same day. Five different types of beer and hard liquor were analyzed for their ethanol concentrations using the MB-FTIR. An American light lager was spiked with different amounts of ethanol to determine if there were any interferences from beer.

To explore the effect of the matrix on the evaluation of ethanol and other analytes, wort and fermenting wort were modeled by the preparation of three different concentrations/specific gravities of Munton's dry Spraymalt light malt and/or ethanol in distilled water. These model systems were evaluated to determine if there any interferences existed during fermentation.

The specific gravity of each wort solution was determined by comparison to measured refractive index values. Specific gravity is the ratio of the density of a sample to the density of water. The specific gravity for each wort solution was calculated by obtaining the refractive index of the wort using a Bausch & Lomb ABBE-3L refractometer, shown in Figure 3.13, and comparing the result to a table that correlates refractive index and specific gravity (Science History Institute, 1950). Alternatively, the density could be compared using a pycnometer.

Figure 3.13: Photograph of the Bausch & Lomb ABBE-3L refractometer used to determine the refractive index and ultimately obtain the specific gravity of the wort solutions

An analysis to determine if there is an interference in the IR spectrum in wort throughout fermentation was performed. The wort solution was spiked with increasing ethanol concentrations to show the growth of ethanol as it increased with each sample and to show no interferences in the IR spectrum for ethanol detection. Each concentration of wort was evaluated with the addition of 10 mL of ethanol (approximately 4.7 %ABV) for comparison across the difference in wort concentration. The wort solutions were prepared by making stock solutions of dry malt extract in water. The specific gravities were determined by pycnometer and hydrometer measurements. Three wort

concentrations were prepared and analyzed for interferences in the IR spectrum. Half of the wort samples were spiked with Red Star® active dry yeast to mimic a brewery fermentation. The amount of yeast used was calculated by a standard yeast addition used in home brewing (9.5 grams of yeast/5.5 gallons of wort).

Outside of the solutions described above, other types of solutions were obtained for further infrared analyses on specific analytes. Diacetyl, one of the products formed in the decomposition of α-acetolactate was used to make standard solutions for analysis on the MB-FTIR. Concentrations ranging between 1% and 5% diacetyl were prepared by diluting the corresponding amount of diacetyl to a 10 mL volumetric flask with D.I. water. The diacetyl solutions were also evaluated on the iS50 FTIR.

Acetone is another product formed in the reaction with ethyl acetoacetate. Acetone standard solutions were prepared for analysis on the MB-FTIR and SB-FTIR in concentrations between 1% and 10%. They were prepared by adding the corresponding volumes of acetone to a 10 mL volumetric flask and diluting with D.I. water.

Acetaldehyde is a product formed by yeast and acetic acid bacteria. The *Acetobacter* class of bacteria produces acetaldehyde by oxidizing ethanol. The amount of acetaldehyde produced by yeast varies with species of the yeast, however, it is a by-product of the alcoholic fermentation (Thomas, 2004). Acetaldehyde standard solutions were analyzed on the MB-FTIR at concentrations ranging between 1% and 20%.

Carbon dioxide in packaged beer was also analyzed. Package carbon dioxide measurements were taken at Crabtree Brewing Company (Greeley, CO) using a Zahm and Nagel CO_2 piercing device, shown in Figure 3.14. This device allows measurement of the volumes of CO_2 that exist in each bottle by comparing the pressure and

temperature of the gas above the liquid with known values. The values recorded from the CO_2 piercer are the pressure in psi (pounds per square inch) and temperature in °F (Figure 3.15). Those data could be compared to the dissolved levels of CO_2 in the beer using the MB-FTIR. The samples evaluated included an extra pale ale, a pale ale, a dry-hopped porter, a wheat/blonde ale, an amber ale, a fruited sour ale, seltzer water, and tonic water.

Figure 3.14: Photograph of a Zahm and Nagel CO_2 piercing device (Zahm &Nagel, n.d.)

TEMPERATURE DEGREES FAHRENHEIT

	0	2	4	6	8	10	12	14	16	18	20	22	24	26	28
32°	1.71	1.9	2.2	2.4	2.6	2.9	3.1	3.3	3.5	3.8	4.0	4.2	4.4	4.7	4.9
33	1.68	1.9	2.1	2.4	2.6	2.8	3.0	3.2	3.5	3.7	3.9	4.1	4.3	4.6	4.8
34	1.64	1.9	2.1	2.3	2.5	2.7	2.9	3.2	3.4	3.6	3.8	4.1	4.3	4.5	4.7
35	1.61	1.8	2.0	2.3	2.5	2.7	2.9	3.1	3.3	3.5	3.8	4.0	4.2	4.4	4.6
36	1.57	1.8	2.0	2.2	2.4	2.6	2.8	3.0	3.3	3.5	3.7	3.9	4.1	4.3	4.5
37	1.54	1.7	2.0	2.2	2.4	2.6	2.8	3.0	3.2	3.4	3.6	3.8	4.0	4.2	4.4
38	1.51	1.7	1.9	2.1	2.3	2.5	2.7	2.9	3.1	3.3	3.5	3.7	3.9	4.1	4.3
39	1.47	1.7	1.9	2.1	2.3	2.5	2.7	2.9	3.1	3.3	3.5	3.7	3.9	4.0	4.3
40°	1.45	1.6	1.8	2.0	2.2	2.4	2.6	2.8	3.0	3.2	3.4	3.6	3.8	4.0	4.2
41	1.42	1.6	1.8	2.0	2.2	2.4	2.6	2.8	2.9	3.1	3.3	3.5	3.7	3.9	4.1
42	1.40	1.6	1.8	2.0	2.1	2.3	2.6	2.8	2.9	3.1	3.3	3.5	3.6	3.8	4.0
43	1.37	1.6	1.7	1.9	2.1	2.3	2.5	2.7	2.8	3.0	3.2	3.4	3.6	3.8	3.9
44	1.35	1.5	1.7	1.9	2.1	2.2	2.4	2.6	2.8	3.0	3.1	3.3	3.5	3.7	3.9
45	1.32	1.5	1.7	1.8	2.0	2.2	2.4	2.5	2.7	2.9	3.1	3.3	3.4	3.6	3.8
46	1.29	1.5	1.6	1.8	2.0	2.2	2.3	2.5	2.7	2.8	3.0	3.2	3.4	3.5	3.7
47	1.26	1.4	1.6	1.8	1.9	2.1	2.3	2.4	2.6	2.8	2.9	3.1	3.3	3.5	3.6
48	1.24	1.4	1.6	1.7	1.9	2.1	2.2	2.4	2.6	2.7	2.9	3.1	3.2	3.4	3.6
49	1.21	1.4	1.5	1.7	1.9	2.0	2.2	2.4	2.5	2.7	2.8	3.0	3.2	3.3	3.5
50°	1.19	1.4	1.5	1.7	1.8	2.0	2.2	2.3	2.5	2.6	2.8	2.9	3.1	3.3	3.4
51	1.17	1.3	1.5	1.6	1.8	2.0	2.1	2.3	2.4	2.6	2.7	2.9	3.1	3.2	3.4
52	1.15	1.3	1.5	1.6	1.8	1.9	2.1	2.2	2.4	2.5	2.7	2.8	3.0	3.2	3.3
53	1.13	1.3	1.4	1.6	1.7	1.9	2.0	2.2	2.3	2.5	2.6	2.8	2.9	3.1	3.3
54	1.11	1.3	1.4	1.6	1.7	1.9	2.0	2.2	2.3	2.4	2.6	2.7	2.9	3.0	3.2
55	1.10	1.2	1.4	1.5	1.7	1.8	2.0	2.1	2.3	2.4	2.6	2.7	2.8	3.0	3.1
56	1.08	1.2	1.4	1.5	1.6	1.8	1.9	2.1	2.2	2.4	2.5	2.6	2.8	2.9	3.1
57	1.06	1.2	1.3	1.5	1.6	1.8	1.9	2.0	2.2	2.3	2.5	2.6	2.7	2.9	3.0
58	1.04	1.2	1.3	1.5	1.6	1.7	1.9	2.0	2.1	2.3	2.4	2.6	2.7	2.8	3.0
59	1.02	1.2	1.3	1.4	1.6	1.7	1.8	2.0	2.1	2.2	2.4	2.5	2.7	2.8	2.9
60°	1.00	1.1	1.3	1.4	1.5	1.7	1.8	1.9	2.1	2.2	2.3	2.5	2.6	2.7	2.9
61	0.98	1.1	1.2	1.4	1.5	1.6	1.8	1.9	2.0	2.2	2.3	2.4	2.6	2.7	2.8
62	0.97	1.1	1.2	1.4	1.5	1.6	1.7	1.9	2.0	2.1	2.3	2.4	2.5	2.6	2.8
63	0.95	1.1	1.2	1.3	1.5	1.6	1.7	1.8	2.0	2.1	2.2	2.4	2.5	2.6	2.7
64	0.93	1.1	1.2	1.3	1.4	1.6	1.7	1.8	1.9	2.1	2.2	2.3	2.4	2.6	2.7
65	0.92	1.1	1.2	1.3	1.4	1.5	1.7	1.8	1.9	2.0	2.2	2.3	2.4	2.5	2.6
66	0.90	1.0	1.2	1.3	1.4	1.5	1.6	1.8	1.9	2.0	2.1	2.2	2.4	2.5	2.6
67	0.89	1.0	1.1	1.2	1.4	1.5	1.6	1.7	1.8	2.0	2.1	2.2	2.3	2.4	2.6
68	0.88	1.0	1.1	1.2	1.3	1.5	1.6	1.7	1.8	1.9	2.0	2.2	2.3	2.4	2.5
69	0.86	1.0	1.1	1.2	1.3	1.4	1.5	1.6	1.8	1.9	2.0	2.1	2.2	2.4	2.5
70°	0.85	1.0	1.1	1.2	1.3	1.4	1.5	1.6	1.7	1.9	2.0	2.1	2.2	2.3	2.4
71	0.84	0.9	1.1	1.2	1.3	1.4	1.5	1.6	1.7	1.8	1.9	2.1	2.2	2.3	2.4
72	0.83	0.9	1.0	1.2	1.3	1.4	1.5	1.6	1.7	1.8	1.9	2.0	2.1	2.2	2.4
73	0.81	0.9	1.0	1.1	1.2	1.4	1.5	1.6	1.7	1.8	1.9	2.0	2.1	2.2	2.3
74	0.79	0.9	1.0	1.1	1.2	1.3	1.4	1.5	1.6	1.8	1.9	2.0	2.1	2.2	2.3
75	0.78	0.9	1.0	1.1	1.2	1.3	1.4	1.5	1.6	1.7	1.8	1.9	2.0	2.2	2.3
76	0.77	0.9	1.0	1.1	1.2	1.3	1.4	1.5	1.6	1.7	1.8	1.9	2.0	2.1	2.2
77	0.76	0.9	1.0	1.1	1.2	1.3	1.4	1.5	1.6	1.7	1.8	1.9	2.0	2.1	2.2
78	0.75	0.9	0.9	1.0	1.1	1.2	1.3	1.4	1.5	1.6	1.7	1.9	2.0	2.1	2.2
79	0.75	0.8	0.9	1.0	1.1	1.2	1.3	1.4	1.5	1.6	1.7	1.8	1.9	2.0	2.1
80°	0.73	0.8	0.9	1.0	1.1	1.2	1.3	1.4	1.5	1.6	1.7	1.8	1.9	2.0	2.1
81	0.72	0.8	0.9	1.0	1.1	1.2	1.3	1.4	1.5	1.6	1.7	1.8	1.9	2.0	2.1
82	0.71	0.8	0.9	1.0	1.1	1.2	1.3	1.4	1.5	1.6	1.6	1.7	1.8	1.9	2.0
83	0.70	0.8	0.9	1.0	1.1	1.2	1.3	1.4	1.4	1.5	1.6	1.7	1.8	1.9	2.0
84	0.69	0.8	0.9	1.0	1.0	1.1	1.2	1.4	1.4	1.5	1.6	1.7	1.8	1.9	2.0
85	0.68	0.8	0.9	0.9	1.0	1.1	1.2	1.3	1.4	1.5	1.6	1.7	1.8	1.9	1.9
86	0.67	0.8	0.8	0.9	1.0	1.1	1.2	1.3	1.4	1.5	1.5	1.6	1.7	1.8	1.9
87	0.66	0.7	0.8	0.9	1.0	1.1	1.2	1.3	1.4	1.4	1.5	1.6	1.7	1.8	1.9
88	0.65	0.7	0.8	0.9	1.0	1.1	1.2	1.2	1.4	1.4	1.5	1.6	1.7	1.8	1.9
89	0.64	0.7	0.8	0.9	1.0	1.1	1.1	1.2	1.3	1.4	1.5	1.6	1.7	1.7	1.8

PRESSURE PER SQUARE INCH

Figure 3.15: Diagram using pressure and temperature and giving the volumes of CO_2 measured in the bottle of a carbonated aqueous solution (Zahm & Nagel, n.d.)

In summary, an analysis to detect diacetyl by using its counterpart, CO_2 was explored. Since there is a one to the one-mole relationship between diacetyl and CO_2 in the oxidative decarboxylation of α-acetolactate, the concentration of α-acetolactate can be determined by measurement of the concentration of CO_2. IR spectroscopy is a rapid analytical technique that can be used to quantify the concentration of CO_2. IR spectroscopy determines the vibration of molecules and their dipole moments to define the functional groups in the analyzed sample. Raman spectroscopy, another type of vibrational spectroscopy, results from the change of the polarizability of a molecule. Performing IR and Raman spectroscopy gives us a full view of vibrational spectroscopic analytical techniques in order to fully understand the sample being analyzed.

CHAPTER IV

RESULTS AND DISCUSSION

A series of analytes were evaluated with various techniques in an effort to develop a method to determine the concentration of diacetyl (and other fermentation products) during beer production. Because carbon dioxide has a 1:1 stoichiometric relationship with diacetyl, we sought to create a new method to detect CO_2 using FTIR. FTIR was chosen as the method because it would be a more-rapid, less-expensive, and comparably sensitive analytical technique to measure diacetyl concentration. As a model of the fermentation system, we chose to explore the reaction of ethyl acetoacetate. The reaction of ethyl acetoacetate generates CO_2 in a two-step process, the first being the deesterification of ethyl acetoacetate and the second being the decarboxylation of the resulting ß-oxoacid.

The mechanism in Figure 4.1 shows the deesterification of ethyl acetoacetate in five steps. All but the second step in this mechanism are fast. The second step is the rate-determining step that utilizes two reactants, giving us a second-order reaction. This reaction can be made to behave in a pseudo-first-order fashion if the concentrations of reactants are well-chosen.

Carbon dioxide is a product of the reaction of acetoacetic acid (the product of the deesterification reaction), as seen in the mechanism in Figure 4.2. The rate of the decarboxylation of acetoacetic acid is fast compared to the deesterification reaction. The investigation of the decarboxylation reaction with ethyl acetoacetate made it possible to

compare this reaction to that of the oxidative decarboxylation reaction of α-acetolactate in fermentation.

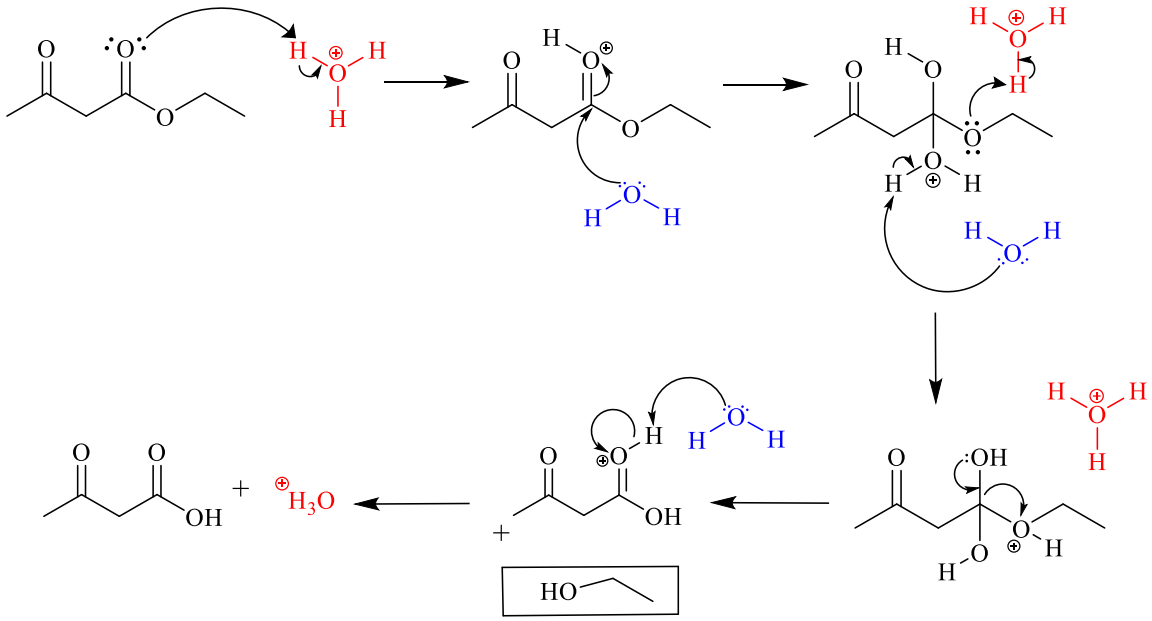

Figure 4.1: Mechanism for the first of two reactions for the deesterification reaction of ethyl acetoacetate in acidic conditions

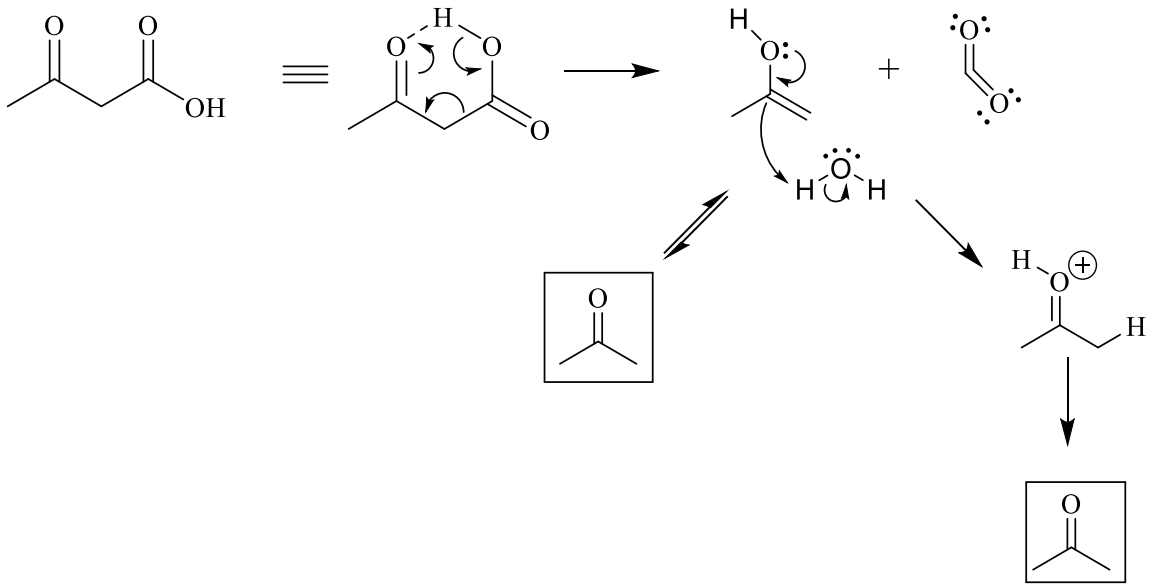

Figure 4.2: Mechanism for the second of two reactions for the decarboxylation reaction of ethyl acetoacetate in acidic conditions

Carbon Dioxide as an Analyte

The analysis of the method began with the evaluation of a readily available source of dissolved CO_2, seltzer water. Seltzer water was chilled in a refrigerator for a minimum of 24 hours to get as much CO_2 dissolved in solution as possible. Seltzer water was analyzed using MB-FTIR by pouring samples directly onto the ZnSe crystal-trough. The IR spectrum showed absorbance $\tilde{\upsilon}$ ~2348 cm^{-1} (the asymmetric stretch of the CO_2), as shown in Figure 4.3. This same seltzer water was analyzed using the Zahm and Nagel CO_2 Piercer, determining that the seltzer water has 1.5 volumes of CO_2. This was determined to be equivalent to 2900 ppm using the pressure and temperature and the plot in Figure 3.15. A set of standards was not obtained due to the difficulty in preparing CO_2 solutions of known concentration. But, based upon 2900 ppm in our standard solution, the limit of detection (LOD) and the limit of quantification (LOQ) were determined to be 73 ppm and 240 ppm respectively.

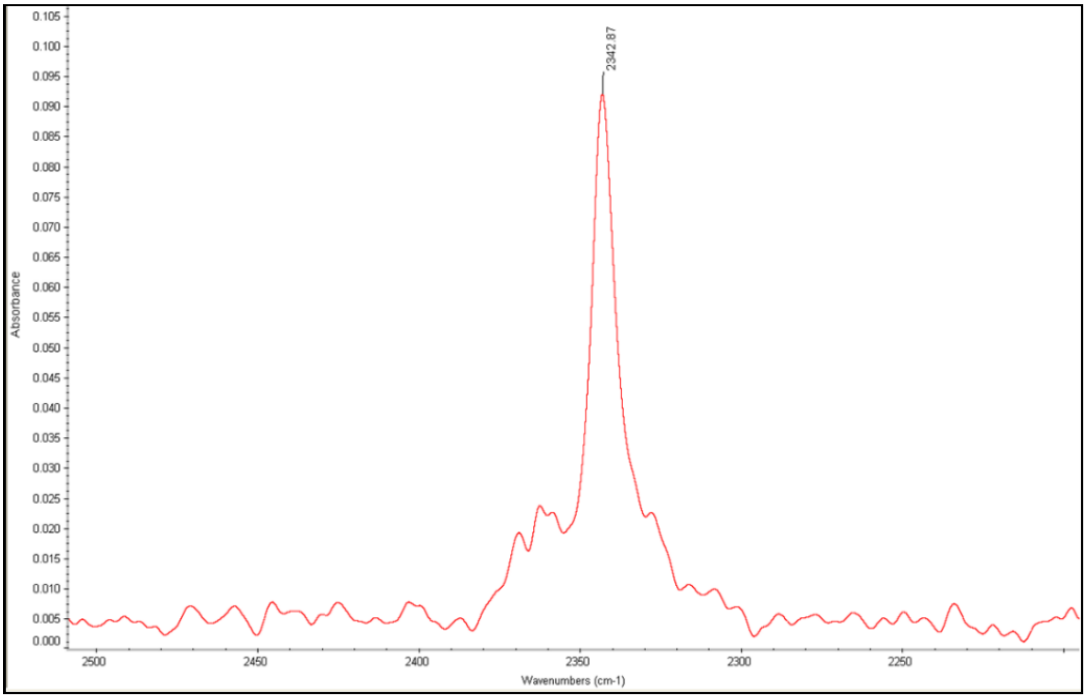

Figure 4.3: IR spectrum of chilled seltzer water to analyze CO_2 asymmetric stretch at $\tilde{\upsilon}$ = 2342.8 cm^{-1}, corresponding to 2900 ppm of CO_2

The seltzer water was then analyzed using the Ge flow cell, to determine if the solution could be detected in a flow-based setup. The seltzer water was chilled for a minimum of 24 hours in a refrigerator before use. Table 4.1 shows the absorbance and area of the maximum signal that was obtained over a 34-minute period. There is a lot of variability in the measurement in this system as evidenced by the changing absorbance and peak area values. According to the Beer-Lambert Law, this implies that the concentration of CO_2 is varying over time due to temperature, pressure, or pathlength fluctuations. Spectral data can be found in the Appendix.

Table 4.1: Seltzer water analysis in the Ge flow cell at 23 ℃ over time

Seltzer Water @ 23℃	$\tilde{\upsilon}_{max}$ (cm^{-1})	A_{max}	$Area_{max}$
0 min	2364.9	0.0330	0.2889
4 min	2360.2	0.0507	0.3866
22 min	2363.5	0.0334	0.2261
33 min	2362.2	0.0661	0.5951
34 min	2361.4	0.0374	0.3303

Fevertree® tonic water, similar to seltzer water but containing quinine, was analyzed using an iS50 FTIR, to see if dissolved CO_2 could be detected with a more sensitive detector. The tonic water was chilled for a minimum of 24 hours and poured directly onto the ZnSe crystal for analysis. The asymmetric C-O stretch was seen at approximately $\tilde{\upsilon}$ ~2343 cm^{-1}. The absorbance bands were compared to data obtained using the Zahm and Nagel CO_2 piercer. The data collected from the CO_2 piercer for two trials gave 2.60 volumes of CO_2, corresponding to 5120 ppm and 2.92 volumes of CO_2, corresponding to 5750 ppm. This analysis was performed with tonic water due to not having any seltzer water in stock when we had access to this instrument. Spectral data and the resulting standard curve can be seen in the Appendix.

The seltzer water was also analyzed using the Raman Spectrometer to determine if the Raman active vibrational mode of CO_2, the symmetric stretch could be detected. The seltzer water was chilled for at least 24 hours in a refrigerator and poured into 1 mL glass vials. The focal length of the sample was changed throughout the four trials to determine the best signal. All four trials showed a large signal to noise ratio, meaning there was a lack of distinctive peaks/signals detected. The low powered laser of our instrument is likely cannot detect the small signals due to the level of noise. We hypothesized that a higher-powered laser could amplify the signals enough to detect CO_2 signals in the Raman spectrum.

Carbon dioxide concentrations were determined in beer solutions to determine if anything in the matrix would interfere with CO_2 detection. Samples of wort were taken from a porter during fermentation vessel and chilled in an ice bath. The samples were contained in screw-cap vials and brought to the MB-FTIR for analysis. Half of the samples taken at the same time stayed in the ice bath and the other half was put into a hot water bath at 100 ℃ for about 10 minutes and then chilled in an ice bath for 24 hours. This was performed to determine if the CO_2 levels would dissolve more readily in chilled solutions versus heated ones. The samples were analyzed on the MB-FTIR for the dissolved CO_2 concentration. We predicted that the solutions that were heated would produce more CO_2 due to the increase in gas formation and after cooling the solutions, more CO_2 would be dissolved in solution. The results of this analysis are shown in Figure 4.4. These results showed many inconsistencies, most likely due to the screw-cap vials possibly allowing CO_2 to escape. A similar analysis was completed at a local brewery, Weldwerks Brewing Company in Greeley, Colorado, by removing samples of wort

throughout an active fermentation over a 43-hour period. Each analysis showed results that were very similar to those produced in the lab. The heated solutions had consistently higher CO_2 absorption values, meaning that these solutions lost their dissolved CO_2 faster than the chilled beer. The data are located in the Appendix.

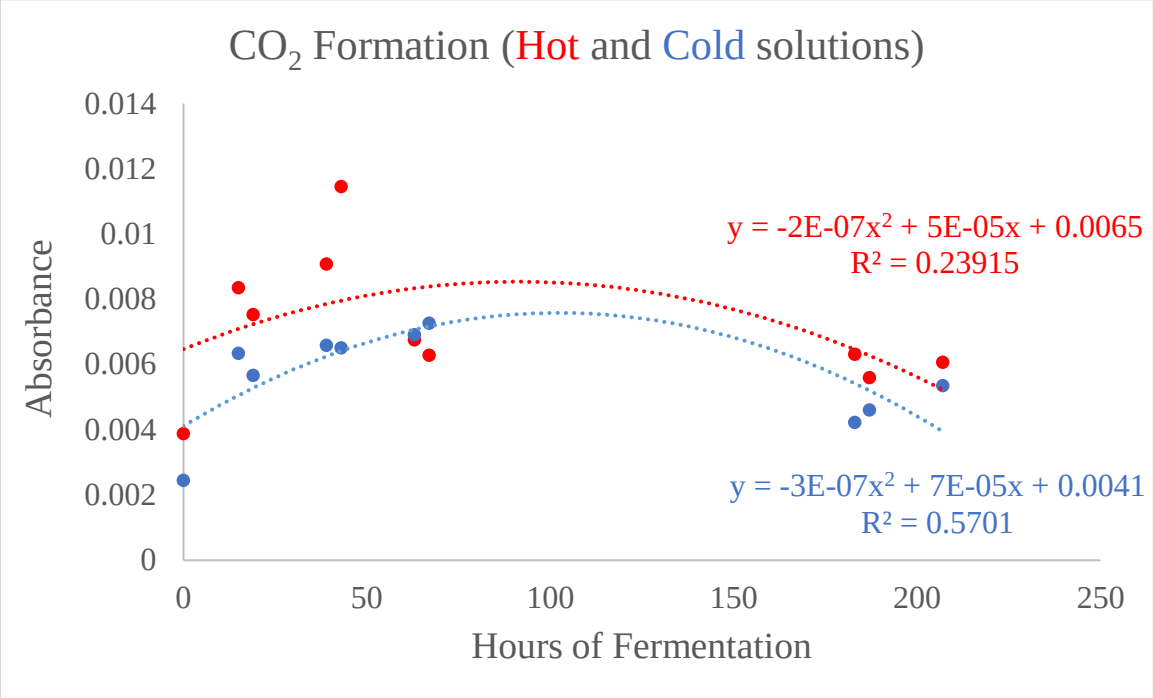

Figure 4.4: Plot showing the results of cooled and heated solutions of wort throughout fermentation using peak height

The total package carbon dioxide concentration was analyzed in commercially obtained beer. The results of the MB-FTIR analysis were compared to the data obtained using the Zahm and Nagel CO_2 piercer. A dry-hopped porter, a pale ale, an extra pale ale, a Belgian-style sour ale, and a strawberry blonde were analyzed (Table 4.2). It was determined that the Belgian style sour was over-carbonated due to gushing that occurred when the bottles were opened normally. The high level of carbonation was observed during the analysis as well. The other beers were analyzed at similar temperatures. Because each was packaged at different pressures the analysis revealed different CO_2

concentrations. The table also shows that this measurement is not dependent upon the style of beer. The packaged CO_2 concentration is only dependent upon the brewery's decision, not on the particular style of beer. The average absorbance values were taken over three different trials.

Table 4.2. Beer styles and their CO_2 concentrations. Belgian style sour was not refrigerated for a 24-hour minimum like the others, $\tilde{\upsilon}$ = 2342.4 cm^{-1}

Beer Style	Temperature (°F)	Pressure (psi)	Average Absorbance	[CO_2] (ppm)
Dry hopped porter	45	18.5	0.154	5543
Pale Ale	43	17	0.143	5474
Extra Pale Ale	45.2	20.1	0.182	5789
Belgian style Sour	76	50	0.305	6281
Strawberry Blonde	43	14.3	0.154	5218

The proposed mechanism shown in Figure 4.1, is of a reaction of ethyl acetoacetate, like α-acetolactate, producing ethanol, acetone, and CO_2. We performed this reaction to evaluate dissolved CO_2 as a function of time, to mimic a fermentation. We assumed that the reaction produced CO_2, in a reasonable timeframe, but performed the reaction using a bubble collection analysis to confirm that fact. The bubble analysis consisted of putting the reaction of ethyl acetoacetate, D.I. water, and 200 proof ethanol into a sample container in a hot water bath. The reaction was performed over three trials at three different temperatures: 323.15 K, 333.15 K, and 343.15 K. The average volume of CO_2 collected was approximately 3.00 mL. The reaction at 341.15 K produced more CO_2 more rapidly than the trials at 333.15 K and 323.15 K. The activation energy was determined to be 54.1 kJ/mol, as we are predicting that the reaction rate is pseudo-first-order, determined by an Arrhenius plot (ln(k) vs 1/T) as shown in Figure 4.5 and ruling out zero-order based on the mechanism.

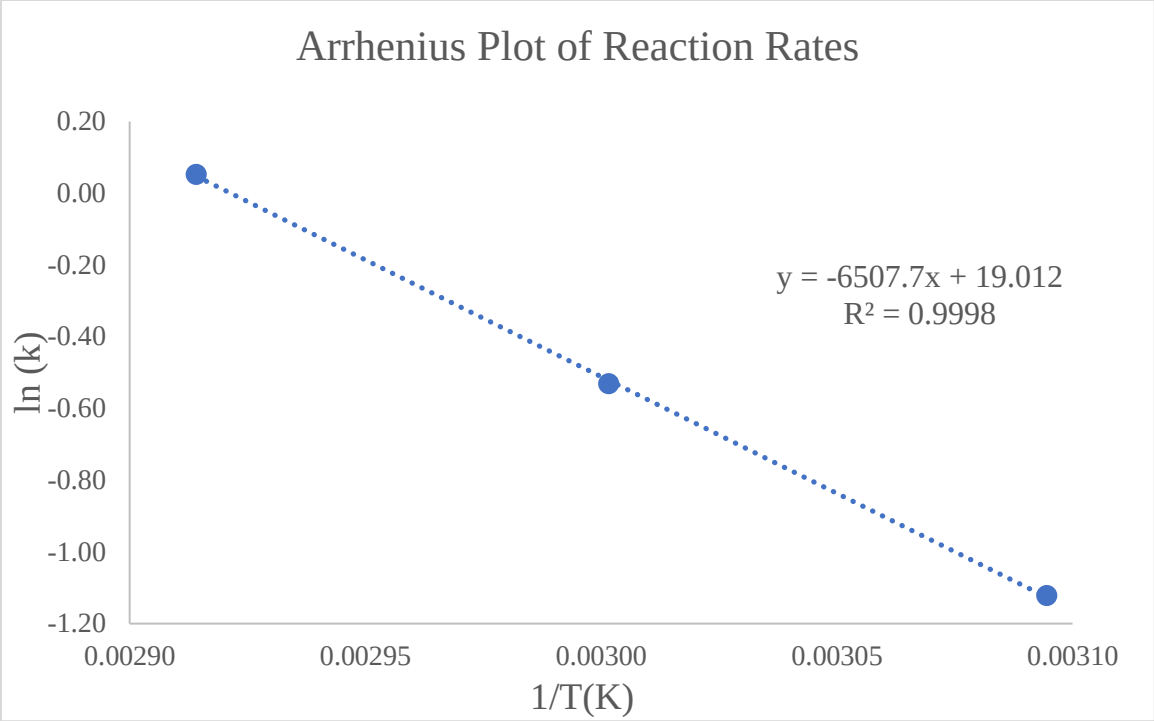

Figure 4.5: Arrhenius plot for the decarboxylation reaction obtained from the bubble analysis

The desertification/decarboxylation reactions of ethyl acetoacetate were analyzed using the MB-FTIR, the Ge flow cell, and the iS50 FTIR. In the MB-FTIR method, carbon dioxide was analyzed at different time intervals, temperatures, and pH values ranging from 4 to 6. The conditions were chosen to imitate the conditions that are typical in a fermentation vessel. Each trial was conducted by placing the reaction into screwcap vials and heating the vials in a hot water bath at temperatures varying from 40 °C to 80 °C (Figure 4.6). The vials were then removed from the hot water bath and cooled in ice for up to 4 hours to dissolve the carbon dioxide. The results of the analysis at 65 °C are shown in Figure 4.7. Absorbance values in the plot were taken at $\tilde{\upsilon}$ = 2348.4 cm^{-1}. Figure 4.8 illustrates another trial of CO_2 formation for a three-hour period at 80 °C at $\tilde{\upsilon}$ = 2342.6 cm^{-1}. Spectral data for each trial are shown in the Appendix.

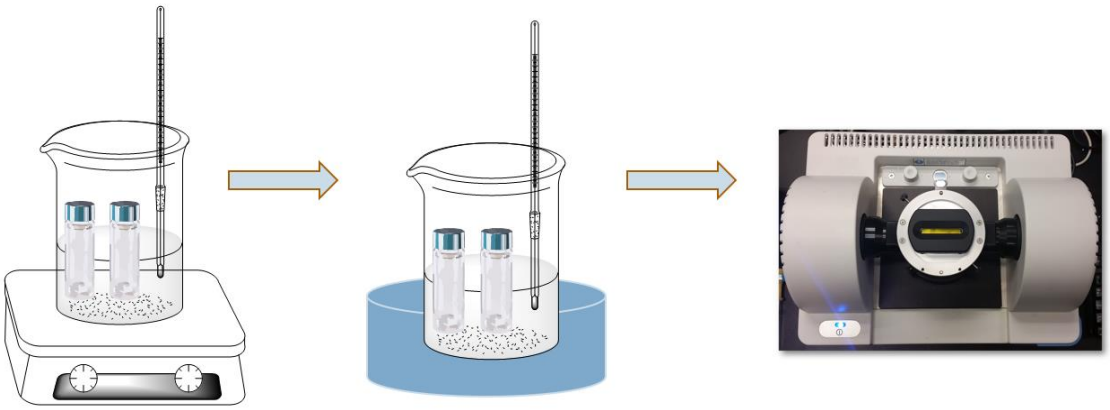

Figure 4.6: CO_2 method diagram for MB-FTIR analysis of reaction with ethyl acetoacetate and the sodium acetate buffer at various temperatures

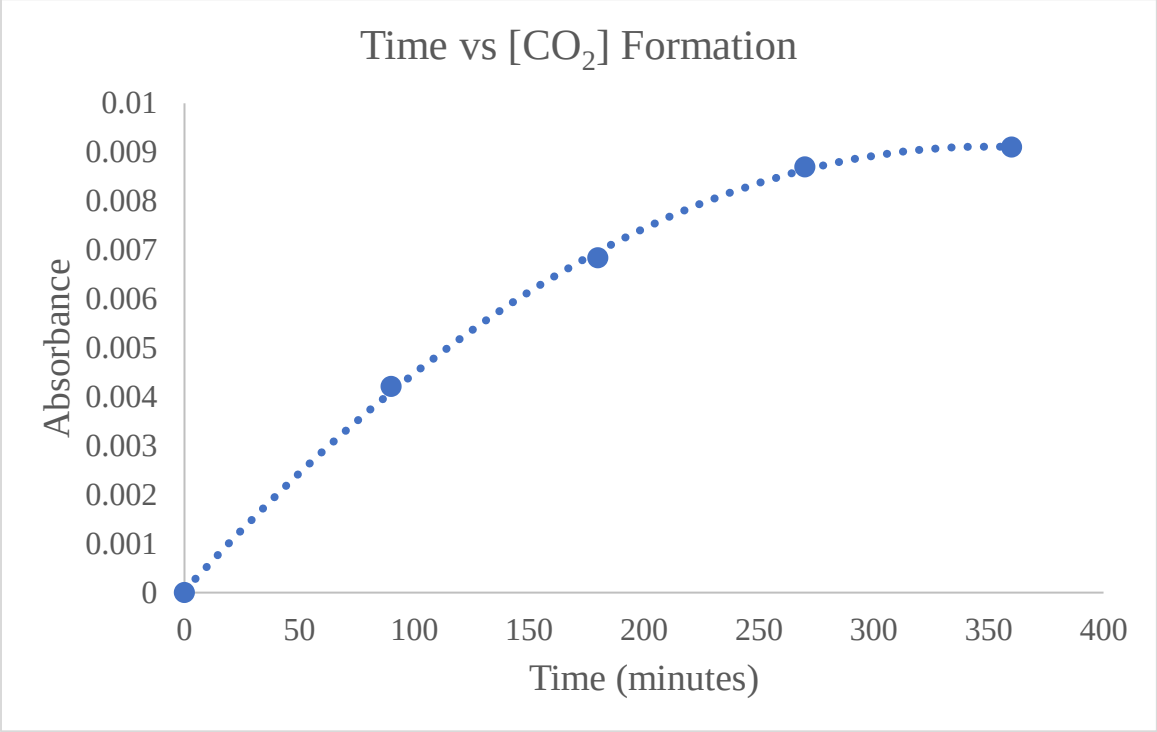

Figure 4.7: Diagram of the amount of CO_2 that was produced over a six-hour period at 65 °C from the MB-FTIR method using peak height

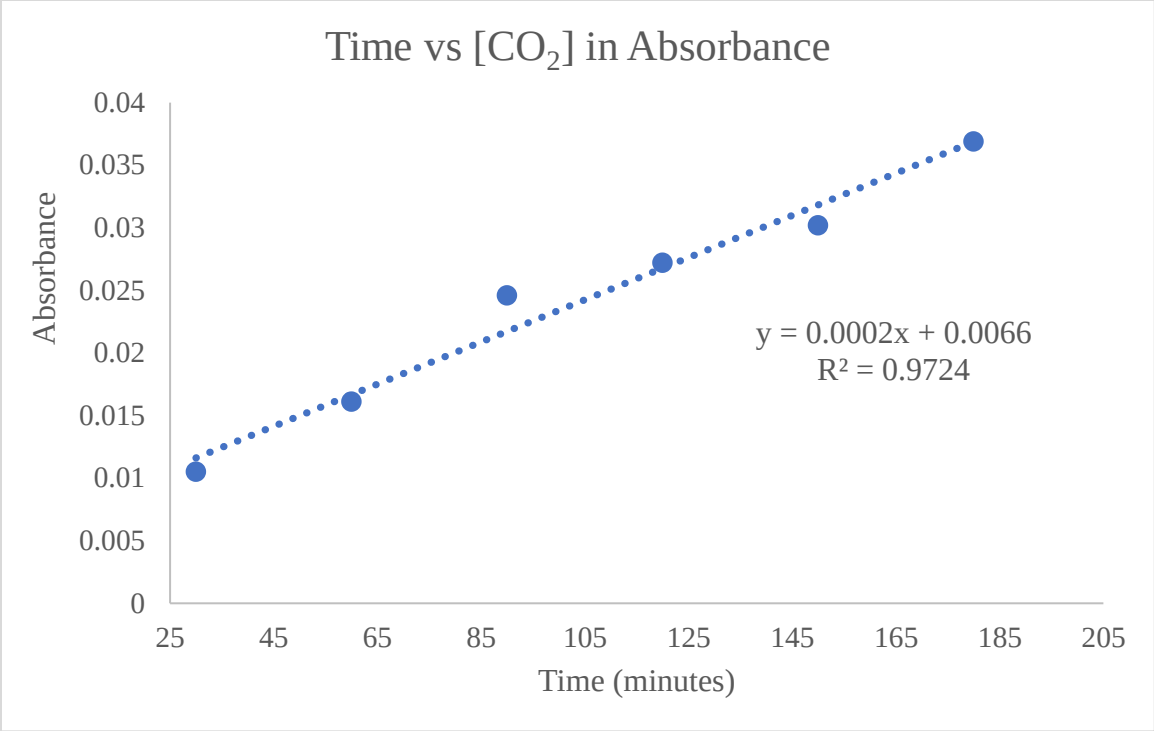

Figure 4.8: Diagram of the amount of CO_2 that was produced over a 3-hour period at 80 °C taken at $\tilde{\upsilon}$ = 2342.6 cm^{-1} from the MB-FTIR method using peak height

The deesterification-decarboxylation reactions of ethyl acetoacetate were analyzed by pumping the reaction mixture through the Ge flow cell. This was performed to determine if results using a flow-based FTIR technique would render similar results to the previous analyses. Multiple trials using different solvents, different temperatures, and different pH values were attempted. The data are collected in Table 4.3. An analysis of the spectra obtained from the reaction in D.I. water and acetonitrile did produce signals around $\tilde{\upsilon}$~1700 cm^{-1} that do not come from interference with the solvents.

Most of the reactions processed through the Ge flow cell did not provide any useful data. Instead, the signal to noise ratio was too small to observe any distinguishable signals. It was determined that a more sensitive detector was required for this analysis. The analysis of the reaction in 85% ethanol showed the largest peak at $\tilde{\upsilon}$ =1048.2 cm^{-1}, this is due to the ethanol, therefore, the peak chosen for the largest peak height was $\tilde{\upsilon}$ =

1738.6 cm^{-1}. The area max for the reaction in 85% ethanol took the ethanol peak into account, as this peak should not have grown or disappeared over time, giving the peak area maximum below.

Table 4.3: Reaction of ethyl acetoacetate with varying solvent, temperature, pH, and reaction times using the Ge flow cell method

Time (min)	Solvent	pH	Temp. (°C)	N_2 purge	$\tilde{\upsilon}_{max\ (}cm^{-1})$	A_{max}	$Area_{max}$
0-120	Sodium acetate	~6	23	N	N/A	N/A	N/A
0-141	Sodium acetate	~6	50	Y	N/A	N/A	N/A
0-120	D.I. water	~6	30, 50, 70	Y	N/A	N/A	N/A
0-120	D.I. water/↑	~6	40, 50	Y	N/A	N/A	N/A
0-120	D.I. water/ Acetonitrile	~6	50, 60, 70	Y	N/A	N/A	N/A
0-200	D.I. water/ Acetonitrile	~5	60	Y	1706.9	0.246	0.141
0-221	D.I. water/ Acetonitrile	~5	70	Y	1703.1	0.192	0.156
0-144	D.I. water/ Acetonitrile	~5	80	Y	1709.6	0.169	0.088
0-216	D.I. water/ Acetonitrile	~5	40	Y	N/A	N/A	N/A
0-75	D.I. water/ Acetonitrile	~5	20	Y	N/A	N/A	N/A
0-230	85% EtOH	~5	30	Y	1738.6	0.412	78.097

N/A = No signal was observed for carbon dioxide

The ethyl acetoacetate reaction was evaluated using the iS50 FTIR to compare these results with more sensitive detectors to the other FTIR analyses. Samples were prepared by adding ethyl acetoacetate to D.I. water. The solutions were poured directly on the ZnSe crystal and analyzed. The IR spectra obtained from the analysis illustrated an absorbance at $\tilde{\upsilon}$ ~1050 cm^{-1}, two large peaks at $\tilde{\upsilon}$~1740-1700 cm^{-1}, another signal at 1300 cm^{-1}, and a multi-peak region between $\tilde{\upsilon}$~1500-1200 cm^{-1} (Figure 4.9). The signal at $\tilde{\upsilon}$ ~1050 cm^{-1} appeared to increase in intensity over the 43-min analysis. No absorbance values consistent with CO_2 signals were observed in the spectrum. This was not unexpected as the iS50 FTIR was not purged of atmospheric CO_2. It is noteworthy that

there is a pH dependence of this reaction. No results could be obtained at pH~6 but some results were obtained at pH ~5.

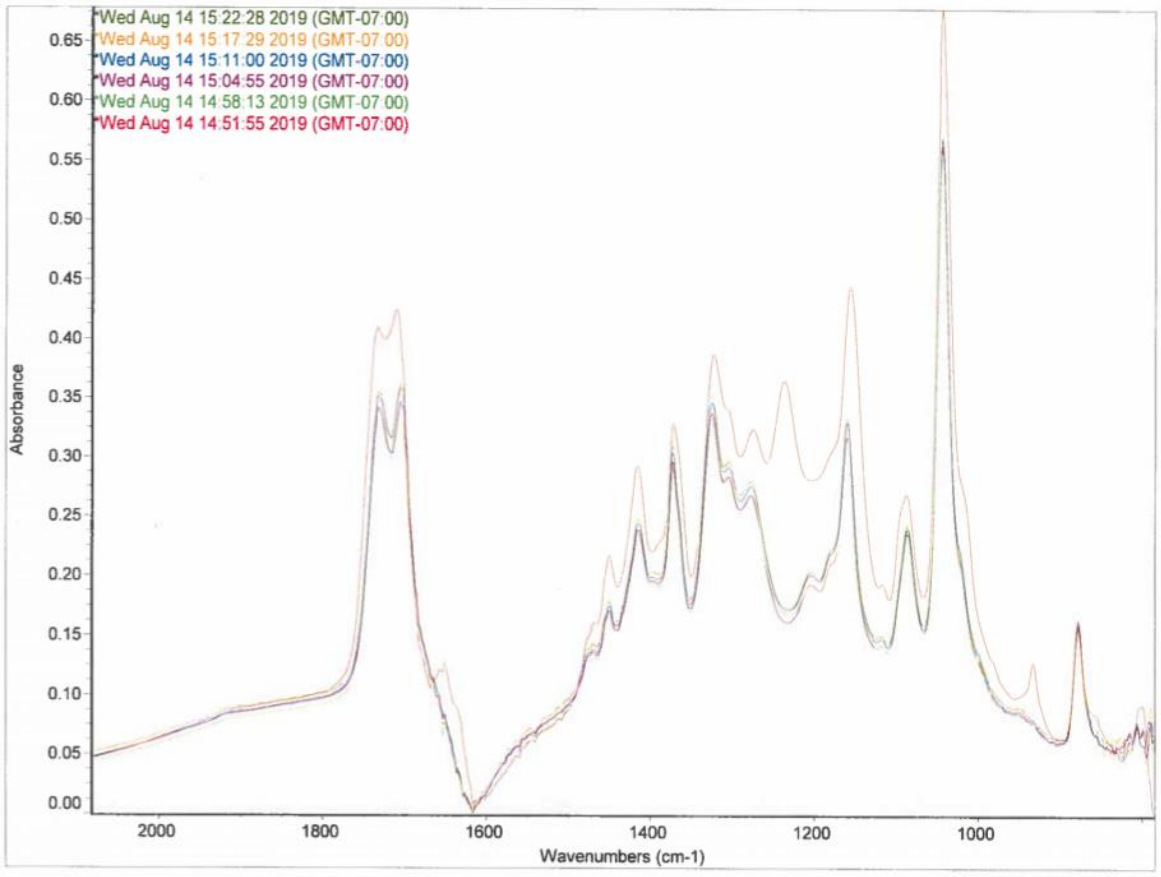

Figure 4.9: IR spectrum of the ethyl acetoacetate reaction using the iS50 FTIR

Ethanol as an Analyte

Ethanol is another product that is formed during the deesterification/ decarboxylation of ethyl acetoacetate. In addition to the use of this analyte for the study of decarboxylation of ethyl esters, ethanol could be a possible analyte for evaluation of the fermentation process or determination of ethanol concentration in finished or packaged beer. The determination of ethanol was accomplished with the SB-FTIR, the MB-FTIR, the iS50 FTIR, the Ge flow cell, and the Raman spectrometer.

Ethanol standards in water were prepared to create a standard curve using the SB-FTIR. Aqueous solutions were made from 0.5% to 20% ethanol by volume using 200 proof ethanol and D.I. water. The concentrations in each standard solution were verified using the refractive index and comparison to the published correlation table (Refractive Index of Ethanol Solutions, 2011). A drop of each solution was then placed on the SB-FTIR crystal and the spectrum obtained. The standard curve created over the average of three trials is seen below in Figure 4.10. The LOD and the LOQ were determined to be 3.40 %ABV and 11.3 %ABV respectively for ethanol. The IR spectra shown in Figure 4.11 illustrates the C-O vibration at $\tilde{\upsilon}$ = 1045.2 cm^{-1} in ethanol.

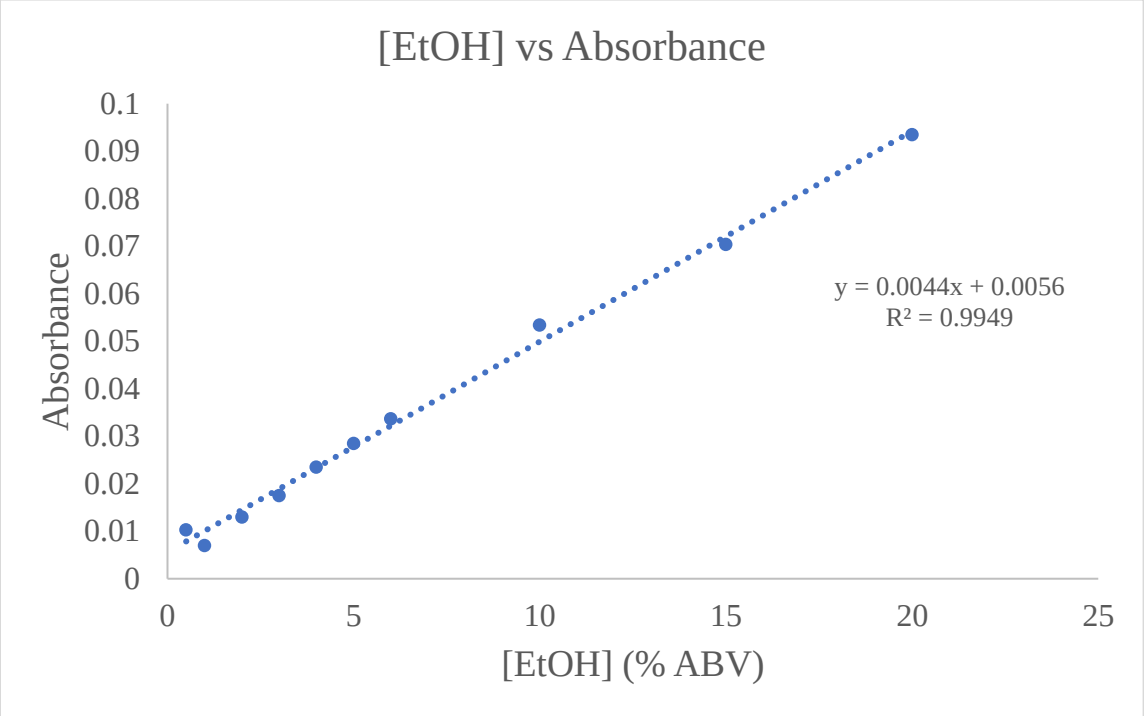

Figure 4.10: Standard curve of ethanol using the SB-FTIR at $\tilde{\upsilon}$ = 1045.2 cm^{-1}

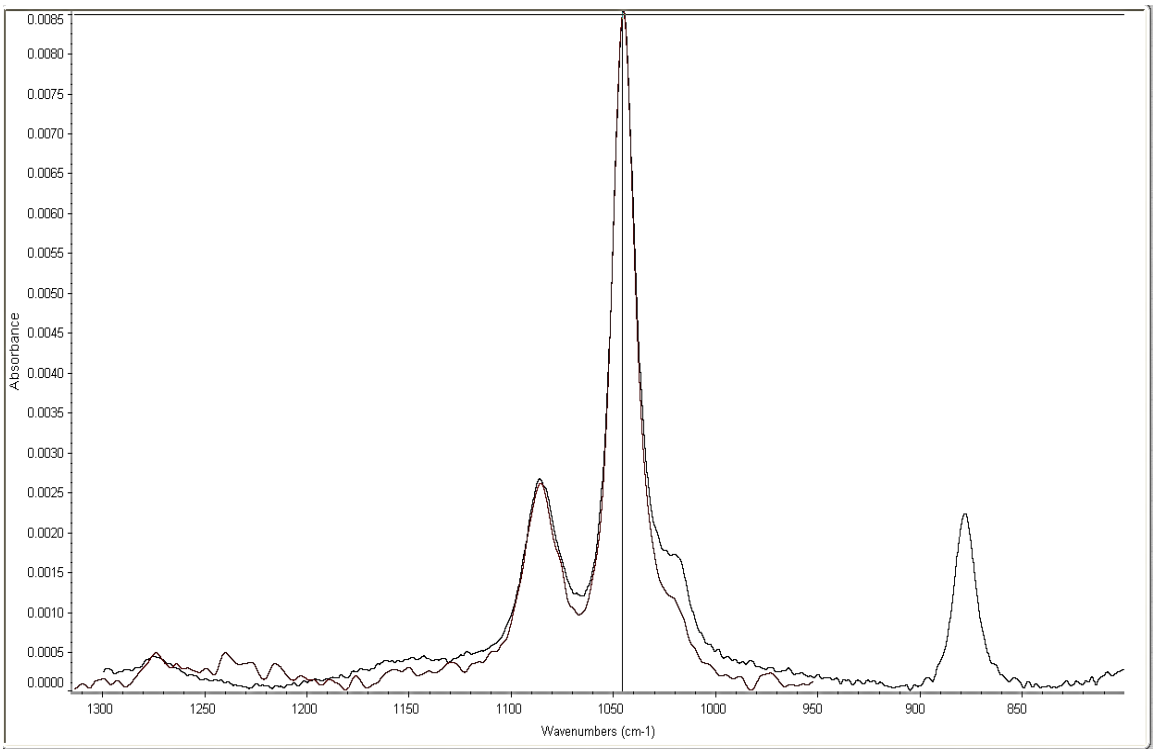

Figure 4.11: IR spectrum of C-O stretch for ethanol using SB-FTIR

The MB-FTIR analysis of ethanol was conducted similarly, although approximately 1.00 mL was required for each analysis. The concentrations of ethanol were verified using their refractive index value and the correlation table (Refractive Index of Ethanol Solutions, 2011). The standard curve for ethanol, shown in Figure 4.12, was developed when calculating the concentration of ethanol in non-alcoholic beer. Another standard curve for ethanol by volume was developed using the MB-FTIR when analyzing full-strength beer in Figure 4.13. A different standard curve for ethanol was developed for ethanol by weight (%ABW) (Figure 4.14). The LOD for ethanol was determined to be 0.500 %ABV and the LOQ was determined to be 1.67 %ABV. Temperature, pressure, and laser alignment/shifting could contribute to the drift seen in the collected data. This changed the absorbance so much that it was essential to create a new standard curve to reference for each analysis daily, as seen in the figures below.

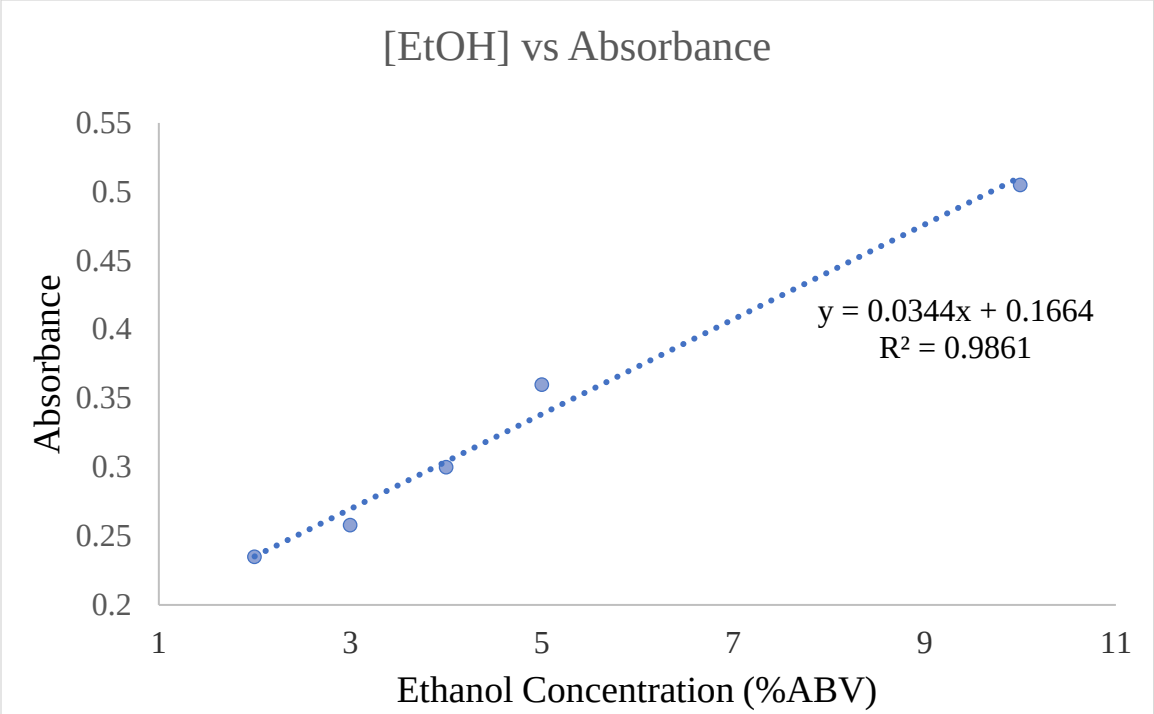

Figure 4.12: Standard curve of ethanol using the MB-FTIR at $\tilde{\upsilon}$ = 1045.1 cm^{-1} for non-alcoholic beer using peak height

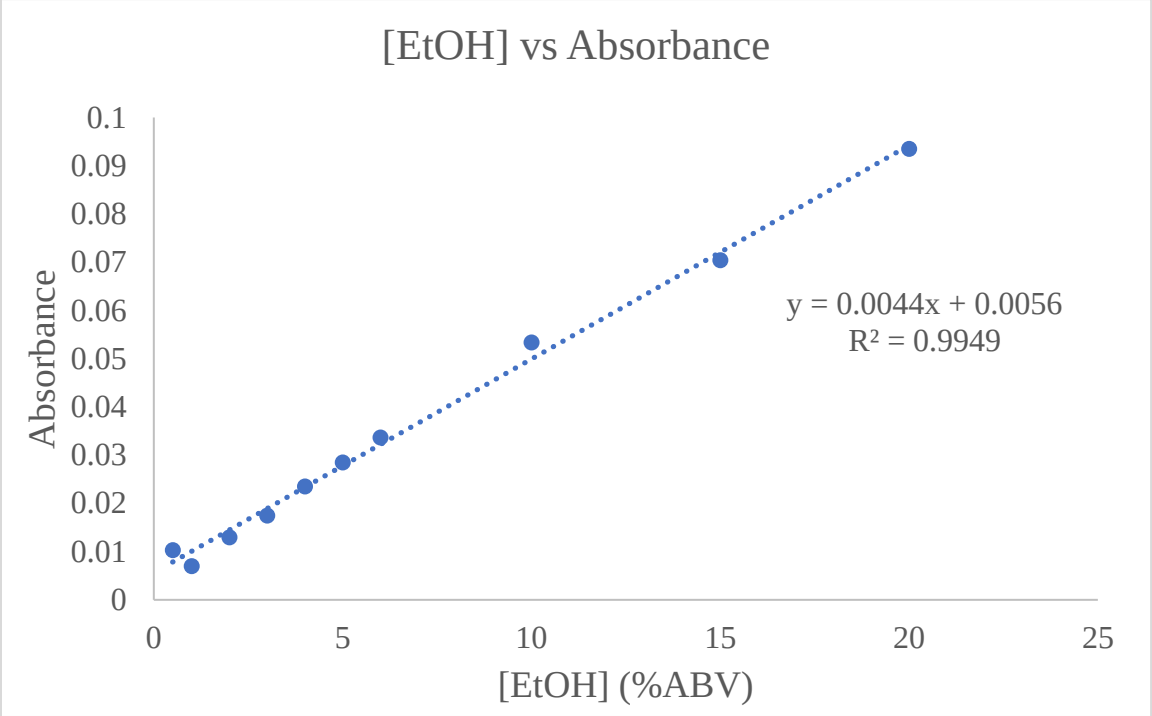

Figure 4.13: Standard curve of ethanol using the MB-FTIR at $\tilde{\upsilon}$ = 1045.2 cm^{-1} for full-strength beer using peak height

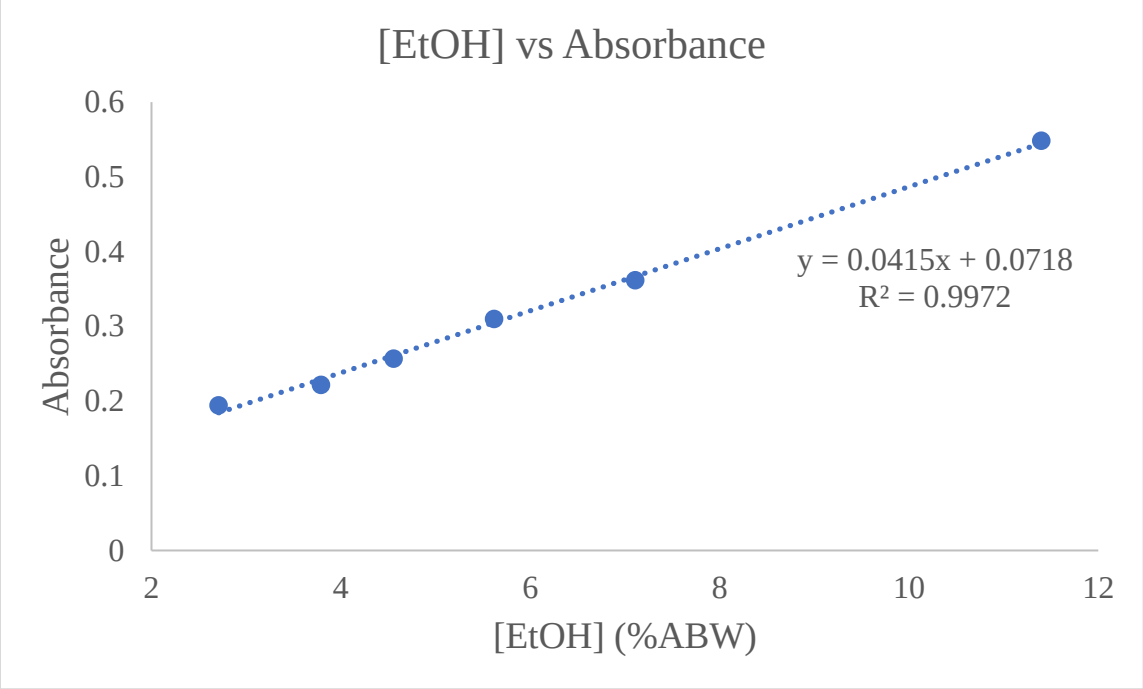

Figure 4.14: Standard curve of ethanol using the MB-FTIR at $\tilde{\upsilon}$ = 1044.2 cm^{-1} using peak height. The baseline of each spectrum was normalized at a signal of interest. However, the signals, when normalized on the same axis, appear on a ridge on the spectrum, which is why the standard curve does not go through the origin. This resulted in a non-zero absorbance at $\tilde{\upsilon}$ = 1044.2 cm^{-1} during the analysis

Ethanol standards were analyzed using the Ge flow cell to determine if a standard curve could be obtained using this analytical method. The ethanol solutions were made using 200 proof ethanol and D.I. water and their concentrations were confirmed using refractive index values. Figure 4.15 shows a standard curve created for ethanol using the Ge flow cell for the concentration of ethanol versus absorbance at $\tilde{\upsilon}$ = 1045.4 cm^{-1}. Figure 4.16 shows the same standard curve for ethanol using the total peak area from $\tilde{\upsilon}$ = 1186.9- 911.6 cm^{-1}. While neither curve passes through the origin (0,0), the standard curve using the total peak area provided less error in the linear regression. In addition, the Ge flow cell worked well in ethanol analysis. The LOD was determined to be 0.250 %ABV and the LOQ was determined to be 0.820 %ABV.

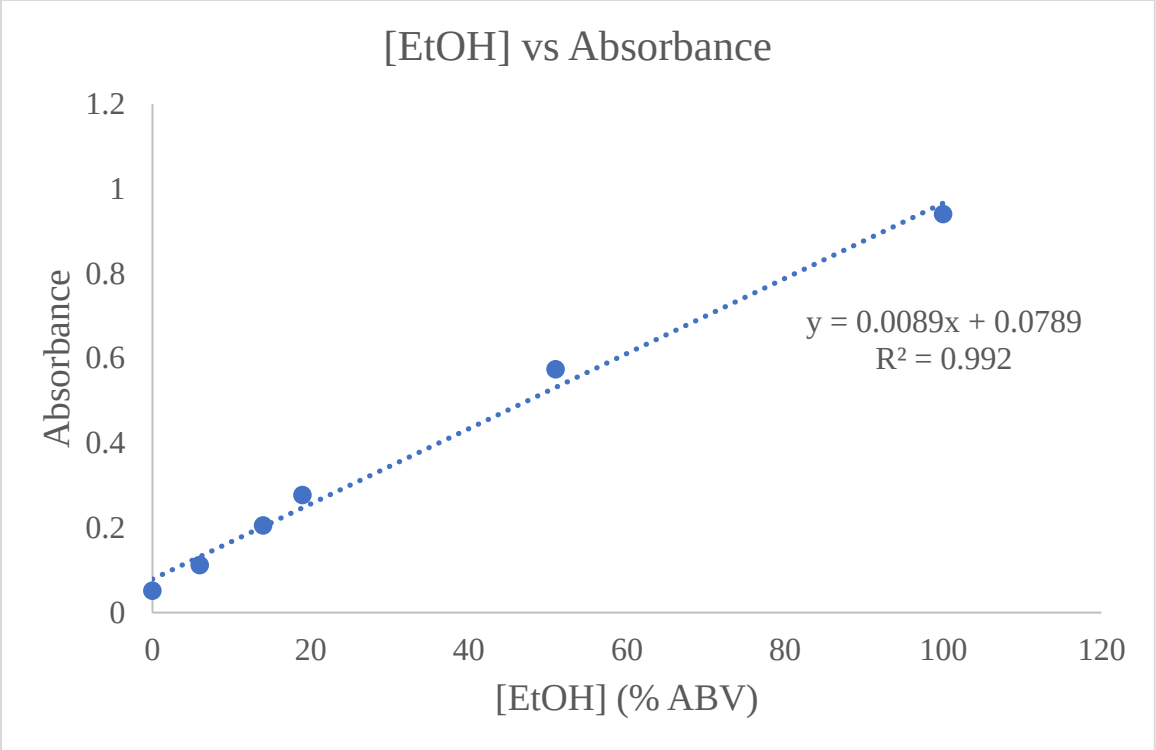

Figure 4.15: Standard curve of [EtOH] versus absorbance using the Ge flow cell using peak height

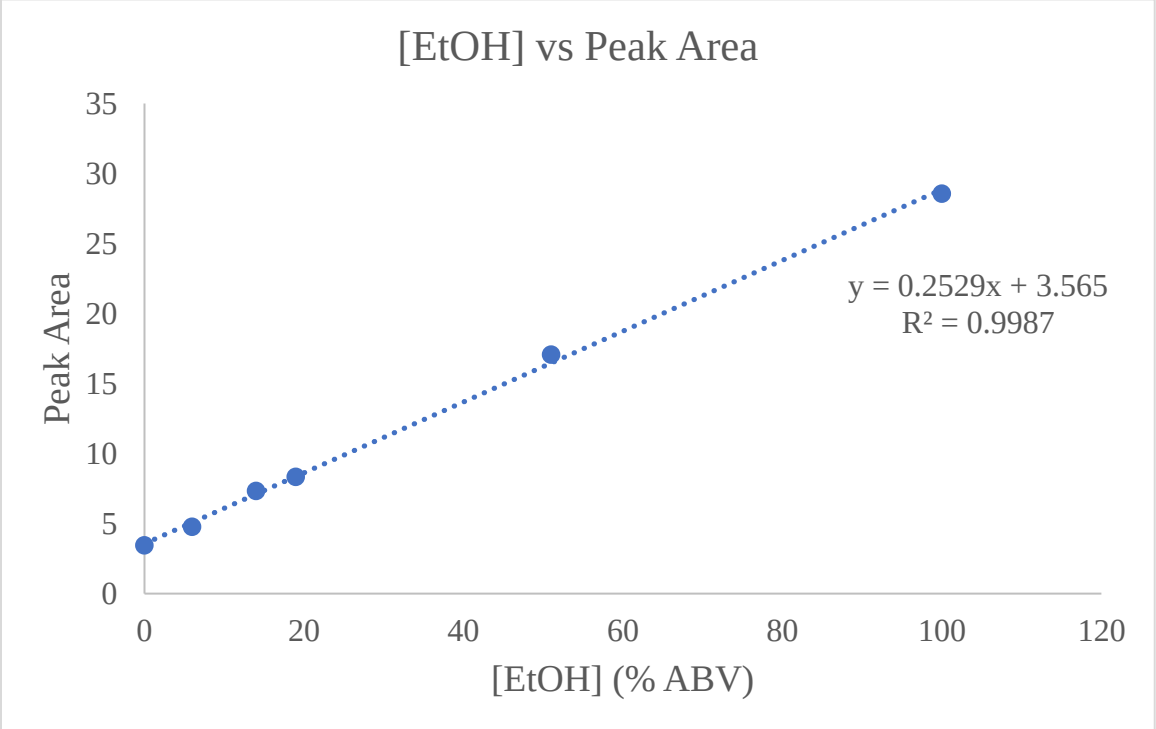

Figure 4.16: Standard curve of [EtOH] versus peak area using the Ge flow cell using peak area

Interferences with Carbon Dioxide

CO_2 is everywhere and the atmosphere currently contains up to 407.4 ppm of CO_2 (Lindsey, 2019). Since we are analyzing CO_2, there is interference in the atmosphere that we are unable to subtract from the background when using the FTIR. We did not have access to move the instrument to the controlled non-CO_2 atmosphere to perform the analysis, so we thought to use nitrogen gas to purge the environment of any CO_2 present when performing the analysis. This meant putting the FTIR inside of a plastic liner, opening the area where the detector is stored while removing the desiccant, placing a nitrogen gas line in this area and then tying and taping the plastic liner shut, but leaving a hole for the CO_2 to escape. The nitrogen line was made from Saint-Gobain Tygon S3™ E-3603 NSF®-51 at a maximum temperature of 165 °F, purchased from Saint-Gobain and connected to a water trap made from a glass tube containing $CaCl_2$ and glass wool, photograph in the Appendix. The nitrogen line was hooked up to a nitrogen tank that was a mixture of nitrogen and air, we were unable to find a pure nitrogen tank readily available for use. Spectral data taken had shown that there was a slight decrease in the CO_2 concentration in the background but not enough to make a difference in the spectral data taken during the reaction with ethyl acetoacetate, this spectral data can be seen in the Appendix. Since the sodium acetate buffer appeared to interfere with the CO_2 absorption, different solvents and solvent systems were employed and can be found in the Appendix.

Ethanol was also analyzed using the iS50 FTIR for comparison of results to the other tested analytical techniques. New ethanol standards were made from 200 proof ethanol and D.I. water. These standards spanned the concentration range from 0.5% to 10% ethanol (%ABV); Figure 4.17 illustrates the results of the analysis. The sample IR

spectra of the analysis are shown in Figure 4.18. The improved detector on the iS50 resulted in a LOD of 0.055 %ABV and a LOQ of 0.183 %ABV.

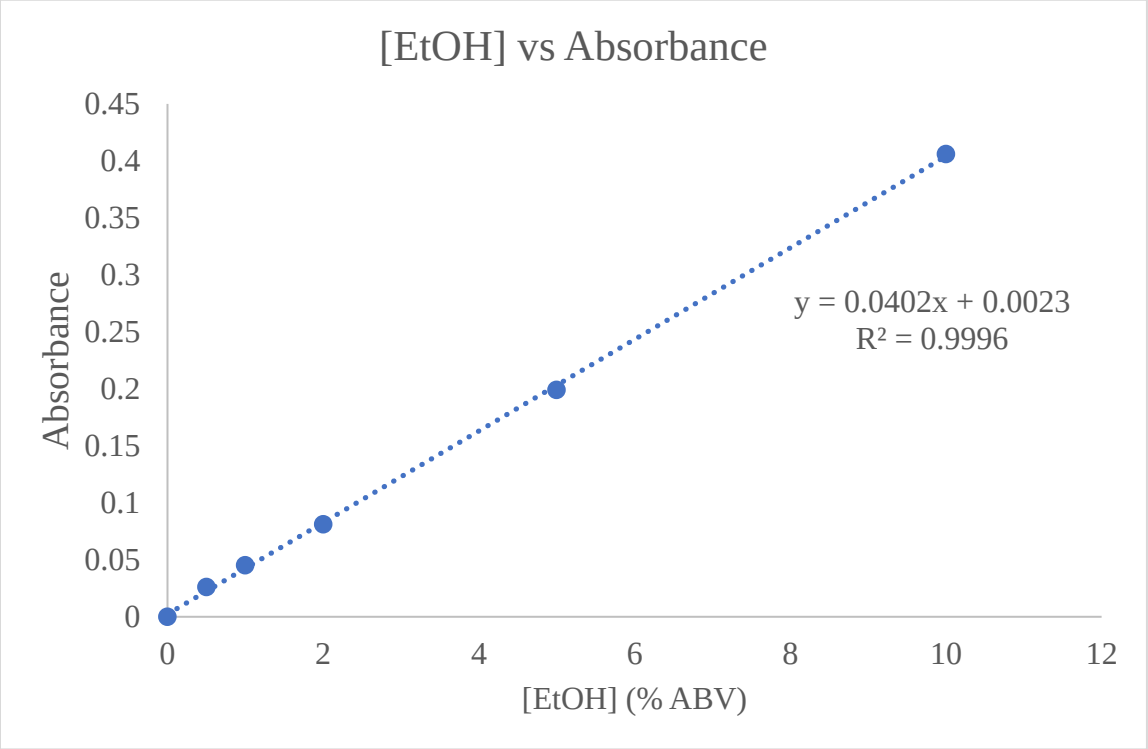

Figure 4.17: Standard curve of ethanol using the iS50 FTIR using peak height

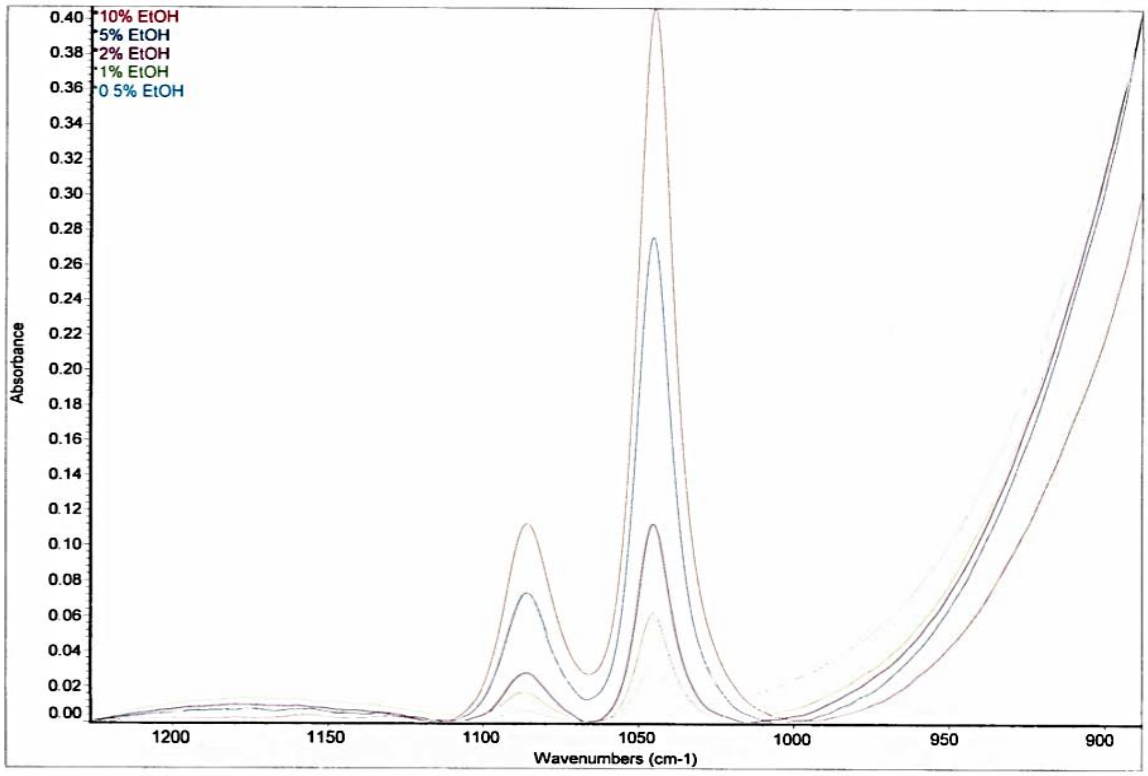

Figure 4.18: IR spectrum of ethanol using the iS50 FTIR at various concentrations

Ethanol contains vibrational modes that are Raman active that could be used to determine ethanol concentrations in solution. The ethanol standard solution was prepared from 200 proof ethanol and D.I. water. The ethanol concentrations were verified using their respective refractive indexes. Table 4.4 shows the data collected from the Raman spectrometer and a standard curve was produced in Figure 4.19, using peak area. These data provide another way to determine ethanol concentrations in aqueous solution. The LOD and LOQ were determined to be 0.446 %ABV and 1.49 %ABV, respectively.

Table 4.4: Raman data for ethanol concentration determination using peak height and peak area

Sample	%ABV by refractometer	Peak height (absorbance units)	Peak area (absorbance units)
1	7%	389.132	3100
2	13%	480.3878	1.07×10^4
3	19%	818.6305	1.71×10^4
4	24%	1001.069	2.69×10^4
5	27%	537.3232	2.02×10^4

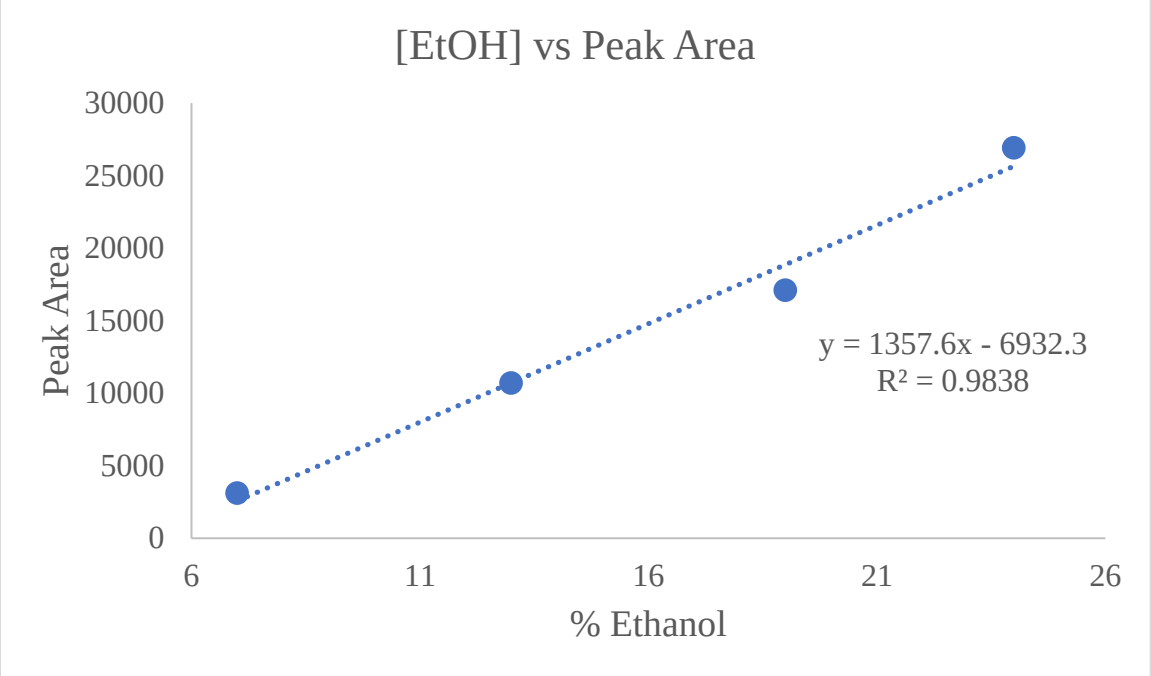

Figure 4.19: Standard curve of ethanol using the Raman spectrometer using peak area

Verification of the application of FTIR to the analysis of beer was accomplished. The first analysis performed using beer as the matrix was done to determine if any trace amounts of ethanol could be detected in non-alcoholic beer. Non-alcoholic beer must contain less than 0.50 %ABV. Four different non-alcoholic beers were analyzed using the MB-FTIR to determine their ethanol concentration, with data shown in Table 4.5. The results illustrate that the %ABV of non-alcoholic drinks can be evaluated easily with our

working standard curve at a LOD of 0.064 %ABV and LOQ of 0.213 %ABV using data from Figure 4.12 above.

Table 4.5: Data for non-alcoholic beer compared to the standard curve

Non-alcoholic beer	$Absorbance_{avg}$	%ABV from the standard curve (%)
1	0.0232	0.507
2	0.0263	0.582
3	0.0197	0.423
4	0.0156	0.324

Since the %ABV of non-alcoholic beer was able to be determined, the next step involved evaluation and comparison of the concentration of ethanol in 3.2 %ABW beer (purchased at a local grocery store) to similar beers at 4.2 %ABV (purchased at a local liquor store). Beer samples were cooled in a refrigerator for at least 24-hours prior to analysis. Approximately 1.00 mL was needed per sample analyzed on the MB-FTIR. The results can be seen in Table 4.6 below. The LOD and the LOQ were determined to be, 0.500 %ABV and 1.67 %ABV, respectively using data from Figure 4.13 above.

Table 4.6: Comparison of 3.2 %ABW beer versus full-strength beer

Beer	Absorbance	Listed %ABV/%ABW	Calculated %ABV/%ABW
Beer 1-Grocery	0.0242	3.2 %ABW	3.38 %ABW
Beer 1-Liquor	0.0239	4.2 %ABV	4.15 %ABV
Beer 2-Grocery	0.0233	3.2 %ABW	3.22 %ABW
Beer 2- Liquor	0.0245	4.2 %ABV	4.30 %ABV
Beer 3- Grocery	0.0266	3.2 %ABW	3.82 %ABW
Beer 3- Liquor	0.0304	4.6 %ABV	5.64 %ABV
Beer 4- Grocery	0.0246	3.2 %ABW	3.46 %ABW
Beer 4- Liquor	0.0319	5.0 %ABV	5.98 %ABV

After comparing the differences in 3.2 %ABV beer versus the same beers bought at the liquor store, the next step was to compare craft beer to the standard curves made. An amber ale, an Oktoberfest/Märzen, a Belgian sour ale, and a double IPA were analyzed using the MB-FTIR method. Table 4.7 gives the results of this analysis over five trials that were averaged with analysis at $\tilde{\upsilon}$ ~1045 cm^{-1}. The IR spectra can be seen in the Appendix. The beers were compared to the standard curve in terms of %ABW.

Table 4.7: Beer styles analyzed for ethanol concentration by MB-FTIR

Sample	Beer Style	Reported %ABV	Calculated %ABW	Calculated %ABV
1[a]	American Amber	5.2%	4.16%	5.20%
2	Oktoberfest/ Märzen	5.8%	4.29%	5.36%
3	Belgian Sour	4.2%	4.93%	6.16%
4	Double IPA	8.2%	6.82%	8.53%

[a]Beer held at room temperature

Another set of data was collected using MB-FTIR to cover a wide range of %ABV's, from 4.2% to 50% using both beer and hard liquor as samples. The data were collected over three trials at $\tilde{\upsilon}$ ~1044 cm^{-1}, data can be seen in Table 4.8. This data was obtained using the ethanol curve in Figure 4.11. An instrumental error can be the cause for the change in the reported values versus the calculated values, including the instrument used in this research or those used at the brewery. Breweries and other manufacturers of alcohol must report their %ABV's with ± 0.30 %ABV of the actual concentration.

Table 4.8: Ethanol determination using average absorbance value by MB-FTIR

Sample	Beer/Liquor style	Reported %ABV	Calculated %ABV
1	American Light Lager	4.2%	3.2%
2	Raspberry Wheat	5.2%	6.0%
3	Red Ale	6.7%	6.9%
4	American Malt liquor	12.2%	11%
5	Cinnamon Schnapps	50%	34%

The last beer analysis obtained was of nine different samples, however, samples 1-3 are the same beer just in different states including being chilled to ~5 ℃, one at stored at room temperature, and one being decarbonated. The rest of the beer samples were chilled to ~5 ℃. The data were collected at $\tilde{\upsilon}$ ~1045 cm^{-1}, over three trials (See Table 4.9.) The instrumental error can be the cause of the change in the reported values versus the calculated values.

Table 4.9: Ethanol determination (%ABV) by MB-FTIR

Sample	Beer Style	Reported %ABV	%ABV
1	RT Amber	5.2%	5.2%
2	Decarb. Amber	5.2%	3.6%
3	Cold Amber	5.2%	3.6%
4	Lemon Rädler	5.5%	4.5%
5	Coffee stout	5.5%	6.4%
6	Dry-hopped Cider	6.7%	5.3%
7	Nitro Saison	6.8%	6.4%
8	Rye IPA	4.0%	3.6%
9	Double IPA	8.5%	8.5%

An American light lager at 5.5 %ABV was processed through the Ge flow cell to determine if the primary alcohol C-O stretch was detectable using this method. The beer was chilled in a refrigerator for a 24-hour minimum period and approximately 240 mL was poured into the sample container, which was kept at room temperature in a water bath. The solution was analyzed over a period of 15 minutes and the absorbance values

were taken at approximately $\tilde{\upsilon}$ ~1046 cm^{-1} and the area of the signal was measured to see if any difference occurred in the spectrum over time. These data can be seen in Table 4.10 below, the IR spectrum is found in the Appendix.

Table 4.10: Data collected from an American light lager using the Ge flow cell

American Light Lager- 5.5 %ABV	$\tilde{\upsilon}_{max}$ (cm^{-1})	A_{max}	$Area_{max}$
0 min	1046.546	0.228	2.823
3 min	1043.545	0.154	3.050
4 min	1046.909	0.166	1.703
5 min	1046.000	0.136	3.020
6 min	1044.591	0.157	2.371
7 min	1044.591	0.188	1.137
9 min	1043.545	0.207	2.592
11 min	1048.046	0.159	2.860
13 min	1045.773	0.154	2.556
15 min	1047.273	0.122	3.818

Based on the data from Table 4.10, there appears to be a noticeable drift in the wavelength of the signal near $\tilde{\upsilon}$~1046 cm^{-1}. In addition, both the absorbance and area of the signal showed significant variability. This is likely due to the limited power of the source in the iS5 FTIR and the significant restriction of power through the Ge flow cell. As such, this would produce a significant error in the determination of ethanol concentration.

Acetone as an Analyte

Acetone, the third product formed in the deesterification/decarboxylation of ethyl acetoacetate was also analyzed to cover all ends of detection using a similar decarboxylation reaction to that of α-acetolactate. Acetone was analyzed using the MB-FTIR and the Ge flow cell. A standard curve for the concentration of acetone using absorbance is shown in Figure 4.20, using the MB-FTIR. The standard curve of acetone using peak area is shown in Figure 4.21. The LOD and the LOQ were determined to be

27.8 ppm acetone and 93.0 ppm acetone, respectively. The standard curve for the concentration of acetone using absorbance values is shown in Figure 4.22, using the MB-FTIR. Figure 4.23 is a standard curve for the concentration of acetone using peak area.

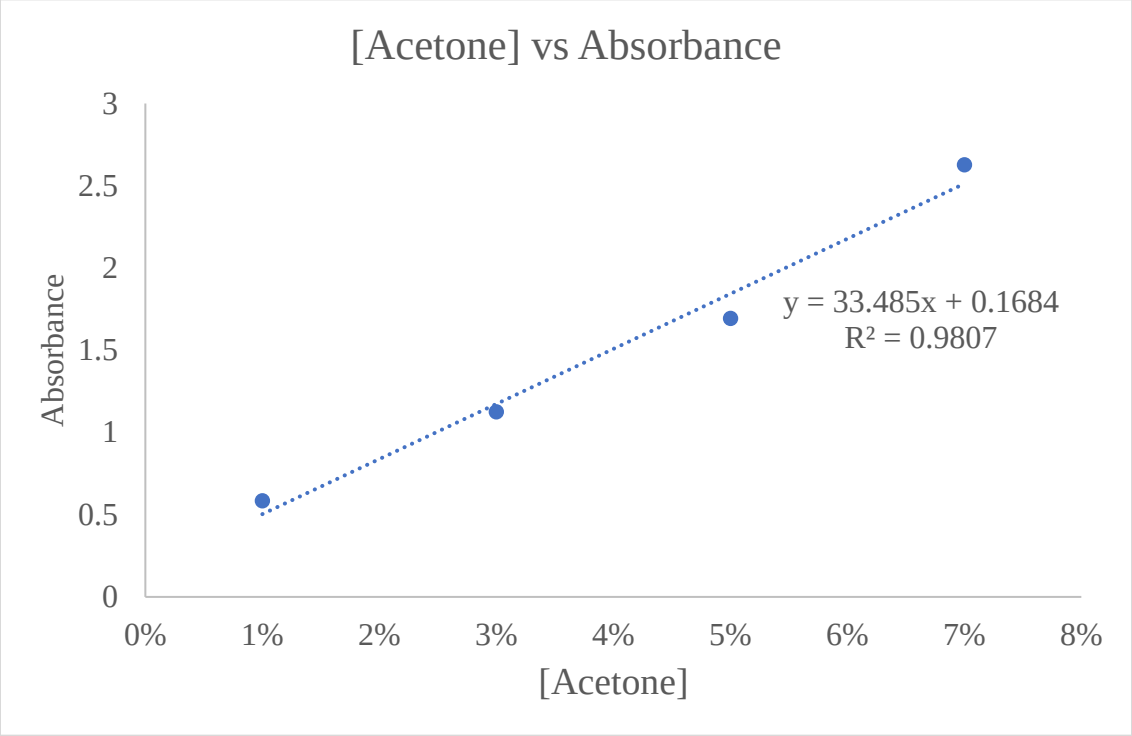

Figure 4.20: Standard curve of acetone using MB-FTIR using the peak height

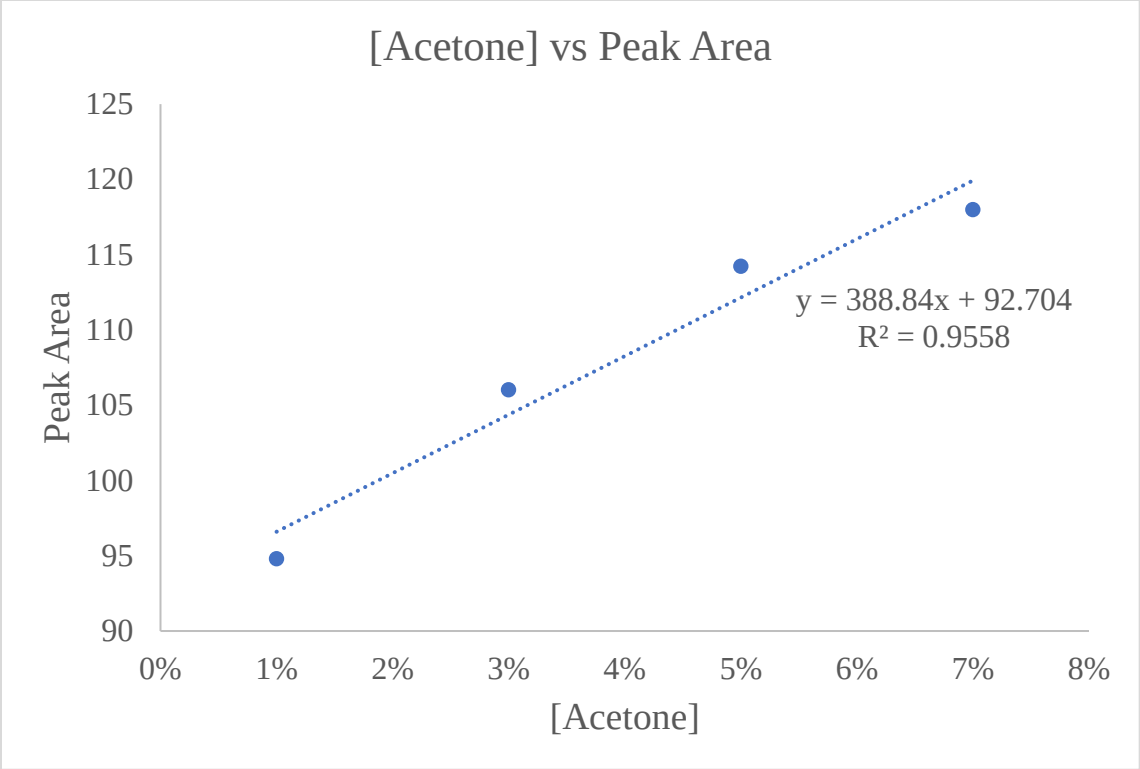

Figure 4.21: Standard curve of acetone using MB-FTIR using peak area

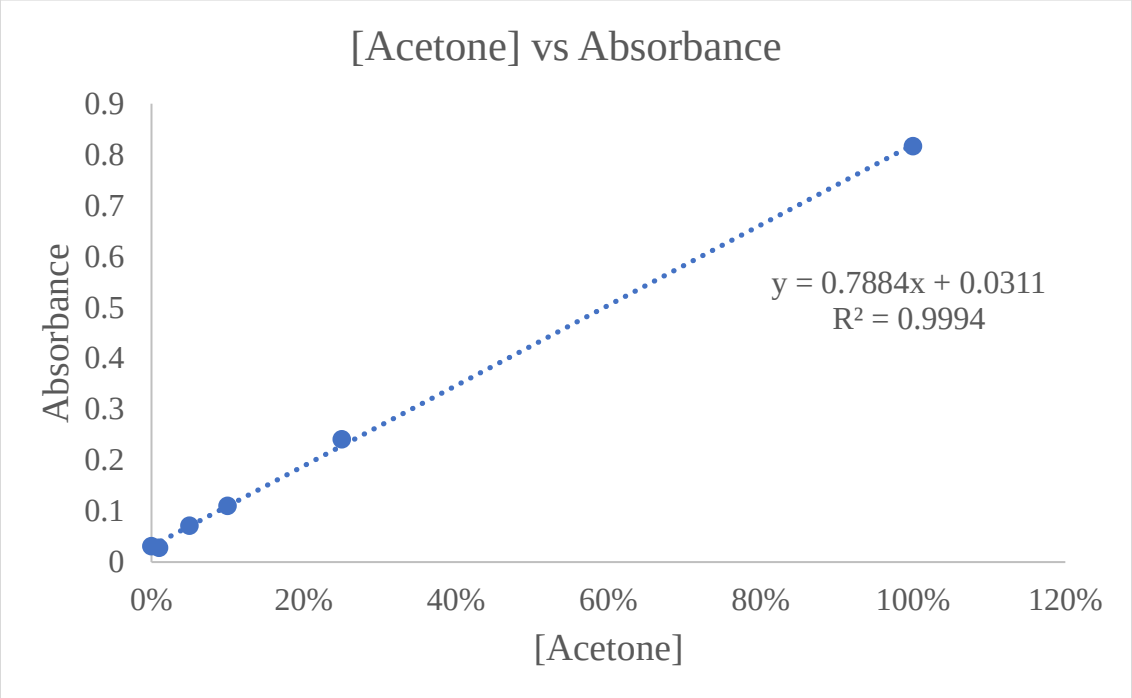

Figure 4.22: Standard curve of acetone using Ge flow cell at $\tilde{\upsilon}$ = 1696.5 cm^{-1} using peak height

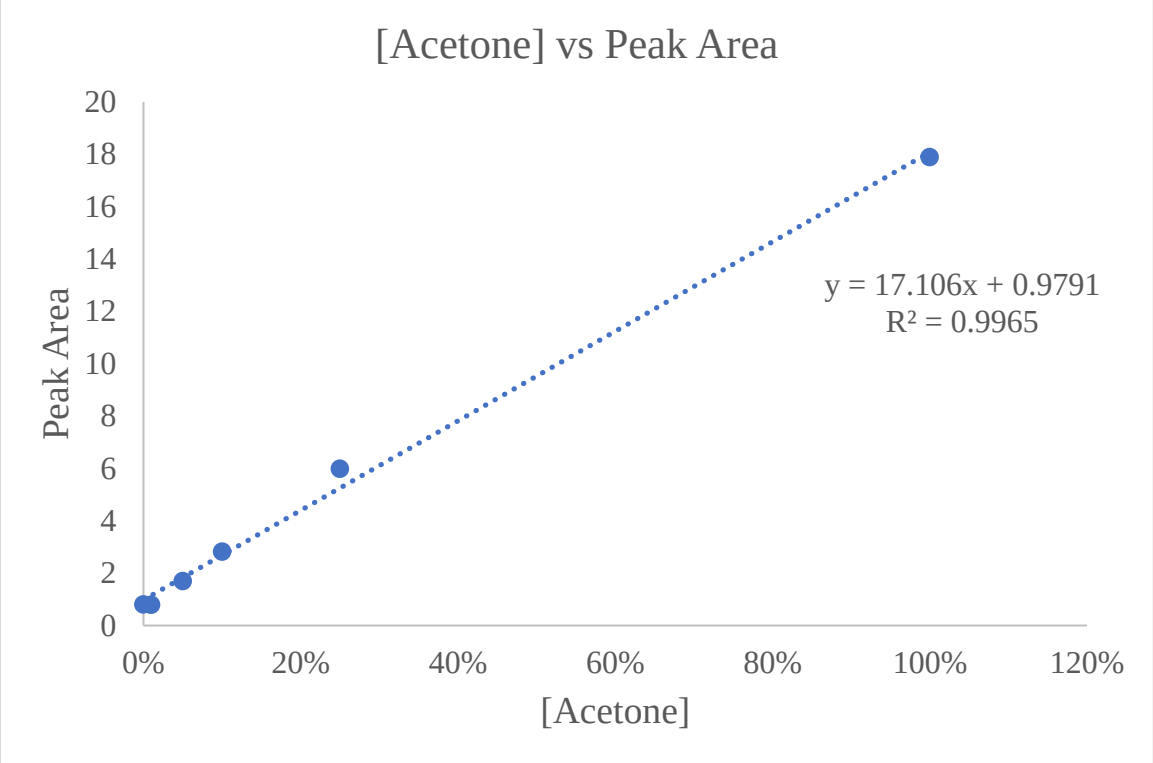

Figure 4.23: Standard curve of acetone using the Ge flow cell utilizing the peak area

Other Interferences on the Infrared Spectrum

An analysis of wort solutions at different concentrations was performed to determine if there any interferences with the analytes existed. Two different wort solutions were made and spiked with different amounts of ethanol to show that the IR signal for the C-O stretch for primary alcohols remained identifiable and quantifiable. Over three trials, the data were collected and averaged to create the plot in Figure 4.24, the spectral data can be seen in the Appendix. The LOD was calculated to be 0.128 %ABV and the LOQ 0.426 %ABV. An American light lager was also analyzed to determine that there were not any interferences with the IR spectrum. Beer samples were spiked with 200 proof ethanol from 1- 15 %ABV and analyzed using the MB-FTIR. The data collected can be seen in the Appendix.

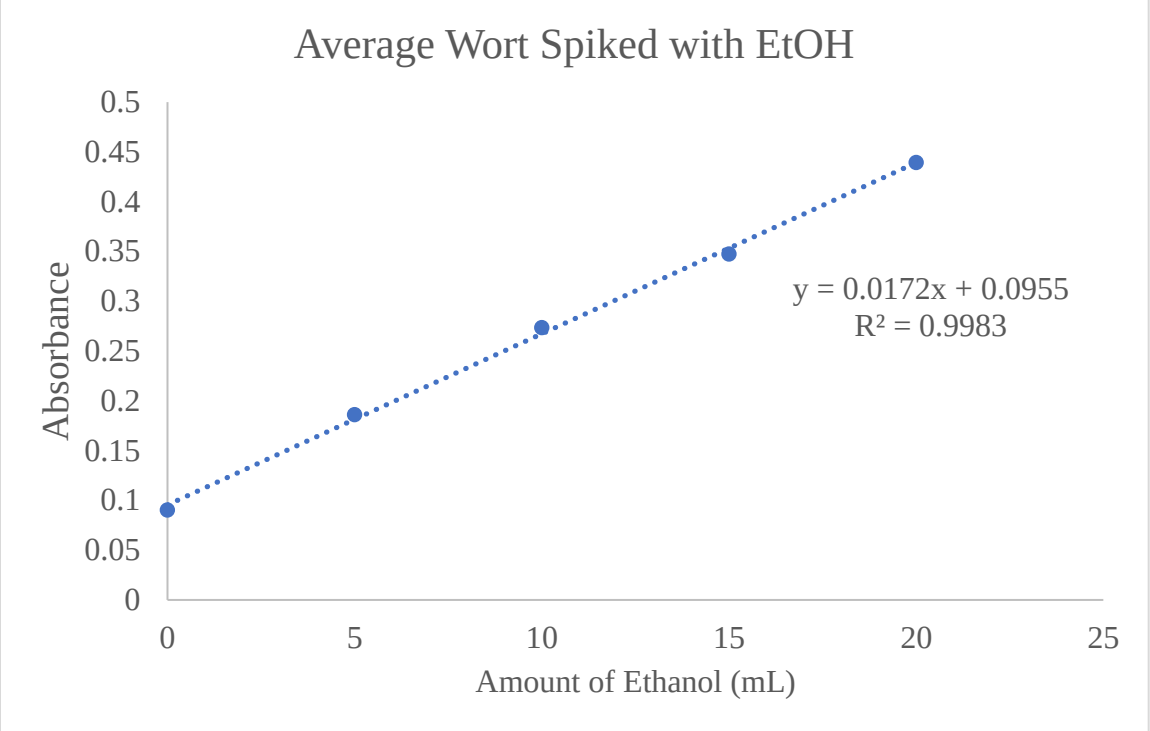

Figure 4.24: Wort spiked with ethanol analysis using MB-FTIR at $\tilde{\upsilon}$ ~1044 cm^{-1} using peak height

There are two more analytes that were analyzed in these experiments, acetaldehyde, and diacetyl itself. Acetaldehyde is another infamous off-flavor that can occur during the brewing process. Acetaldehyde contains known IR active signals meaning that it has dipole interactions. The key signals for acetaldehyde are $\tilde{\upsilon}$~1700 cm^{-1} for the C=O stretch, $\tilde{\upsilon}$ ~1400 cm^{-1} for the C-H rocking, $\tilde{\upsilon}$ ~900 cm^{-1} and $\tilde{\upsilon}$ ~800 cm^{-1} for the CH_3 rocking, $\tilde{\upsilon}$ ~700 cm^{-1} for the C-H wagging and, $\tilde{\upsilon}$ ~500 cm^{-1} for the C-C=O stretch (Evans & Bernstein, 1956). A 0.040 M stock solution of acetaldehyde was made; from this, serial dilutions were made to create standard solutions of acetaldehyde. The collected data can be seen in Figure 4.25. Noticeable IR signals were seen at $\tilde{\upsilon}$ = 1715 cm^{-1}, $\tilde{\upsilon}$ = 1385 cm^{-1}, and $\tilde{\upsilon}$ = 1095 cm^{-1}. A ^{1}H-NMR (Proton Nuclear Magnetic Resonance) spectrum was processed to determine the purity of the original stock solution of acetaldehyde. An ^{1}H-NMR spectrum can be seen with 13 different signals indicating

impurities present. It was determined that the original acetaldehyde solution was 63% pure acetaldehyde and the rest of the solution is a mixture of diastereomers, the acetaldehyde formed a complex seen in Figure 4.26 and the dominant diastereomers in solution in Figure 4.27. Since the original solution was determined to be 63% pure, the 0.040 M solution was determined to be 25% acetaldehyde and 75% D.I. water.

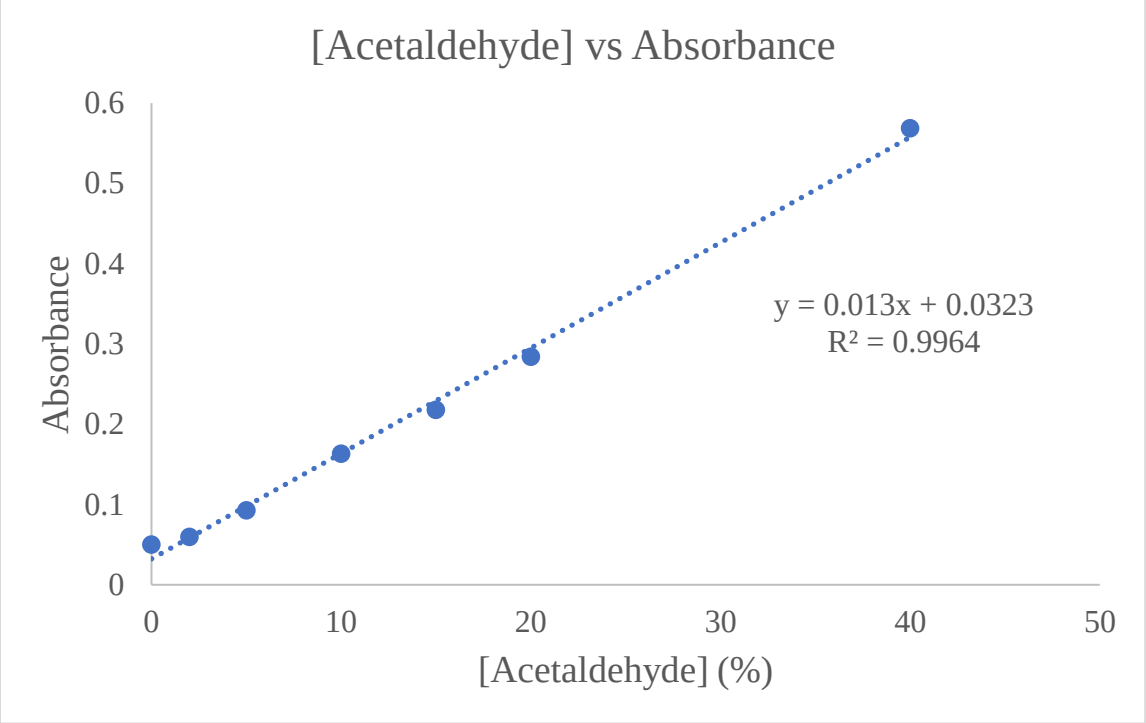

Figure 4.27: Plot of [Acetaldehyde] versus absorbance using the MB-FTIR for $\tilde{\upsilon}$~ 1715 cm^{-1}, corresponding to the C=O stretch using peak height

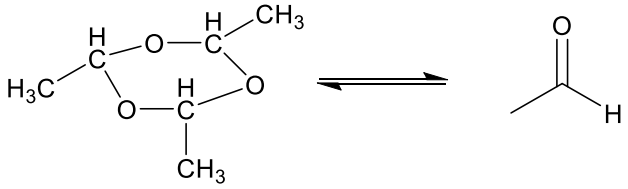

Figure 4.28: Acetaldehyde complex in equilibrium with a single acetaldehyde molecule

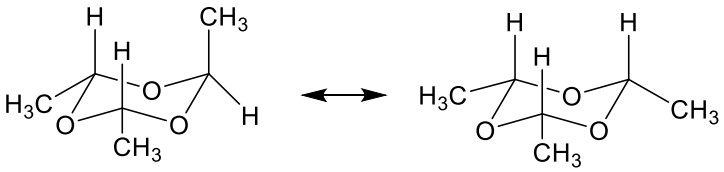

Figure 4.29: The two prominent diastereomers contributing to the many ˈH-NMR signals

Diacetyl, the compound we have been trying to find a method to analyze was also used to see what its IR spectrum looked like at different concentrations. Diacetyl concentrations were analyzed using the iS50 FTIR. Diacetyl solutions were created by using 100% diacetyl from Sigma Aldrich and making 1%-10% dilutions. There were a few signals of interest present at $\tilde{\upsilon}$ ~1700 cm^{-1}, a large stretch from $\tilde{\upsilon}$ ~1650 cm^{-1} to $\tilde{\upsilon}$ ~1500 cm^{-1}, peak growth at $\tilde{\upsilon}$ ~1350 cm^{-1}, $\tilde{\upsilon}$ ~1100 cm^{-1}, and a strong peak at $\tilde{\upsilon}$ ~1045 cm^{-1} for 10% diacetyl, the IR spectrum can be seen in Figure 4.28. The LOD and the LOQ were determined to be: 0.073% and 2.45%, respectively.

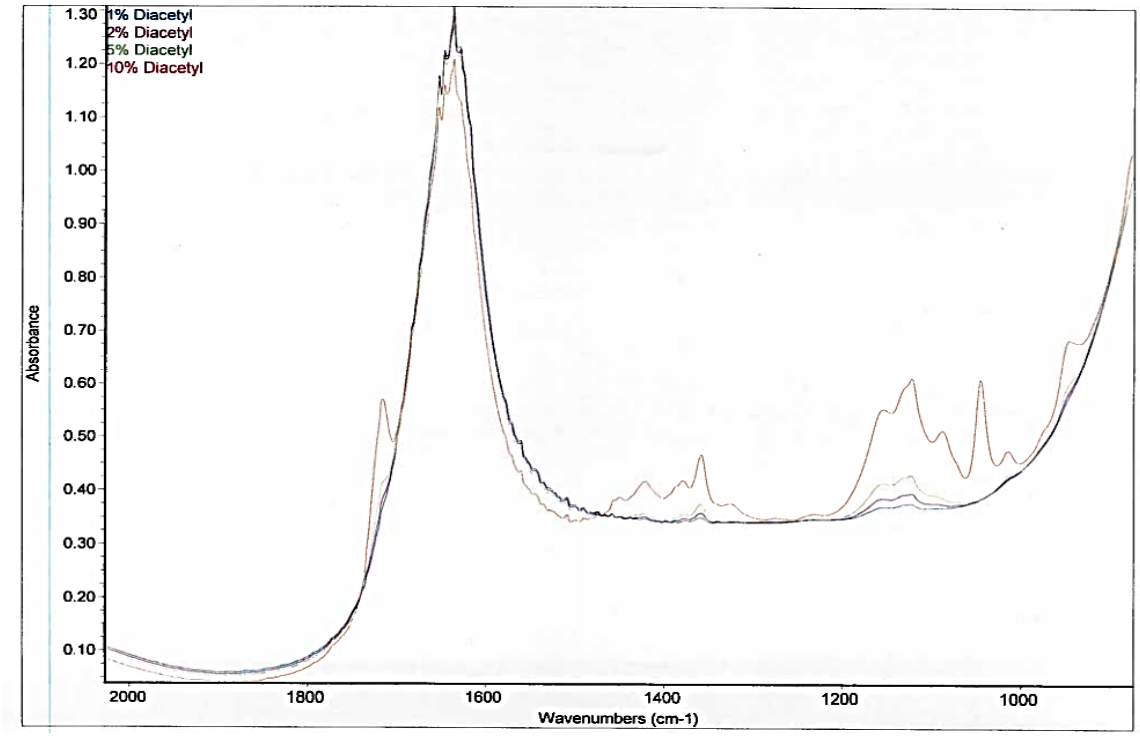

Figure 4.28: IR spectrum of diacetyl using the iS50 FTIR

CHAPTER V

CONCLUSION AND FUTURE WORK

The primary goal for this research was to create a new technique in order to detect and analyze diacetyl in fermenting wort through an indirect analyte. A hypothesis was advanced to detect diacetyl in solution by measurement of the concentration of dissolved CO_2.

Methods for the analysis of diacetyl using FTIR in this matrix (or any other for that matter) do not appear to exist in the literature. This is most likely due to the lack of sensitivity of the typical FTIR spectrometer. There are also no inline nor online detection methods to measure the concentration of diacetyl. Using FTIR requires no sample prep and the goal was to create a device that would be online with a fermentation vessel to detect dissolved CO_2 in solution. This would increase the efficiency in a brewery; brewers would not have to guess the stage of fermentation.

Utilizing the rapid and inexpensive method of ATR-FTIR and complementing the research with Raman spectroscopy gave us a way to explore and examine which method would provide the best results. We utilized five different instrumental techniques for analysis. These five methods included: single bounce FTIR (SB-FTIR), Multi-bounce FTIR(MB-FTIR), the Ge flow cell, the iS50 FTIR, and the Raman spectrometer.

The use of the SB-FTIR as an instrumental method for the detection of CO_2 gave a significant amount of error. Its limit of detection was too high to accurately and precisely determine the concentration of CO_2 in solution. When the SB-FTIR was used

for ethanol as an analyte, the results gave a LOD of 3.40 ±0.16 %ABV and a LOQ of 11.3 ±0.16 %ABV. This shows that the method is not very precise for ethanol as an analyte. Overall, this method is not one that should be considered for use in the indirect determination of CO_2.

The use of the MB-FTIR as an instrumental method for the detection of CO_2 was performed using seltzer water and the reaction with ethyl acetoacetate. The limit of detection was determined to be 528 ±0.033 ppm and the LOQ was determined to be 1760 ±0.033 ppm for the concentration of CO_2 in solution. When the MB-FTIR was used for ethanol as an analyte the LOD was determined to be 0.500 ±0.01 %ABV and the LOQ was determined to be 1.67 ±0.01 %ABV. Acetone was another analyte that was analyzed using MB-FTIR, obtaining results such as a LOD of 27.8 ±0.01 ppm and a LOQ of 93.0 ±0.01 ppm. Acetaldehyde was analyzed using the MB-FTIR. The LOD calculated for the acetaldehyde was 2.66 ±0.071% and the LOQ was determined to be 8.87 ±0.071%. Overall, this method should be considered for use in the indirect determination of CO_2.

The use of the Ge flow cell as an instrumental method for the detection of CO_2 gave a significant amount of error. Its limit of detection was too high to accurately and precisely determine the concentration of CO_2 in solution. When the Ge flow cell was used for ethanol as an analyte, the LOD was determined to be 0.250 ±0.001 %ABV and the LOQ was determined to be 0.820 ±0.001 %ABV. Acetone concentrations were also detected using the Ge flow cell. The LOD determined for acetone was 180 ±0.01 ppm and the LOQ was determined to be 590 ±0.01 ppm. Overall, this method is not one that should be considered for use in the indirect determination of CO_2.

The use of the iS50-FTIR as an instrumental method was used for the detection of dissolved CO_2, diacetyl and ethanol. The LOD for dissolved CO_2 was determined to be 22.5 ppm and the LOQ was determined to be 74.9 ppm. The LOD for diacetyl was determined to be 0.734% and the LOQ was determined to be 2.45%. The ethanol analysis gave a LOD of 0.055 %ABV and a LOQ of 0.183 %ABV. Overall, this method should be considered for use in the indirect determination of diacetyl, but also worked well in the direct measurement of diacetyl and ethanol.

The use of the Raman spectrometer as an instrumental method for the detection of CO_2 gave a significant amount of error. There were not any useful signals available to perform a LOD and LOQ analysis for seltzer water. When the Raman spectrometer was used for ethanol as an analyte, the results gave a LOD of 0.450 %ABV and a LOQ of 1.49 %ABV. Overall, this method works and is relatively precise for the measurement of ethanol, the CO_2 signals were unable to be detected in the spectrum.

Table 5.1 collects each of the different methods and analytes and compares their LOD and LOQ for the analysis. For CO_2, the best instrumental method appears to be the iS50 FTIR using the multi-bounce trough ATR cell. While the relative standard deviation (RSD) was unable to be determined for this method due to the limited time on the instrument, the iS50 was able to drop the LOD by a factor of 20. This puts the analysis of dissolved CO_2 into the range needed for indirect measurement of diacetyl. The best method for the analysis of ethanol appears to be the Ge flow cell. A very low LOD with the smallest RSD indicates that this is the better method for measuring %ABV in beer. This was also true when the analyte was acetone; the flow cell had the lower LOD and the better RSD. The use of these IR methods to determine the concentration of diacetyl or

acetaldehyde is not recommended. The LOD in both cases was >2% v/v which is significantly greater than the largest concentration in a typical fermentation. Moreover, the RSD for acetaldehyde was quite significant.

Table 5.1: Comparison of RSD for different methods and analytes

Analyte: CO_2			
Method	LOD (ppm)	LOQ (ppm)	RSD (of LOD)
SB-FTIR	–[a]	–	–
MB-FTIR	528 ±0.033	1760 ±0.033	0.00667%
Ge Flow Cell	–[a]	–	–
iS50 FTIR	22.5	74.9	–[b]
Raman	–[a]	–	–[b]

Analyte: Ethanol			
Method	LOD (%ABV)	LOQ (%ABV)	RSD (of LOD)
SB-FTIR	3.40 ±0.16	11.3 ±0.16	4.78%
MB-FTIR	0.500 ±0.01	1.67 ±0.01	1.38%
Ge Flow Cell	0.250 ±0.001	0.820 ±0.001	0.300%
iS50 FTIR	0.055	0.183	–[b]
Raman	0.450	1.49	–[b]

Analyte: Acetone			
Method	LOD (ppm)	LOQ (ppm)	RSD (of LOD)
MB-FTIR	27.8 ±0.01	93.0 ±0.01	0.025%
Ge Flow Cell	180 ±0.01	590 ±0.01	0.00384%

Analyte: Diacetyl			
Method	LOD (%)	LOQ (%)	RSD (of LOD)
iS50 FTIR	0.734	2.45	–[b]

Analyte: Acetaldehyde			
Method	LOD (%)	LOQ (%)	RSD (of LOD)
MB-FTIR	2.66 ±0.071	8.87 ±0.071	26.7%

a = no data were available because the method was unable to detect the analyte;
b = because of limited time on the instrument, not enough data were collected to determine the standard deviation.

Future work for this project should focus on improving the current instrumental setup, obtaining a research-grade ATR-FTIR, applying the developed instrumental

method in a brewery setting, and evaluating other important analytes in solution throughout fermentation to improve brewery efficiency.

One of the ways to improve the current setup would be to get a better pump to push liquid through the flow cell. The HPLC pump works for this task but the data indicate that significant decarbonation occurs as the sample flows through the pump. This is especially an issue if the analyte is CO_2.

Since fermentation goes through temperature changes, it would be ideal to have a Peltier temperature controller. A temperature controller would allow samples to be heated and then instantly cooled for analysis. It would also allow the user to obtain all samples at a fixed temperature. This would allow more accurate measurements than using an ice bath and a hot bath.

Improvement of the detector on the Nicolet iD5 FTIR spectrometer is also recommended for future work. Additionally, a more powerful IR source or a convex lens to focus the IR energy through the flow cell would be very important. This would allow the sample to absorb and transmit a more powerful infrared signal which would increase the sensitivity of the technique. Finally, since atmospheric CO_2 interferes with the background, operation of the IR in a glove box or other controlled atmosphere chamber would help eliminate the background signals from CO_2.

In fact, better instrumentation would solve many of the issues that were discovered during this research. The limited operation of the ThermoFischer iS50 FTIR spectrometer proved that this instrument would alleviate many issues. However, the cost of the instrumentation would need to be considered.

The ideal instrument found in the brewery would require, at the minimum, a non-decarbonating pump, a flow cell, a detector similar to the MTG detector, a powerful IR source to optimize the energy directed towards the detector, a Peltier heater and cooler to adjust the temperature of the beer, and software to transform ATR-FTIR data. FTIR would allow for an inexpensive, fast-performing, and comparable method to the ASBC and Analytica-EBC methods for analyzing diacetyl and the other analytes determined in this analysis.

Lastly, there are thousands of analytes that are found during yeast fermentation that are of interest to the brewer. An FTIR capable of performing multiple analyte measurements simultaneously would provide instant and useful information about the quality and progress of fermentation. Obtaining information for multiple analytes in fermentation can indicate yeast performance. The better the yeast perform, the reuptake remaining diacetyl could lead to better and more consistency during production. The efficiency of moving the beer from fermentation to conditioning will allow brewers to produce more beer and better beer.

REFERENCES

American Society of Brewing Chemists Methods of Analysis (2014) Beer method 2: Specfic gravity. *American Society of Brewing Chemists*, St. Paul, MN. ASBC publications and technical committees. doi: 10.1094/ASBCMOA-Beer-2

American Society of Brewing Chemists Methods of Analysis (1964). Beer Methods 25B, 25C, 25E; Broad spectrum method for VDK, Micro dimethyl glyoxime method, Gas chromatographic method. *American Society of Brewing Chemists*, St. Paul, MN. ASBC publications and technical committees. doi: 10.1094/ASBCMOA-Beer-25

Avery, A. (2018). Avery brewing company. Retrieved September 26, 2018, from https://www.averybrewing.com/

Baker, J. (2018). Brewers Association craft beer in 2018. Retrieved August 10, 2018, from https://www.craftbeer.com/editors-picks/ba-releases-craft-beer-in-2018-headlines

Barros, A., Rodrigues, J. A., Almeida, P. J., & Oliva-Teles, M. T. (1999). Determination of glyoxal, methylglyoxal, and diacetyl in selected beer and wine, by HPLC with UV spectrophotometric detection, after derivatization with *o*-phenylenediamine. *Journal of Liquid Chromatography & Related Technologies*, *22*(13), 2061-2069. doi:10.1081/jlc-100101786

Bryn, K., Ulstrup, J. C., & Stormer, F. (1973). Effect of acetate upon the formation of acetoin in *Klebsiella* and *Enterobacter* and its possible practical application in a rapid Voges-Proskauer test. *Applied Microbiology*, *25*(3), 511–512.

Buckee, G., & Mundy, A. (1994). Determination of vicinal diketones in beer by gas chromatography (headspace technique)-collaborative trial. *Journal of the Institute of Brewing*, *100*(4), 247-253. doi:10.1002/j.2050-0416.1994.tb00820.x

Buijten, J. C., & Holm, B. (1979). An automated distillation method for the determination of diacetyl in beer: a comparison of analysis by autoanalyzer and gas chromatography. *Journal of Automatic Chemistry*, *1*(2), 91-94. doi:10.1155/s1463924679000286

Burikov, S., Dolenko, T., Patsaeva, S., Starokurov, Y., & Yuzhakov, V. (2010). Raman and IR spectroscopy research on hydrogen bonding in water-ethanol systems. *Molecular Physics, 108*(18), 2427-2436. doi:10.1080/00268976.2010.516277

Carter, C. F., Lange, H., Ley, S. V., Baxendale, I. R., Wittkamp, B., Goode, J. G., & Gaunt, N. L. (2010). ReactIR flow cell: a new analytical tool for continuous flow chemical processing. *Organic Process Research & Development, 14*(2), 393-404. doi:10.1021/op900305v

Damiani, P., & Burini, G. (1998). Determination of diacetyl in butter as 2,3-diaminonaphthalene derivative, using a fluorometric procedure or reverse phase liquid chromatography with fluorescence detection. *Journal Association Official Analytical Chemistry, 7*(3), 462-465.

Davis, A. R., & Oliver, B. G. (1972). A vibrational-spectroscopic study of the species present in the CO_2-H_2O system. *Journal of Solution Chemistry, 1*(4), 329-339. doi:10.1007/bf00715991

Dejong, R., Verhagen, L., & Strating, J. (1987). Analysis of vicinal diketones in beer by high-performance liquid-chromatography. *Journal of The Institute of Brewing 93*(3), 164.

DeltaNu. (2012). Advantage 200A benchtop Raman spectrometer, *Intevac Photonics-Delta Nu.*1-4.

Edinburgh Instruments. (2019). Raman scattering in fluorescence emission spectra – common errors in fluorescence spectroscopy. Retrieved August 1, 2018, from https://www.edinst.com/blog/raman-scattering-blog/

European Brewers Convention-Analytica. (1998). Method 9.24.1. *Vicinal diketones in beer: gas chromatographic method in Analytica-EBC*. (5th ed.). Maastricht, Netherlands. Nürnberg : Hans Carl, Fachverlag.

European Brewers Convention-Analytica. (1998). Method 9.24.2. *Vicinal diketones in beer*: *spectrophotometric method in Analytica-EBC*. (5th ed.). Maastricht, Netherlands. Nürnberg : Hans Carl, Fachverlag.

Evans, J. C., & Bernstein, H. J. (1956). The vibrational spectra of acetaldehyde and acetaldehyde-d_1. *Canadian Journal of Chemistry, 34*(8), 1083-1092. doi:10.1139/v56-141

Gardiner, D. J. (1989). Introduction to Raman scattering. *Practical Raman Spectroscopy,* 1-12. Berlin, Heidelberg: Springer Berlin Heidelberg doi:10.1007/978-3-642-74040-4_1

Geisler, J., & Weiß, N. (2015). Vicinal diketone (diacetyl and 2,3-pentanedione) measurement in beer using an Eppendorf biospectrometer, Research center Weihenstephan for brewing and food quality short protocol 8, 1-2.

Grecsek, T., & Ruppel, H. (2005). Brewing quantitative control applications using headspace sampling-gas chromatography, Field Application Report, PerkinElmer.

Griffiths, P. R., & de Haseth, J. A. (2007). *Fourier transform infrared spectrometry*. (2nd ed.). Hoboken, New Jersey, John Wiley & Sons Inc.

Harrison, G., Byrne, W., & Collins, E. (1965). Metric methods available for the determination of diacetyl (2, 3-butanedione) in various biological materials. *Directors of Arthur Guinness Son & Co.* (Dublin) Ltd, 71, 336-341. doi.org/10.1002/j.2050-0416.1965.tb02067.x

Heaney, D. (2012). Pycnometer, *Scientific Direct*, Retrieved April 9, 2018. from https://www.sciencedirect.com/topics/engineering/pycnometer.

Hellma Analytics. (n.d.) Comprehensive catalog of FTIR and UV-Vis accessories and supplies. Retrieved November 15, 2018, from www.Piketech.com.

Henry, W. (1803) Experiments on the quantity of gases absorbed by water, at different temperatures, and under different pressures. *Philosophical Transactions of the Royal Society of London*, *93*, 29-274. doi:10.1098/rstl.1803.0004

Holzammer, C. C., & Braeuer, A. S. (2019). Raman spectroscopic study of the effect of aqueous salt solutions on the inhibition of carbon dioxide gas hydrates. *Journal of Physical Chemistry B*, *123*(10), 2354-2361. doi:10.1021/acs.jpcb.8b11040.

Jackson, P., Robinson, K., Puxty, G., & Attalla, M. (2009). In situ Fourier transform-infrared (FT-IR) analysis of carbon dioxide absorption and desorption in amine solutions. *Energy Procedia*, *1*(1), 985-994. doi:10.1016/j.egypro.2009.01.131

King, A. D., & Coan, C. R. (1971). Solubility of water in compressed carbon dioxide, nitrous oxide, and ethane. Evidence for hydration of carbon dioxide and nitrous oxide in the gas phase. *Journal of the American Chemical Society*, *93*(8), 1857-1862. doi:10.1021/ja00737a004

Laakso, O., Haapala, M., Jaakkola, P., Laaksonen, R., Nieminen, J., Pettersson, M., Himberg, J. (2000). The use of low-resolution FT-IR Spectrometry for the analysis of alcohols in breath. *Journal of Analytical Toxicology*, *24*(4), 250-256. doi:10.1093/jat/24.4.250

Landaud, S., Lieben, P., & Picque, D. (1998). Quantitative analysis of diacetyl, pentanedione and their precursors during beer fermentation by an accurate GC/MS method. *Journal of the Institute of Brewing*, *104*(2), 93-99. doi:10.1002/j.2050-0416.1998.tb00981.x

Li, X., Duerkop, A., & Wolfbeis, O. S. (2009). A fluorescent probe for diacetyl detection. *Journal of Fluorescence*, *19*(4), 601-606. doi:10.1007/s10895-008-0450-y

Lindsey, R. (2019). Climate change: Atmospheric carbon dioxide. *NOAA Climate.gov*. Retrieved October 16, 2019, from https://www.climate.gov/news-features/understanding-climate/climate-change-atmospheric-carbon-dioxide.

Martineau, B., Acree, T., & Henick-Kling, T. (1994). A simple and accurate GC/MS method for the quantitative analysis of diacetyl in beer and wine. *Biotechnology Techniques*, *8*(1), 7-12. doi:10.1007/bf00207625

Martín-Ramos, P., Fernández-Coppel, I. A., Ruíz-Potosme, N. M., & Martín-Gil, J. (2018). Potential of ATR-FTIR spectroscopy for the classification of natural resins. *Biology, Engineering, Medicine and Science Reports*, *4*(1), 03-06. doi:10.5530/bems.4.1.2.

McCarthy, S. L. (1995). Analysis of diacetyl and 2,3-pentanedione in beer by HPLC with fluorometric detection. *Journal of the American Society of Brewing Chemists*, *53*(4), 178-181. doi:10.1094/asbcj-53-0178

Mendelsohn, R. (2007). Fourier transform infrared spectrometry, *Journal of the American Chemical Society*, *129*(43), 13358–13358.

Mirabella, F. (1993). Practical spectroscopy series; internal reflection spectroscopy: theory and applications, Marcel Dekker, Inc., 17-52.

Nicolet™ iD Foundation Adapter. (n.d.). Retrieved March 24, 2019, from https://www.thermofisher.com/order/catalog/product/IQLAADGAAGFAJAMAYW

Nicolet™ iS5 FTIR Spectrometer. (n.d.). Retrieved February 17, 2019, from https://www.thermofisher.com/order/catalog/product/IQLAADGAAGFAHDMAZA

Nicolet™ iS50 FTIR Spectrometer. (n.d.). Retrieved May 15, 2019, from https://www.thermofisher.com/order/catalog/product/912A0760

Pejin, J., Grujic, O., Markov, S., Kocic-Tanackov, S., Tanackov, I., Cvetkovic, D., & Djurendic, M. (2006). Application of GC/MS method using SPE columns for quantitative determination of diacetyl and 2,3-pentanedione during beer fermentation. *Journal of the American Society of Brewing Chemists*, *64*(1), 52-60. doi:10.1094/asbcj-64-0052

Refractive Index of Ethanol Solutions. (2011). Refractive index of ethanol solutions Retrieved June 26, 2018, from http://www.refractometer.pl/refraction-datasheet-ethanol.

Rege, S. U., & Yang, R. T. (2001). A novel FTIR method for studying mixed gas adsorption at low concentrations: H_2O and CO_2 on NaX zeolite and γ-alumina. *Chemical Engineering Science, 56*(12), 3781-3796. doi:10.1016/s0009-2509(01)00095-1.

Renger, R. S., van Hateren, S. H., & Luyben, K. C. A. M. (1992). The formation of esters and higher alcohols during brewery fermentation; The effect of carbon dioxide pressure. *Journal of the Institute of Brewing, 98*(6), 509-513. doi:10.1002/j.2050-0416.1992.tb01137.x

Rodrigues, J. A., Barros, A. A., Cruz, J. M. M., & Ferreira, A. A. (1997). Determination of diacetyl in beer using differential-pulse polarography. *Journal of the Institute of Brewing*, *103*(5), 311-314. doi:10.1002/j.2050-0416.1997.tb00962.x

Rodrigues, J. A., Barros, A. A., & Rodrigues, P. G. (1999). Differential pulse polarographic determination of α-dicarbonyl compounds in foodstuffs after derivatization with *o*-phenylenediamine. *Journal of Agricultural and Food Chemistry, 47*(8), 3219-3222. doi:10.1021/jf980856b

Rodrigues, P. G., Rodrigues, J. A., Barros, A. A., Lapa, R. A. S., Lima, J. L. F. C., Machado Cruz, J. M., & Ferreira, A. A. (2002). Automatic flow system with voltammetric detection for diacetyl monitoring during brewing process. *Journal of Agricultural and Food Chemistry, 50*(13), 3647-3653. doi:10.1021/jf011625z

Schaden, S., Haberkorn, M., Frank, J., Baena, J. R., & Lendl, B. (2004). Direct determination of carbon dioxide in aqueous solution using mid-infrared quantum cascade lasers. *Applied Spectroscopy, 58*(6), 667-670. doi:10.1366/000370204872971

Schädle, T., Pejcic, B., Myers, M., & Mizaikoff, B. (2016). Portable mid-infrared sensor system for monitoring CO_2 and CH_4 at high pressure in geosequestration scenarios. *ACS Sensors, 1*(4), 413-419. doi:10.1021/acssensors.5b00246

Science History Institute. (1950). Bausch & Lomb "abbe-56" Refractometer. *Analytical Chemistry, 22*(4), 50A-50A. doi:10.1021/ac60040a758

Thomas, T. (2004). Acetaldehyde, a key yeast metabolite and oxidation product, *Waterhouse Lab UC Davis*. Retrieved April 28, 2019, from https://waterhouse.ucdavis.edu/whats-in-wine/acetaldehyde

Wang, J., Wang, X., Hui, X., Hua, S., Li, H., & Gao, W. (2017). Determination of diacetyl in beer by a precolumn derivatization-HPLC-UV method using 4-(2,3-dimethyl-6-quinoxalinyl)-1,2-benzenediamine as a derivatizing reagent. *Journal of Agricultural and Food Chemistry*, *65*(12), 2635-2641. doi:10.1021/acs.jafc.7b00990

Watson, H., Decloedt, A., Vanderputten, D., & Van Landschoot, A. (2018). Variation in gluten protein and peptide concentrations in Belgian barley malt beers. *Journal of the Institute of Brewing*, *124*(2), 148-157. doi:10.1002/jib.487

Yunfei, B., Hao, W., and Shun, N., (2012). Determination of diacetyl (butanedione) and pentanedione in beer by HS-GC. College of Food Science and Nutritional Engineering, China Agriculture University. *Agilent Technologies*, Application Note, 1-4.

Zahm & Nagel. (n.d.). CO_2 and air testing. Retrieved November 25, 2019, from http://www.zahmnagel.com/product-category/testing-equipment/co2-and-air-testing

APPENDIX

SB-FTIR

The SB-FTIR was used to explore ethanol spectra at varying concentrations. Ethanol concentrations were not verified using the refractometer. The following table illustrates Trials 1, 2, and 3 out of 10. Below is also the standard curve of ethanol measured at 1045 cm^{-1}.

The following plot of Ethanol versus Absorbance illustrates the standard curve of the signal at $\tilde{\upsilon}$ ~1045 cm^{-1} overall 10 trials.

SB-FTIR							
Trial 1	ῡ=1045.202	Trial 2	ῡ=1045.812	Trial 3	ῡ=1045.812	Avg	
0	0	0	0	0	0	0	0
1	0.00568	1	0.00622	1	0.00669	1	0.006197
2	0.00925	2	0.00849	2	0.00710	2	0.008280
3	0.01410	3	0.01290	3	0.01460	3	0.013867
4	0.01920	4	0.01710	4	0.01600	4	0.017433
5	0.02310	5	0.02060	5	0.02360	5	0.022433
6	0.02730	6	0.02460	6	0.02740	6	0.026433
10	0.04590	10	0.04070	10	0.04360	10	0.043400

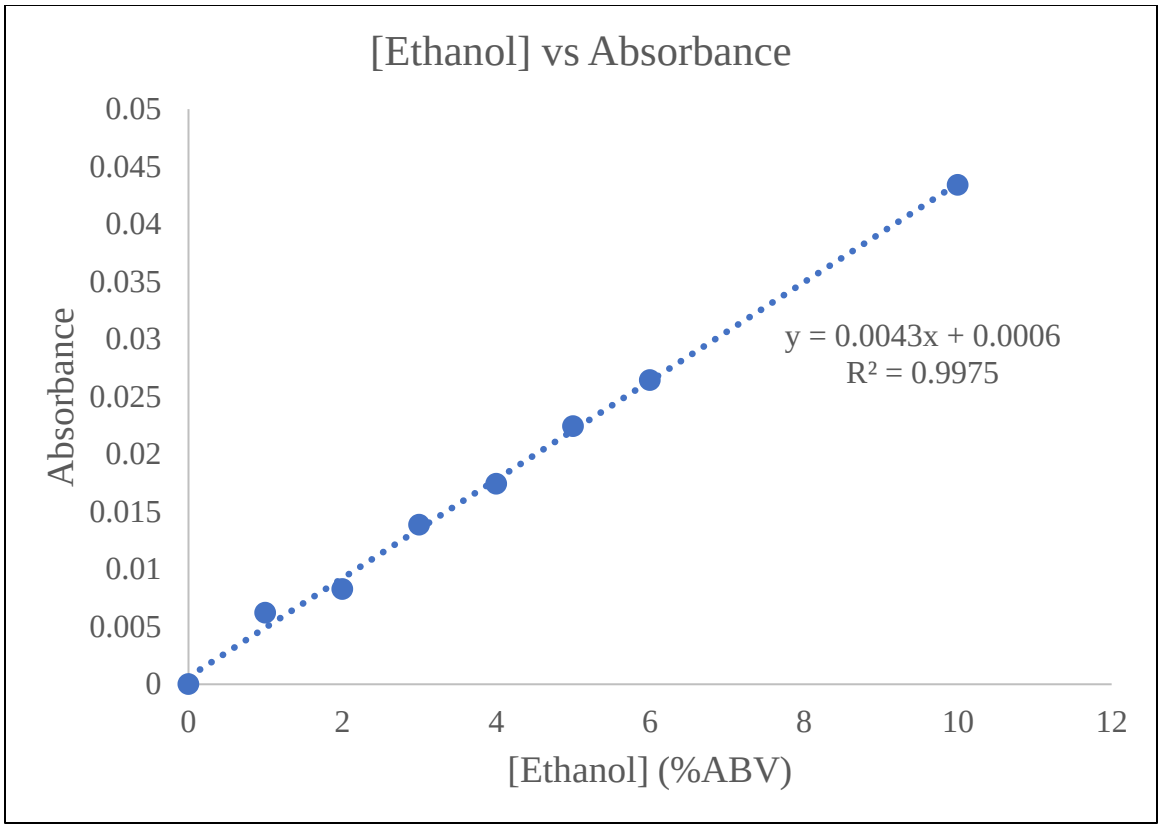
[Ethanol] vs Absorbance
Absorbance
0.05
0.045
0.04
0.035
0.03
0.025
0.02
0.015
0.01
0.005
0
0
2
4
6
8
10
12
[Ethanol] (%ABV)
y = 0.0043x + 0.0006
R² = 0.9975

MB-FTIR

The reaction of ethyl acetoacetate using a sodium phosphate buffer was performed at varying temperatures, using the MB-FTIR. Below is a table containing data for Trial 3 of 17. A plot at 75 ℃ and at 80 ℃ are shown below respectively. A plot of the data obtained from the decarboxylation of ethyl acetoacetate as a function of time is below. Data were from the reaction performed at 80 ℃. Data were from the reaction performed at 75 ℃. An IR spectrum of the data collected 75 ℃ is shown below giving results at $\tilde{\upsilon}$ = 2349.9 cm^{-1}.

65 ℃		75 ℃		80 ℃	
Time(min)	Absorbance	Time(min)	Absorbance	Time(min)	Absorbance
0	0	0	0	0	0
90	0.00421	1.5	0.0144	1.5	0.00265
180	0.00684	3	0.3939	3	0.01260
270	0.00870	4.5	0.4107	4.5	0.00621
360	0.00910	6	0.4289	6	0.00343

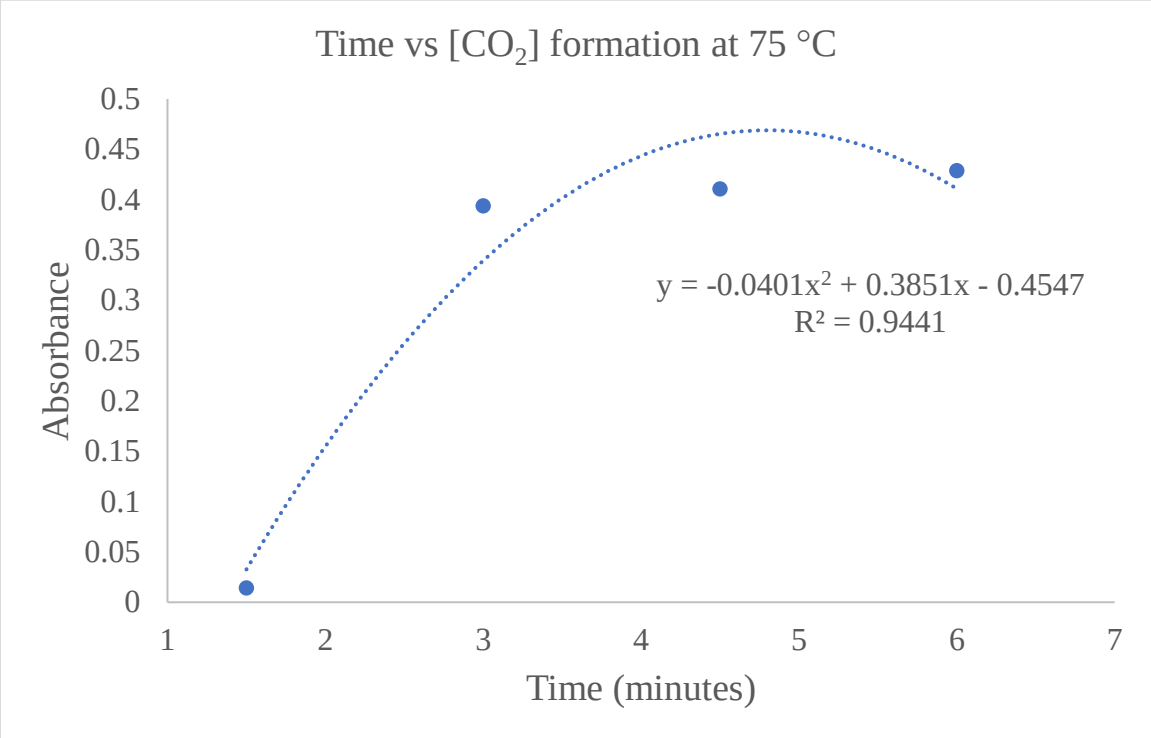

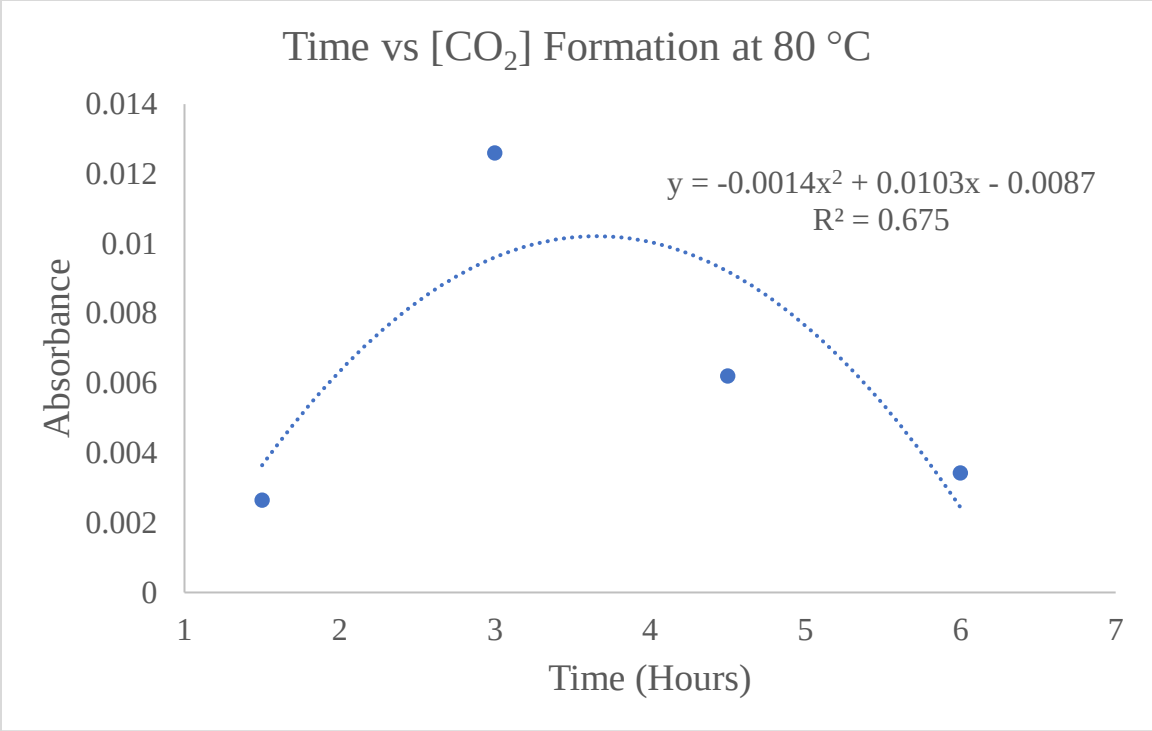
Time vs [CO2] Formation at 80 °C
y = -0.0014x2 + 0.0103x - 0.0087
R2 = 0.675
Absorbance
0.014
0.012
0.01
0.008
0.006
0.004
0.002
0
1
2
3
4
5
6
7
Time (Hours)

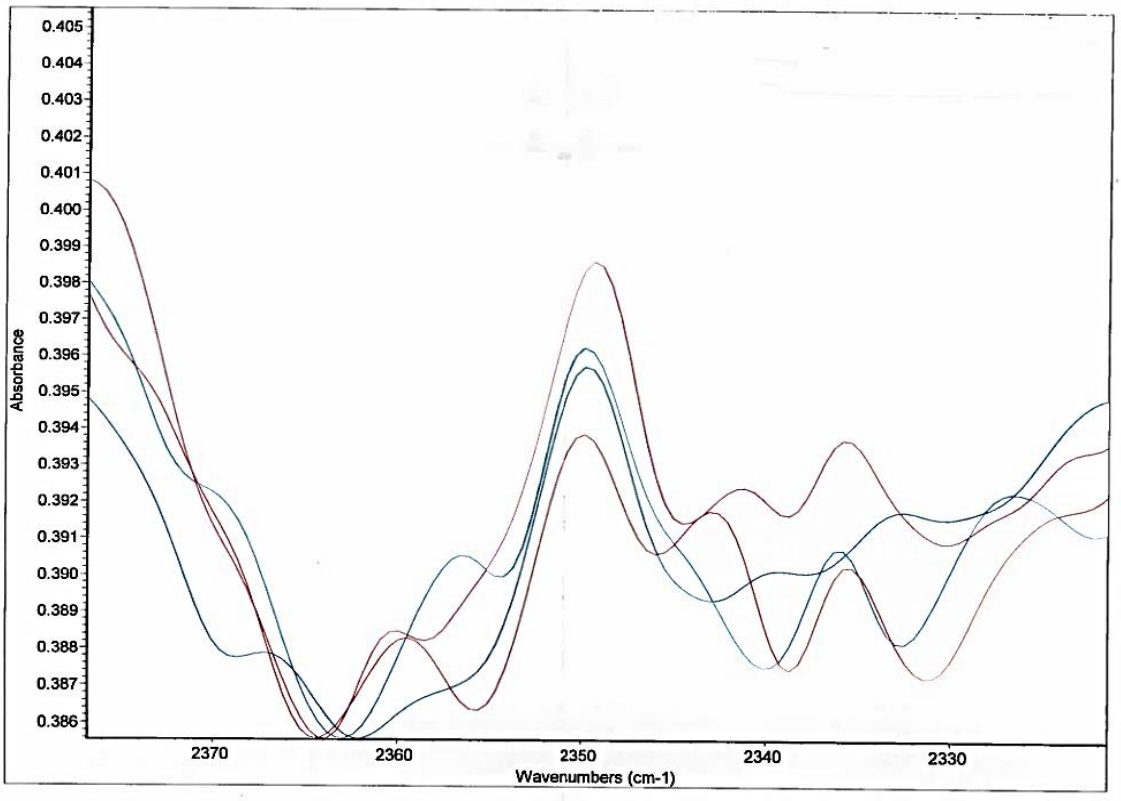
Absorbance
0.405
0.404
0.403
0.402
0.401
0.400
0.399
0.398
0.397
0.396
0.395
0.394
0.393
0.392
0.391
0.390
0.389
0.388
0.387
0.386
2370
2360
2350
2340
2330
Wavenumbers (cm-1)

An ethanol analysis at varying concentrations was performed using the MB-FTIR. Ethanol concentrations were verified using the refractometer. Trials 1-5 out of 45 are in the table below. The ethanol percent was evaluated by comparison to the refractive index of the solution. Each sample was evaluated five times Below is a plot resembling the collected data. A stacked IR spectrum of the C-O signal for ethanol solutions and a deconvoluted IR signal for 11% ethanol are shown below illustrating that the major signal at 1045 cm^{-1} is unobstructed by other signals.

Ethanol	Trial 1	Trial 2	Trial 3	Trial 4	Trial 5	Average
%ABV	Absorbance	Absorbance	Absorbance	Absorbance	Absorbance	Absorbance
0	0	0	0	0	0	0
2.7	0.194	0.2	0.201	0.201	0.201	0.2
3.8	0.228	0.208	0.222	0.226	0.224	0.222
4.6	0.259	0.253	0.257	0.258	0.256	0.257
5.6	0.307	0.302	0.312	0.314	0.312	0.31
7.1	0.367	0.371	0.355	0.362	0.352	0.361
11	0.547	0.569	0.555	0.548	0.554	0.555

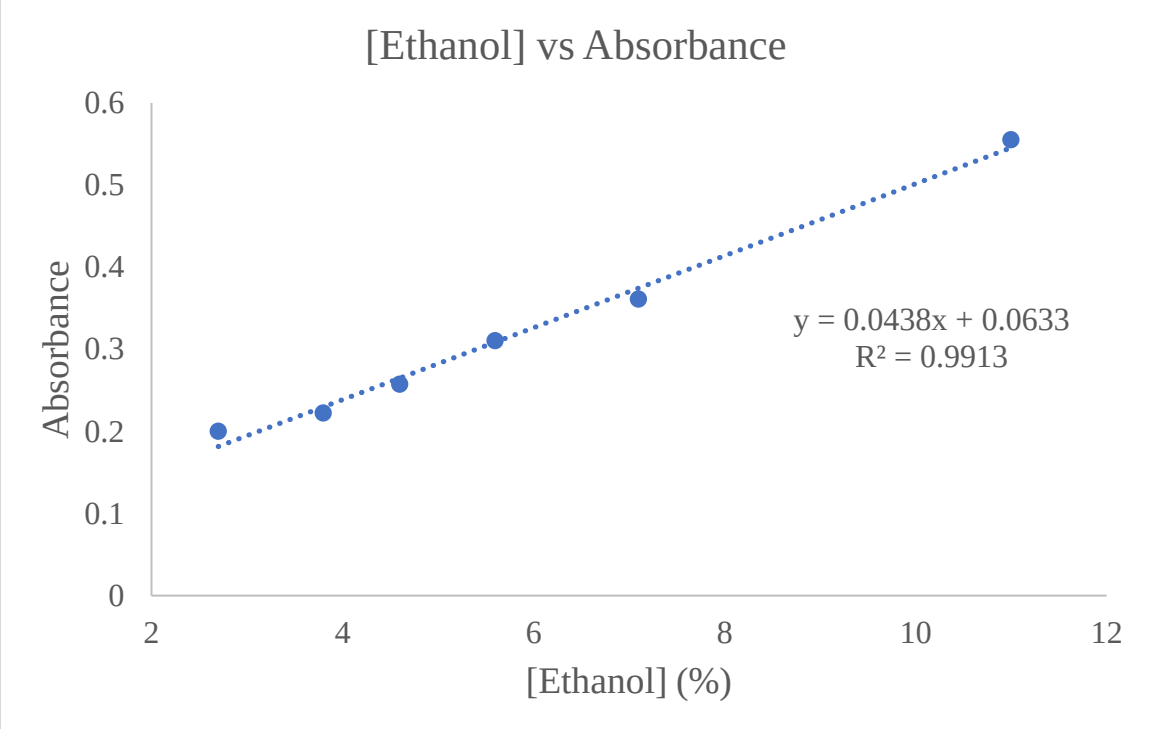

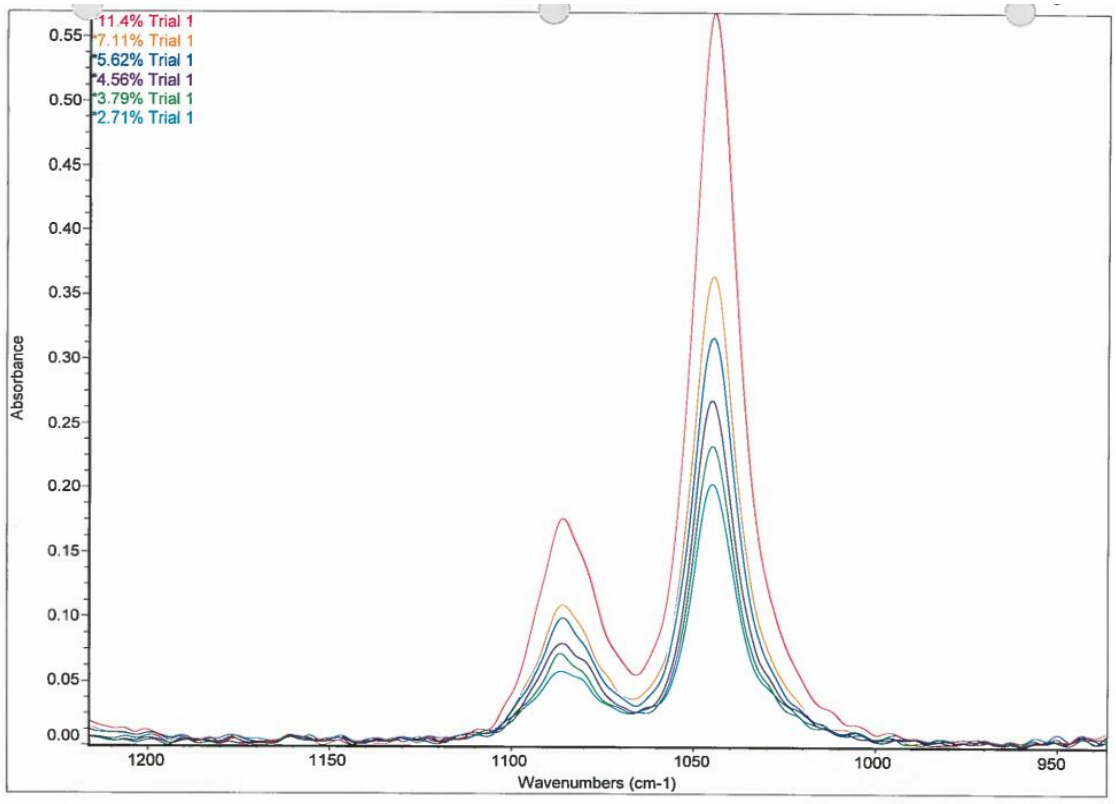
*11.4% Trial 1
*7.11% Trial 1
*5.62% Trial 1
*4.56% Trial 1
*3.79% Trial 1
*2.71% Trial 1
Absorbance
0.55
0.50
0.45
0.40
0.35
0.30
0.25
0.20
0.15
0.10
0.05
0.00
1200
1150
1100
1050
1000
950
Wavenumbers (cm-1)

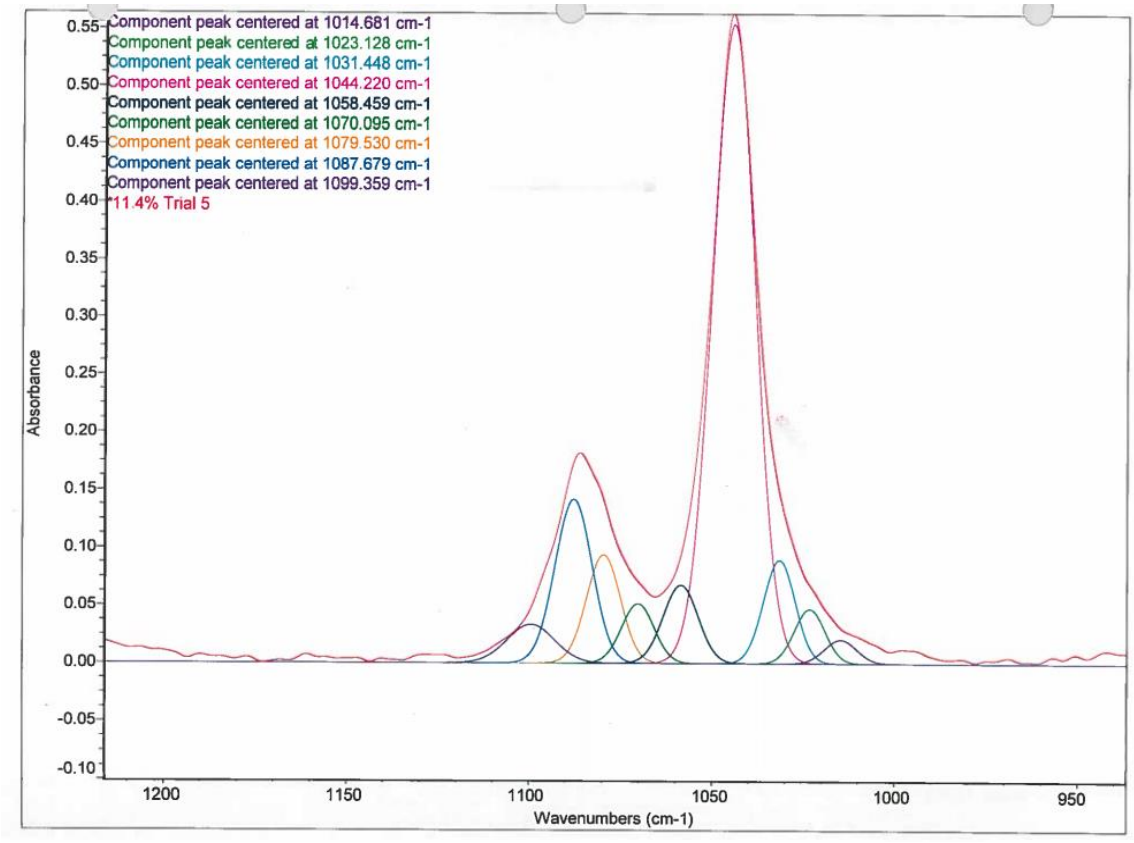
Component peak centered at 1014.681 cm-1
Component peak centered at 1023.128 cm-1
Component peak centered at 1031.448 cm-1
Component peak centered at 1044.220 cm-1
Component peak centered at 1058.459 cm-1
Component peak centered at 1070.095 cm-1
Component peak centered at 1079.530 cm-1
Component peak centered at 1087.679 cm-1
Component peak centered at 1099.359 cm-1
*11.4% Trial 5
Absorbance
0.55
0.50
0.45
0.40
0.35
0.30
0.25
0.20
0.15
0.10
0.05
0.00
-0.05
-0.10
1200
1150
1100
1050
1000
950
Wavenumbers (cm-1)

Acetone solutions were analyzed using the MB-FTIR. Concentrations could not be verified using the refractometer due to the lack of an acetone reference table. Trials 1-3 out of 15. Below is the table of the data collected from the IR spectrum. A plot of this data is also included, giving a standard curve of acetone using MB-FTIR. The IR spectrum of stacked data is also included, to show the various signals representing the vibrations of each degree of freedom acetone contains.

Acetone					
MB-FTIR	Absorbance				ῡ =1701.293
Trial	1%	3%	5%	7%	
1	0.565	1.128	1.668	2.850	
2	0.590	1.129	1.710	2.526	
3	0.598	1.120	1.703	2.506	
Average	0.584333	1.125667	1.693667	2.627333	

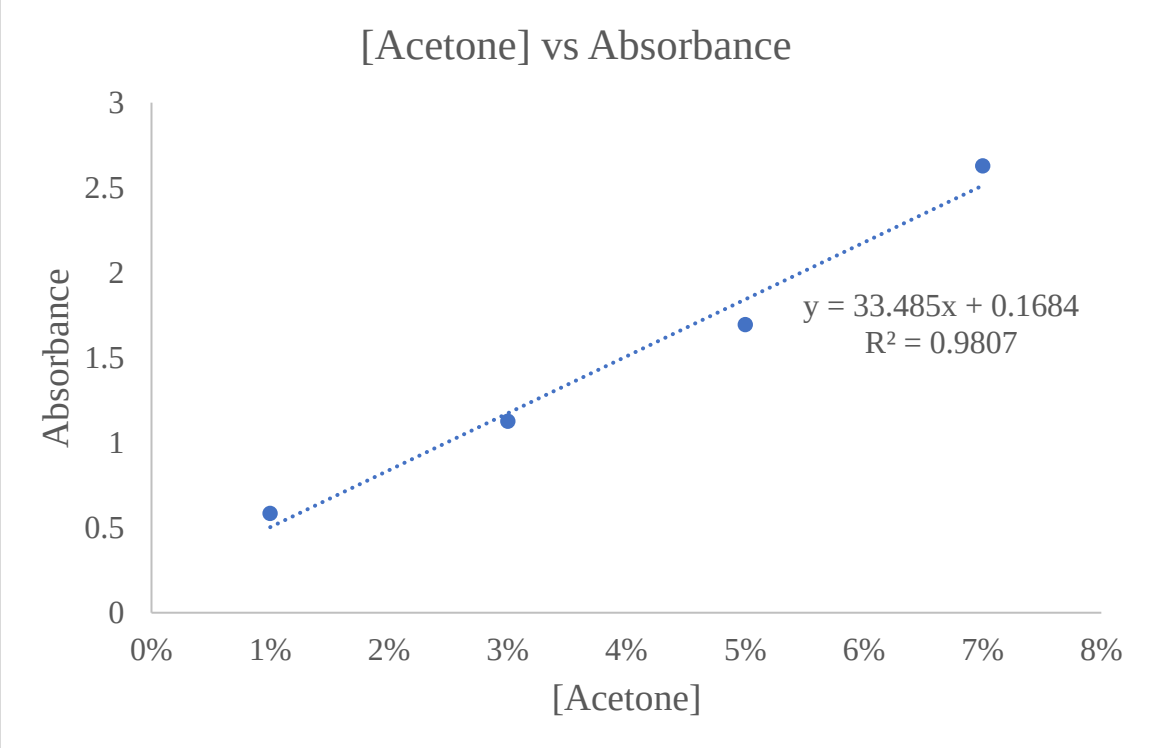

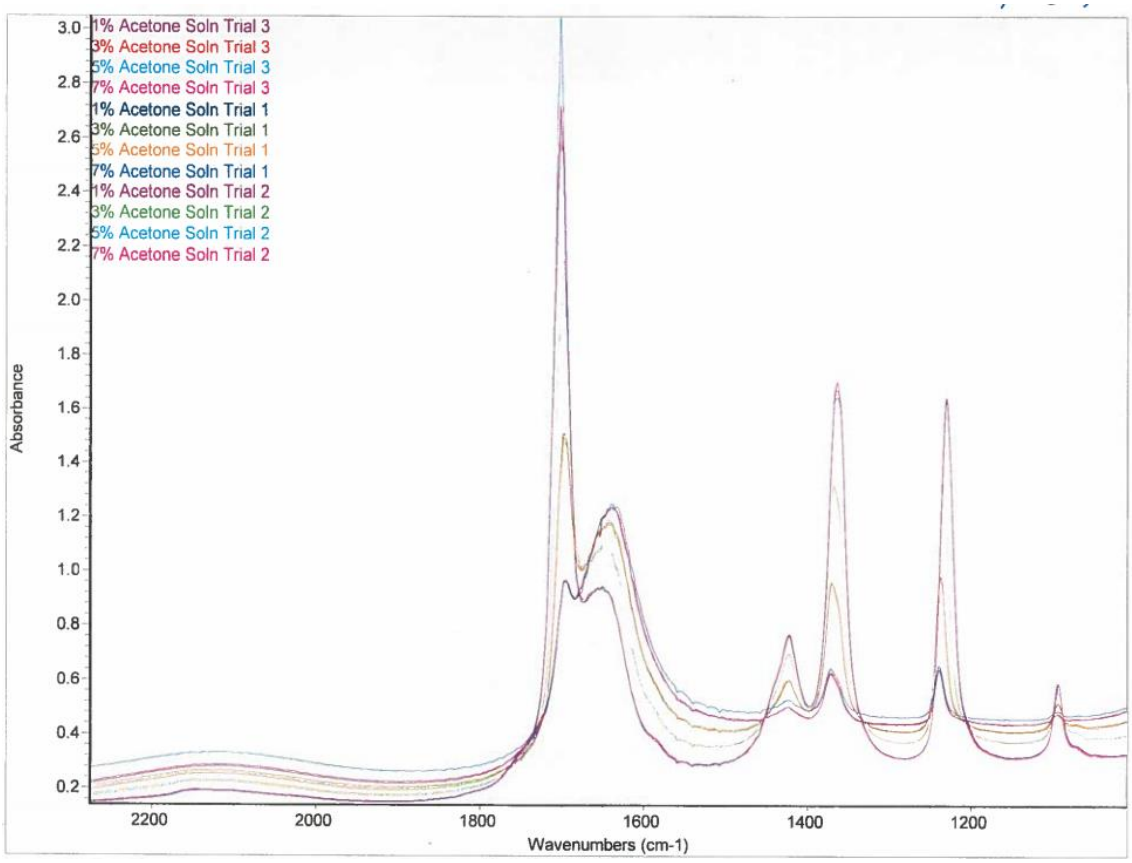
1% Acetone Soln Trial 3
3% Acetone Soln Trial 3
5% Acetone Soln Trial 3
7% Acetone Soln Trial 3
1% Acetone Soln Trial 1
3% Acetone Soln Trial 1
5% Acetone Soln Trial 1
7% Acetone Soln Trial 1
1% Acetone Soln Trial 2
3% Acetone Soln Trial 2
5% Acetone Soln Trial 2
7% Acetone Soln Trial 2
Absorbance
3.0
2.8
2.6
2.4
2.2
2.0
1.8
1.6
1.4
1.2
1.0
0.8
0.6
0.4
0.2
2200
2000
1800
1600
1400
1200
Wavenumbers (cm-1)

Acetaldehyde, another common off-flavor in beer, was analyzed using the MB-FTIR. Absorbance values and two different peak areas were analyzed. Trial 1 of 1. Below are two tables of the collected data, one for the absorbance values at three different wavenumbers, the other of the two areas. The peak areas for Area-1 show negative values, this is due to the area taken with more inversion of noise versus signals of noise. Below is the full IR spectrum of the collected data for each wavenumber and peak area of acetaldehyde.

Avg	1715	Avg	1382	Avg	1096	Avg	Area 1	Avg	Area 2
0	0.049667	1	0.057333	1	0.071667	1	-0.7623	1	2.026267
2	0.059333	2	0.061333	2	0.087	2	-0.56033	2	4.446967
5	0.092333	5	0.092333	5	0.155667	5	0.417	5	9.678
10	0.163	10	0.160667	10	0.286667	10	1.998	10	19.47433
15	0.217667	15	0.227333	15	0.417667	15	3.758333	15	30.421
20	0.283667	20	0.300667	20	0.566333	20	5.549333	20	42.82767
40	0.568333	40	0.595333	40	1.173	40	11.15033	40	93.54233

Average	Area-1	Average	Area-2
1	-0.76230	1	2.026267
2	-0.56033	2	4.446967
5	0.417000	5	9.678000
10	1.998000	10	19.47433
15	3.758333	15	30.42100
20	5.549333	20	42.82767
40	11.15033	40	93.54233

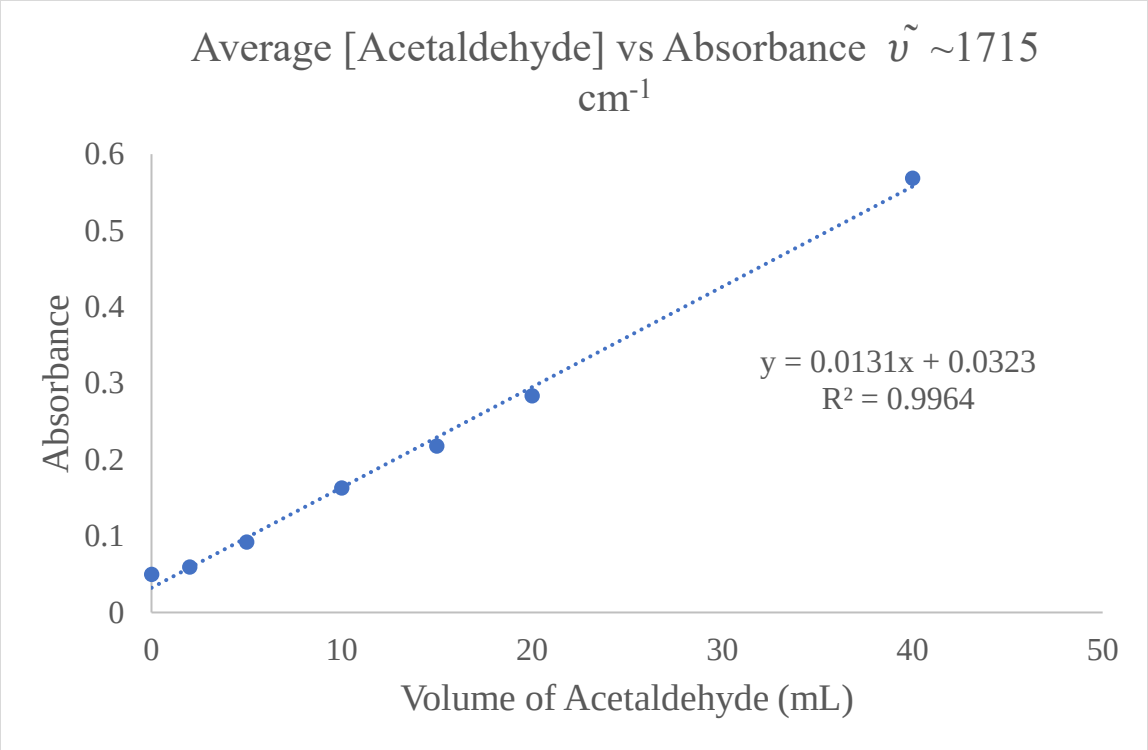
Average [Acetaldehyde] vs Absorbance $\tilde{\upsilon}$ ~1715 cm-1
Absorbance
0.6
0.5
0.4
0.3
0.2
0.1
0
y = 0.0131x + 0.0323
R² = 0.9964
0
10
20
30
40
50
Volume of Acetaldehyde (mL)

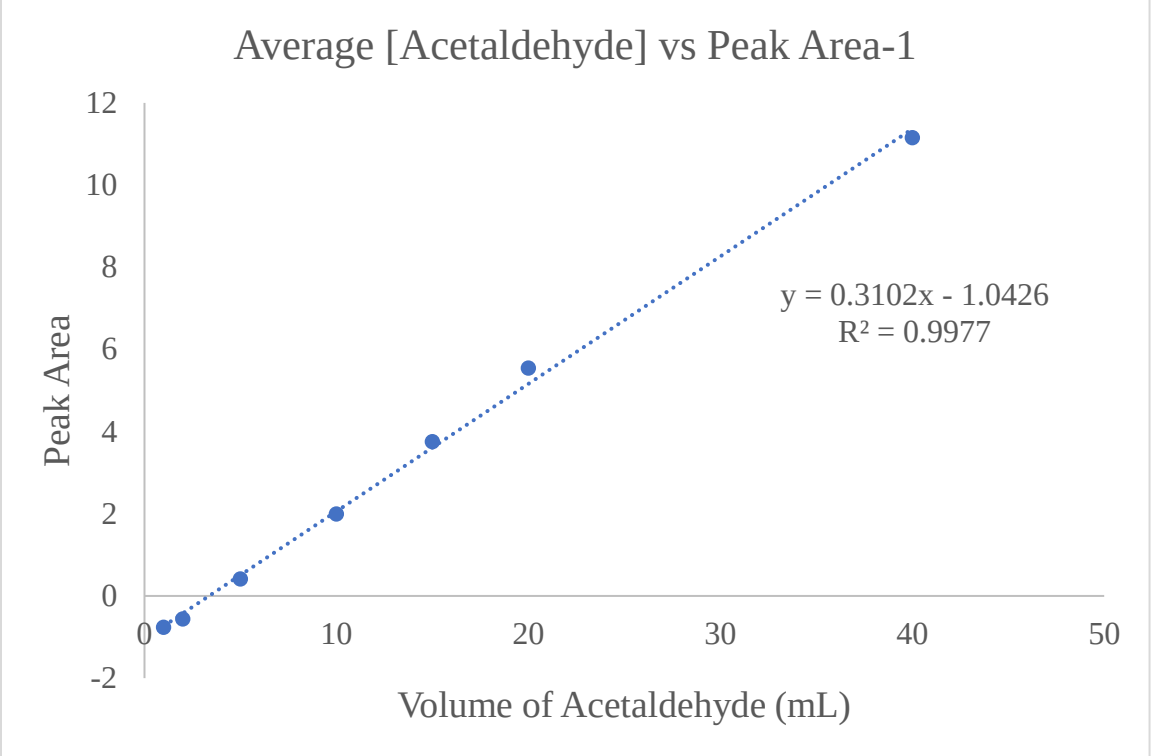
Average [Acetaldehyde] vs Peak Area-1
Peak Area
12
10
8
6
4
2
0
-2
y = 0.3102x - 1.0426
R² = 0.9977
0
10
20
30
40
50
Volume of Acetaldehyde (mL)

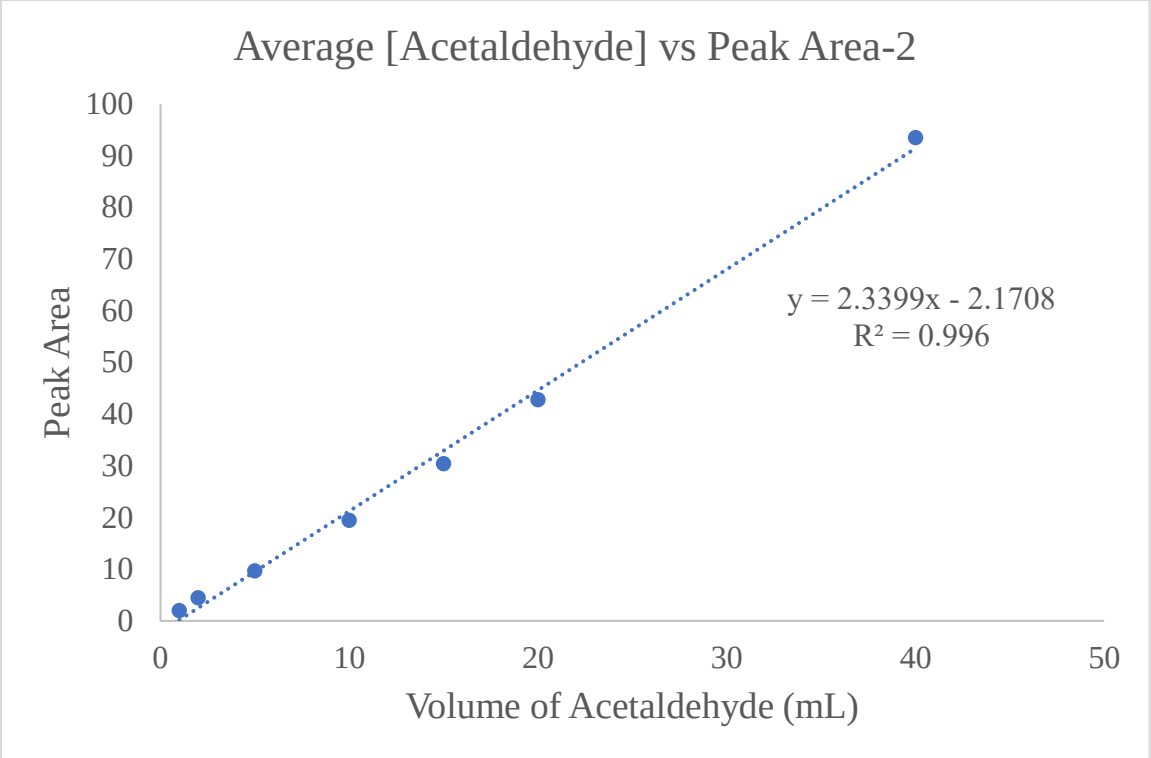
Average [Acetaldehyde] vs Peak Area-2
Peak Area
Volume of Acetaldehyde (mL)
y = 2.3399x - 2.1708
R² = 0.996
0
10
20
30
40
50
60
70
80
90
100

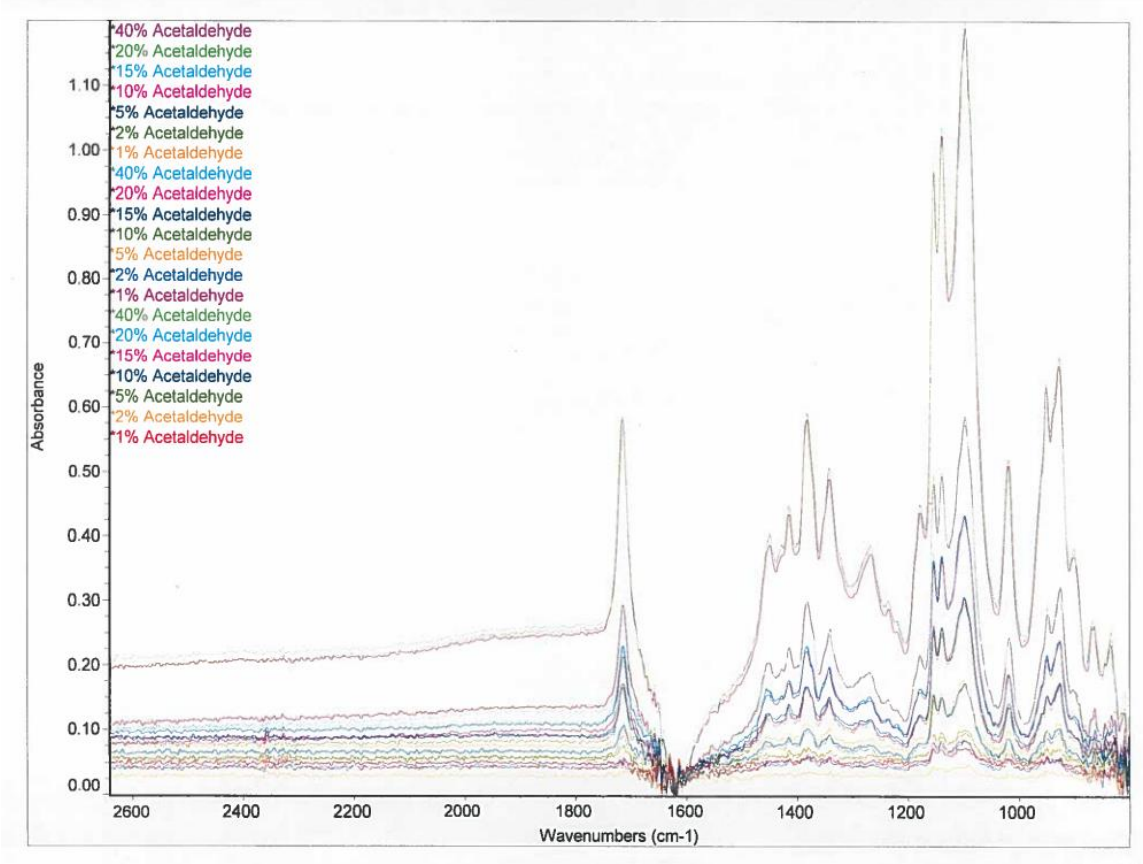
40% Acetaldehyde
20% Acetaldehyde
15% Acetaldehyde
10% Acetaldehyde
5% Acetaldehyde
2% Acetaldehyde
1% Acetaldehyde
40% Acetaldehyde
20% Acetaldehyde
15% Acetaldehyde
10% Acetaldehyde
5% Acetaldehyde
2% Acetaldehyde
1% Acetaldehyde
40% Acetaldehyde
20% Acetaldehyde
15% Acetaldehyde
10% Acetaldehyde
5% Acetaldehyde
2% Acetaldehyde
1% Acetaldehyde
Absorbance
Wavenumbers (cm-1)
0.00
0.10
0.20
0.30
0.40
0.50
0.60
0.70
0.80
0.90
1.00
1.10
2600
2400
2200
2000
1800
1600
1400
1200
1000

A porter style of beer was made on campus and those wort solutions were taken from a fermentation vessel over a 207-hour period. The data collected is in the results section, however, the IR spectra both hot and cold (respectively) at 63 hours are below.

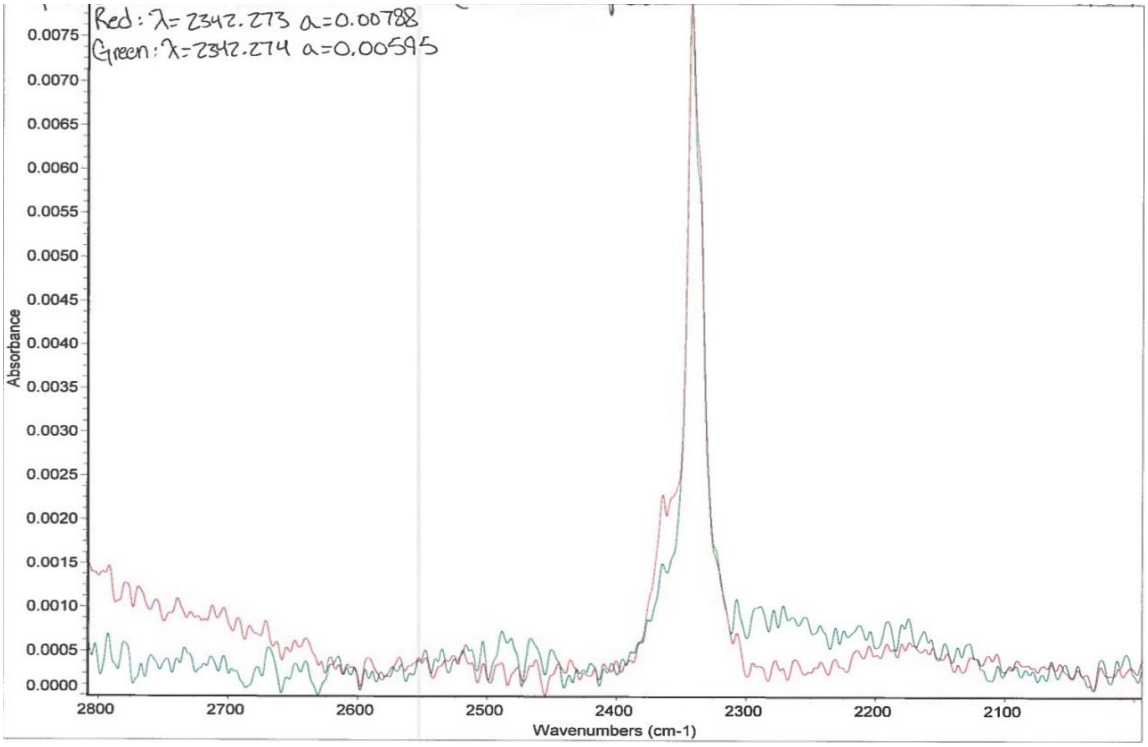

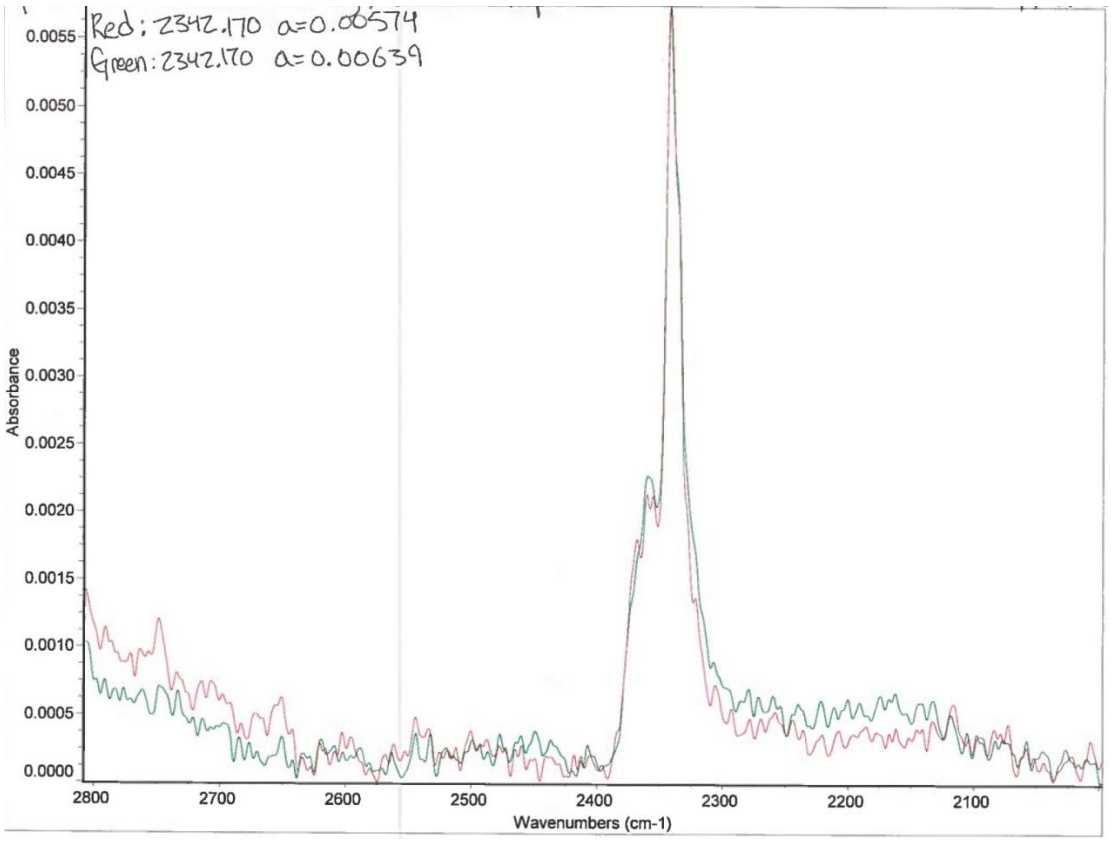

A wort solution was made at 1.0389 specific gravity and spiked with 10.00 mL of 200 proof ethanol (~4.7 %ABV) with the addition of Red Star® active dry yeast. Half of the solutions did not have a yeast addition; the other half did. Trial 1 of 1. Below is a table showing the results collected from the IR spectra for the solutions containing yeast. Below are plots for the data collected for 3 different wavenumbers that were analyzed. There are two IR spectra below of superimposed trials onto one another, one for the solutions containing yeast, the other for the solutions not containing yeast.

Avg mL	1045 cm^{-1} Absorbance	Avg mL	1084 cm^{-1} Absorbance	Avg mL	879 cm^{-1} Absorbance
0	0.090333	0	0.067667	0	0.031000
5	0.186000	5	0.097667	5	0.054333
10	0.273667	10	0.122333	10	0.069000
15	0.347333	15	0.140000	15	0.084667
20	0.439333	20	0.179333	20	0.112000

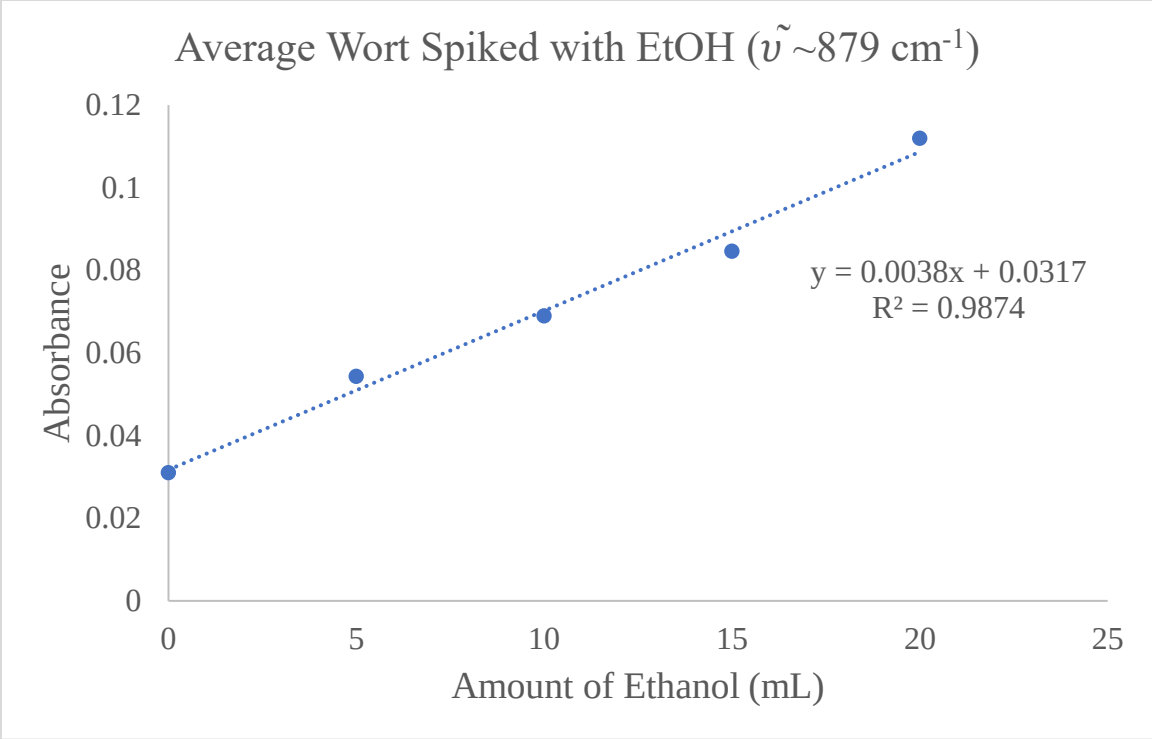
Average Wort Spiked with EtOH ($\tilde{\upsilon}$ ~879 cm^{-1})
Absorbance
0.12
0.1
0.08
0.06
0.04
0.02
0
y = 0.0038x + 0.0317
R² = 0.9874
0
5
10
15
20
25
Amount of Ethanol (mL)

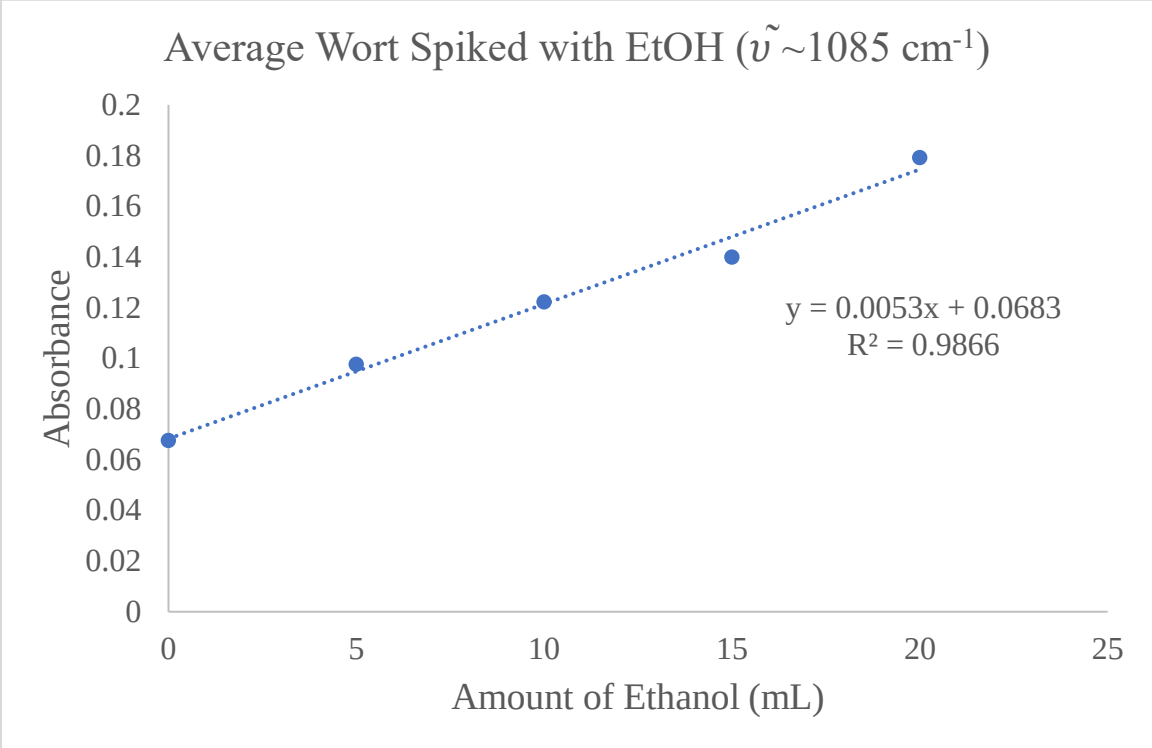
Average Wort Spiked with EtOH ($\tilde{\upsilon}$ ~1085 cm^{-1})
Absorbance
0.2
0.18
0.16
0.14
0.12
0.1
0.08
0.06
0.04
0.02
0
y = 0.0053x + 0.0683
R² = 0.9866
0
5
10
15
20
25
Amount of Ethanol (mL)

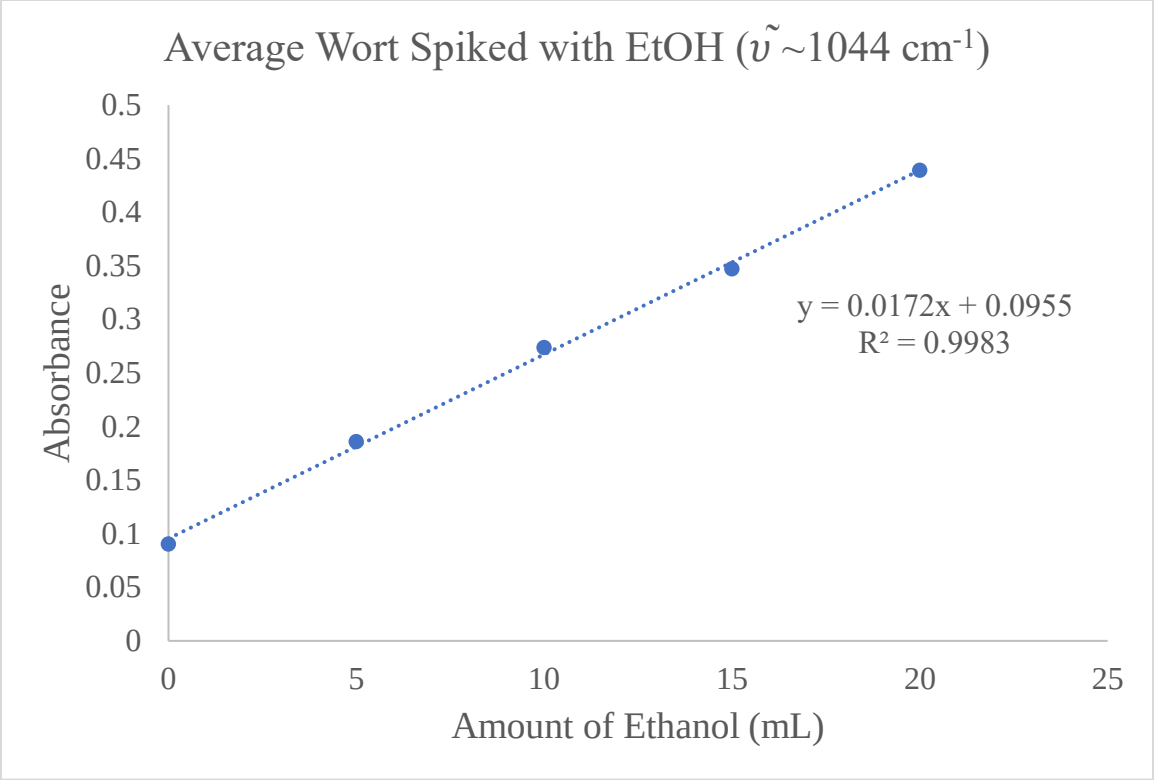
Average Wort Spiked with EtOH ($\tilde{\upsilon}$ ~1044 cm^{-1})
Absorbance
0.5
0.45
0.4
0.35
0.3
0.25
0.2
0.15
0.1
0.05
0
0
5
10
15
20
25
Amount of Ethanol (mL)
y = 0.0172x + 0.0955
R² = 0.9983

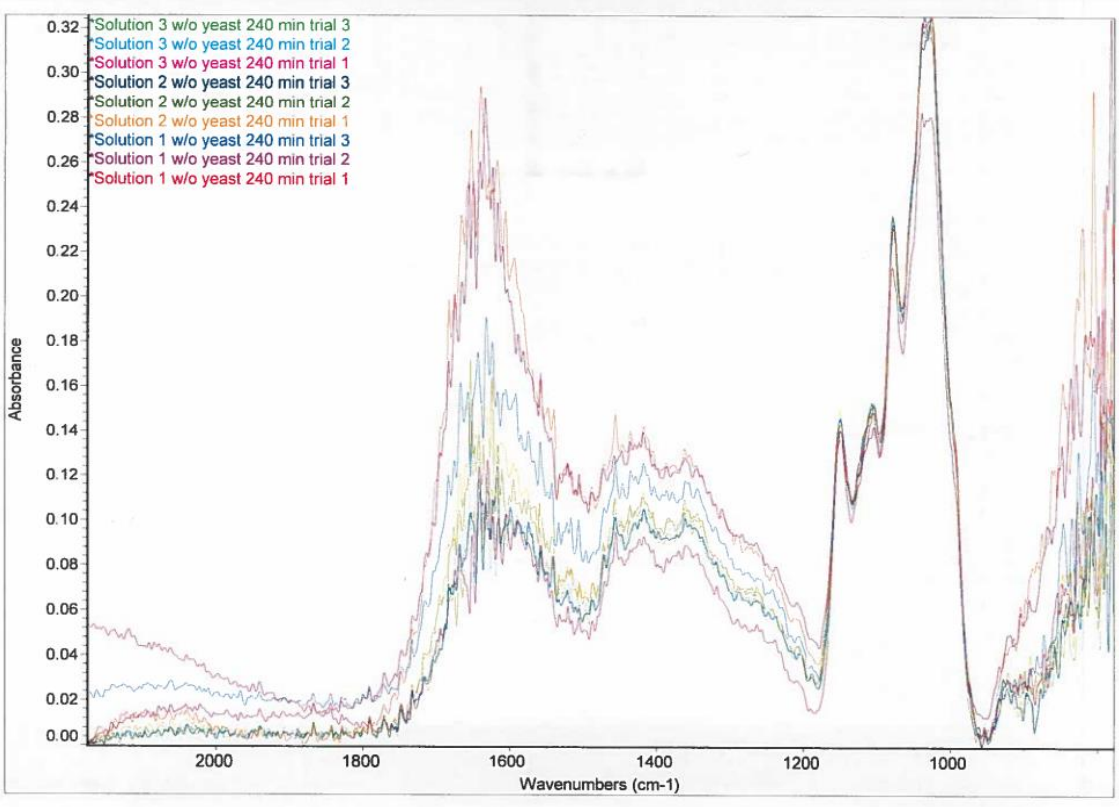
Solution 3 w/o yeast 240 min trial 3
Solution 3 w/o yeast 240 min trial 2
Solution 3 w/o yeast 240 min trial 1
Solution 2 w/o yeast 240 min trial 3
Solution 2 w/o yeast 240 min trial 2
Solution 2 w/o yeast 240 min trial 1
Solution 1 w/o yeast 240 min trial 3
Solution 1 w/o yeast 240 min trial 2
Solution 1 w/o yeast 240 min trial 1
Absorbance
0.32
0.30
0.28
0.26
0.24
0.22
0.20
0.18
0.16
0.14
0.12
0.10
0.08
0.06
0.04
0.02
0.00
2000
1800
1600
1400
1200
1000
Wavenumbers (cm-1)

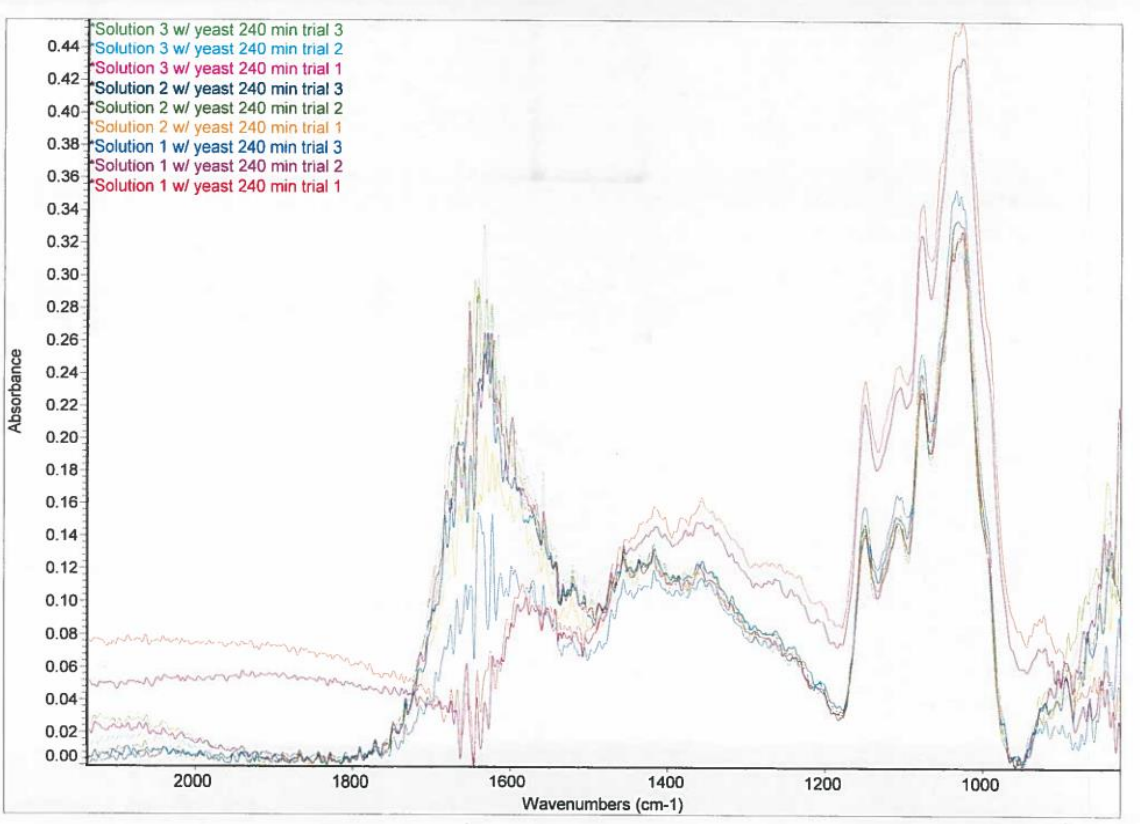
Solution 3 w/ yeast 240 min trial 3
Solution 3 w/ yeast 240 min trial 2
Solution 3 w/ yeast 240 min trial 1
Solution 2 w/ yeast 240 min trial 3
Solution 2 w/ yeast 240 min trial 2
Solution 2 w/ yeast 240 min trial 1
Solution 1 w/ yeast 240 min trial 3
Solution 1 w/ yeast 240 min trial 2
Solution 1 w/ yeast 240 min trial 1
Absorbance
0.44
0.42
0.40
0.38
0.36
0.34
0.32
0.30
0.28
0.26
0.24
0.22
0.20
0.18
0.16
0.14
0.12
0.10
0.08
0.06
0.04
0.02
0.00
2000
1800
1600
1400
1200
1000
Wavenumbers (cm-1)

Beer solutions were analyzed using the MB-FTIR. Below is the IR spectrum for one of the beer samples (Double IPA) at $\tilde{\upsilon}$ ~1045 cm^{-1}. The table of data is in the results.

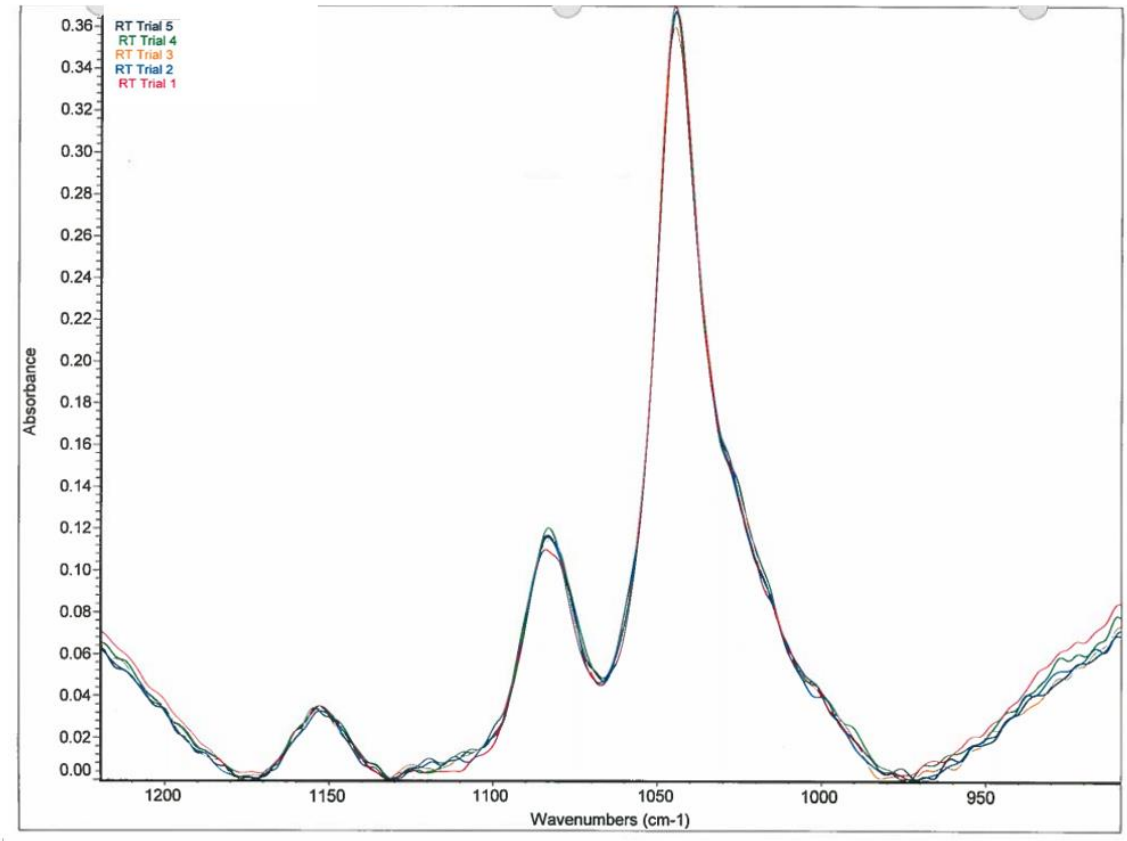

An American light lager (4.6 %ABV) was spiked with 200 proof ethanol to determine if there would be any interferences in the spectrum at $\tilde{\upsilon}$ ~1045 cm^{-1}. This was performed using the MB-FTIR, trial 1 of 1. It was determined that there are no interferences at the ethanol signal, the dissolved CO_2 is seen around $\tilde{\upsilon}$ = ~2450 cm^{-1}.

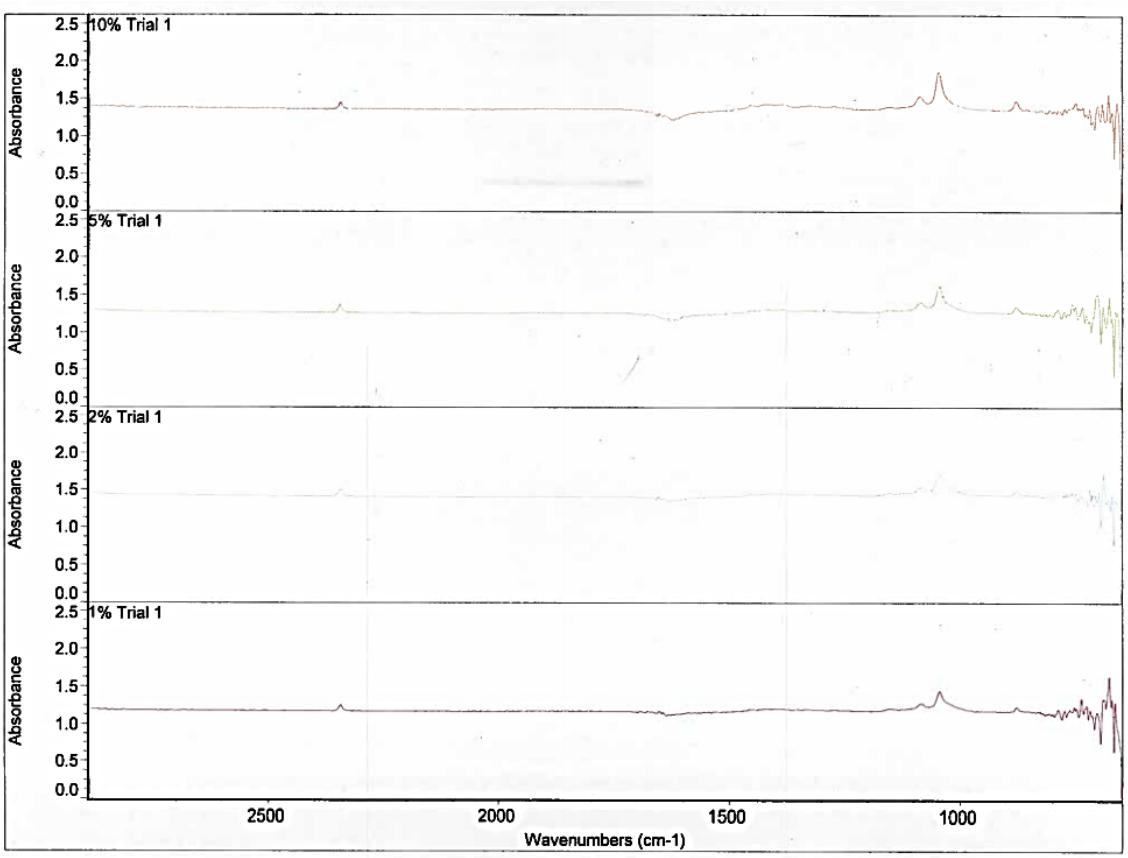

Ge Flow Cell

The reaction of ethyl acetoacetate in a sodium acetate buffer was analyzed using the Ge flow cell. The data organized into tables and graphs are located in the results section. Below is the IR spectral data with the N_2 gas purge. The sodium acetate buffer was interfering with signals; therefore, another buffer was selected. This was the conclusion after seeing no signals show in the IR spectrum.

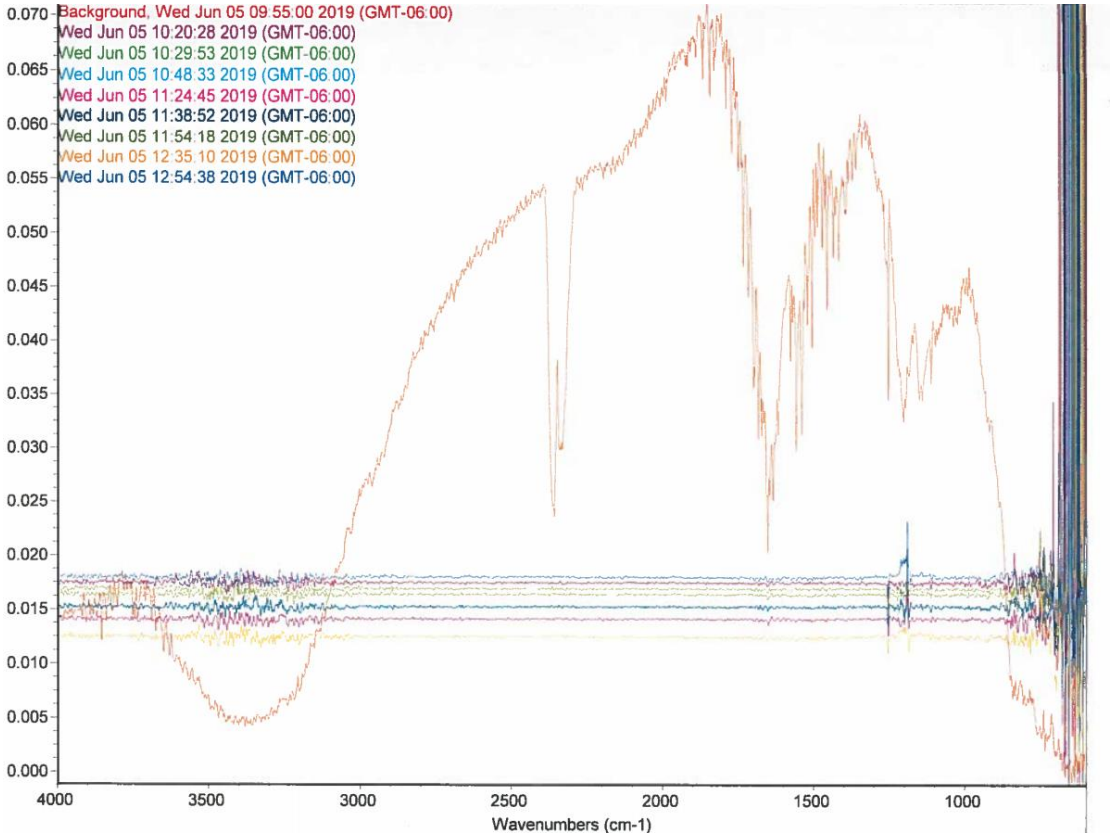

The reaction of ethyl acetoacetate in an acetonitrile and D.I. water solution was analyzed using the Ge flow cell. Data is in tables and graphs in the results section. Below is the IR spectral data with the N_2 gas purge. The signals shown below resemble the inversion of signals. This is due to more interference from the solvent mixtures (acetonitrile and water).

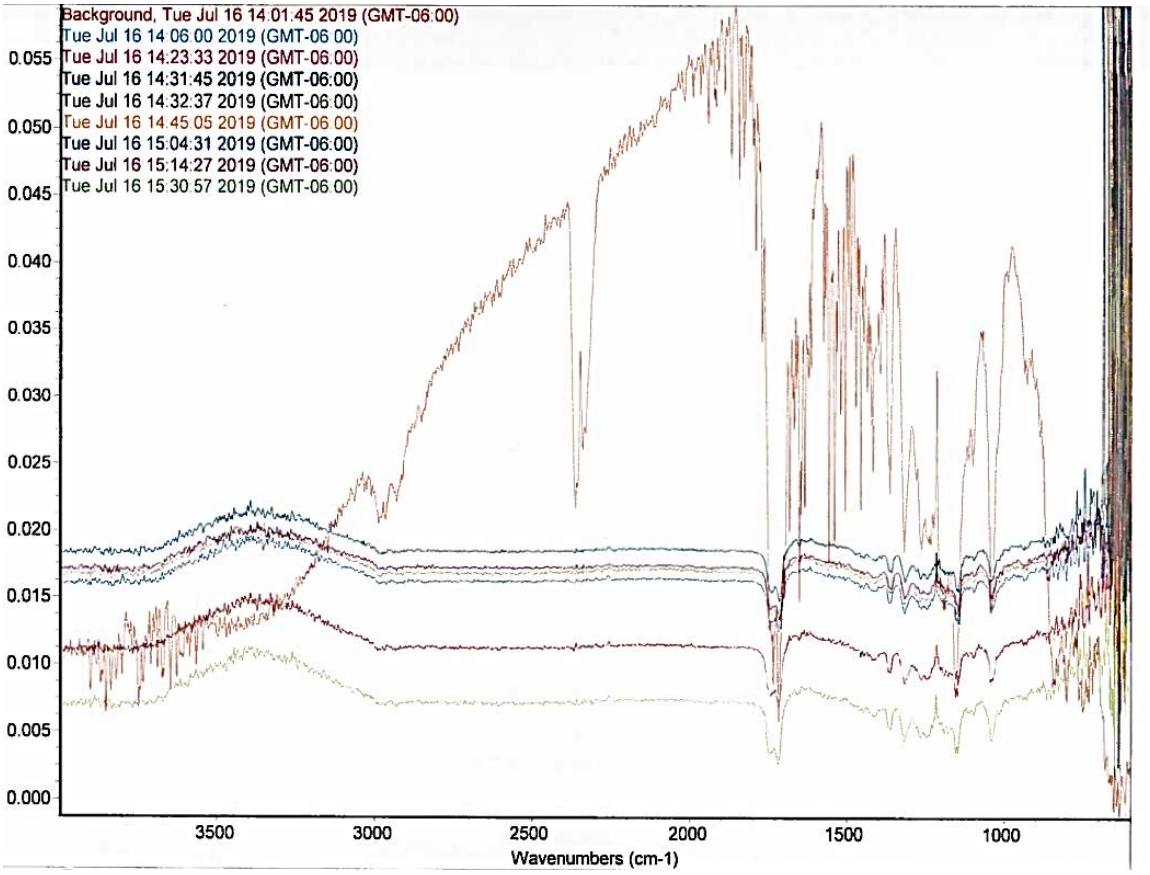

A seltzer water analysis was performed on the Ge flow cell. Below is an IR spectrum showing potential dissolved CO_2 signals. The seltzer water was chilled in a refrigerator for 24 hours minimum.

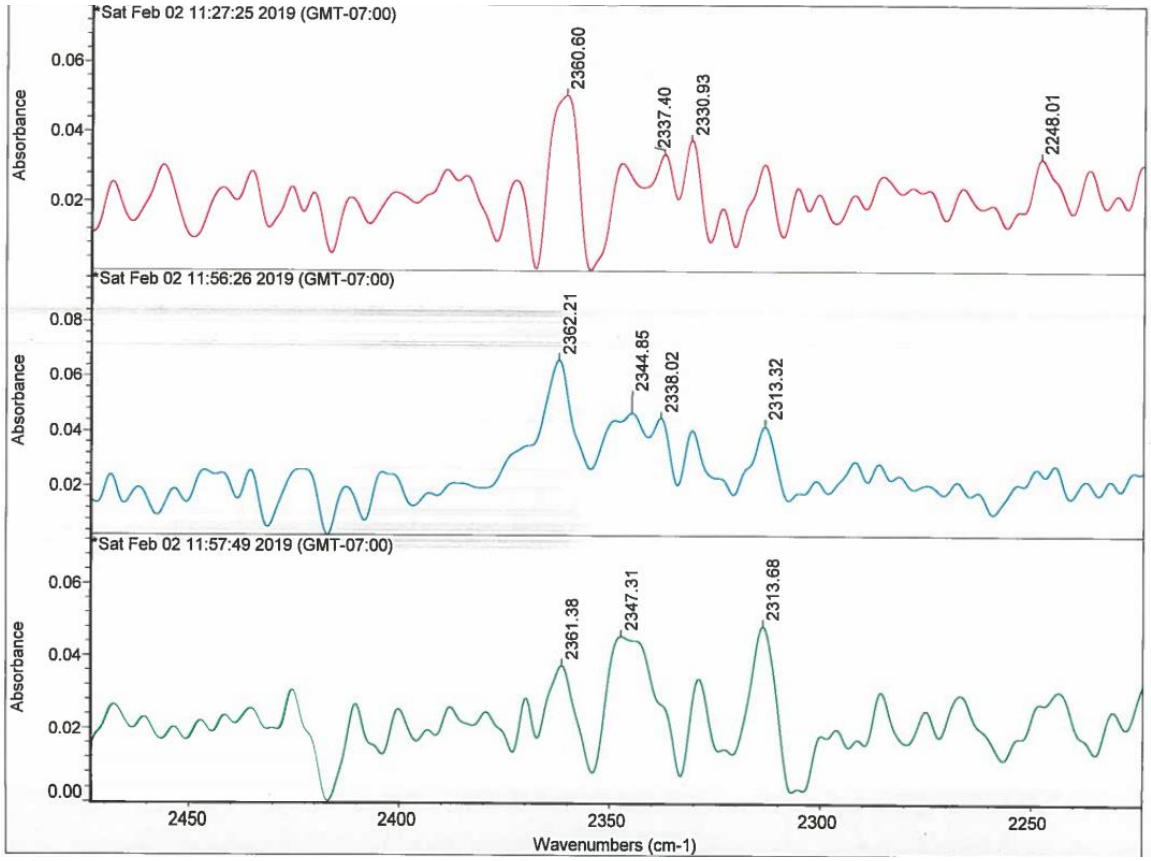

An American light lager (5.5 %ABV) was analyzed using the Ge flow cell to determine if ethanol signals could be detected during a 20-minute time-frame. The IR spectrum is below showing no significant signals for the CO_2 region due to decarbonation through the flow cell. The table below is the data collected from the IR spectrum of trial 1 of 3.

Beer	
Time (min)	Peak area
0	2.823
3	3.05
4	1.701
5	3.02
7	2.371
9	1.137
11	2.592
13	2.86
15	2.556
17	3.818

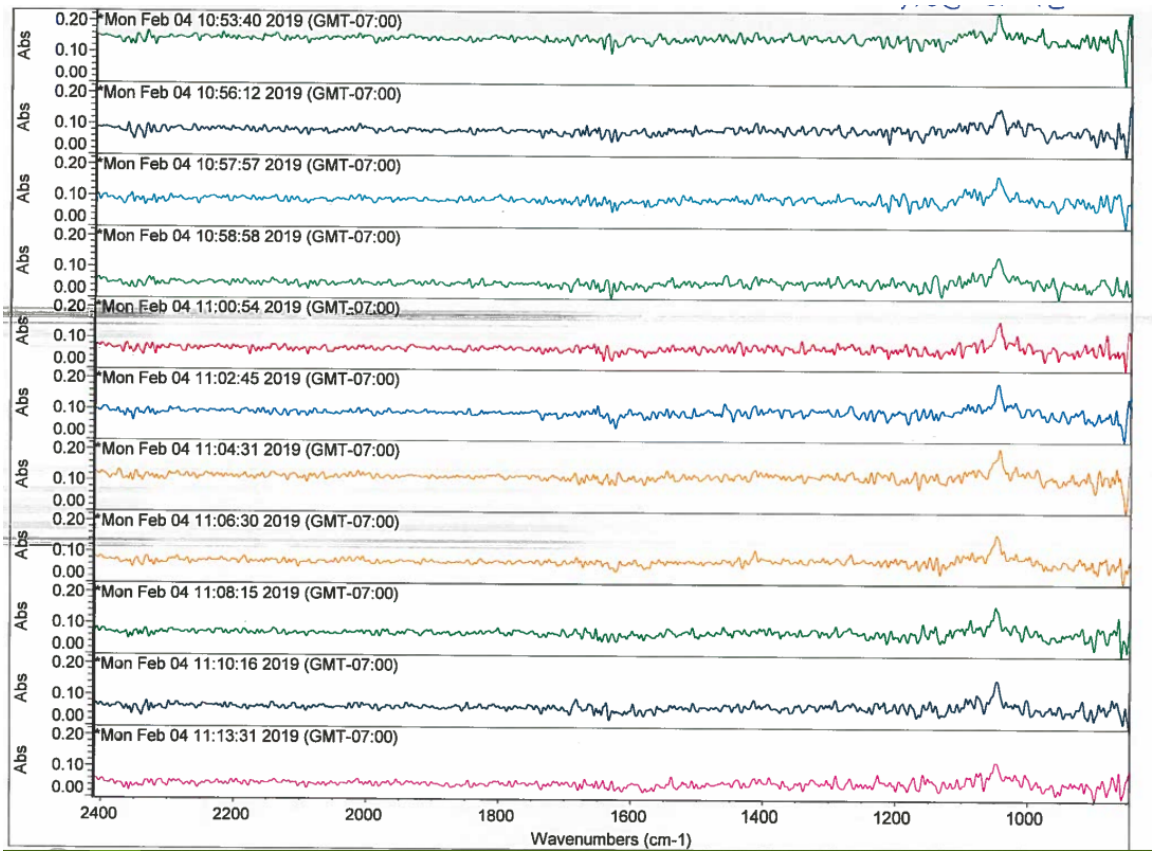

Beer	
Time (min)	Peak area
0	2.823
3	3.05
4	1.701
5	3.02
7	2.371
9	1.137
11	2.592
13	2.86
15	2.556
17	3.818

An ethanol analysis was performed using the Ge flow cell. Below is the table of data from the IR spectrum for [Ethanol] versus Absorbance at $\tilde{\upsilon}$ = 1048.3 cm^{-1}. for Trial 3 of 8, along with the standard curve. Also, below is the table for the data collected from the IR spectrum for peak area and the plot for the [Ethanol] vs Peak Area.

Trials	0%	1%	3%	5%	17%	41%	100%
1	0.093	0.076	0.104	0.114	0.161	0.294	0.454
2	0.08	0.086	0.112	0.135	0.162	0.298	0.483
3	0.094	0.085	0.109	0.113	0.187	0.294	0.648
4	0.072	0.069	0.116	0.111	0.236	0.279	0.694
5	0.066	0.073	0.127	0.153	0.235	0.299	0.757
Average	0.081	0.0778	0.1136	0.1252	0.1962	0.2928	0.6072
SD	0.0135	0.0015	0.0115	0.0195	0.037	0.0025	0.1515

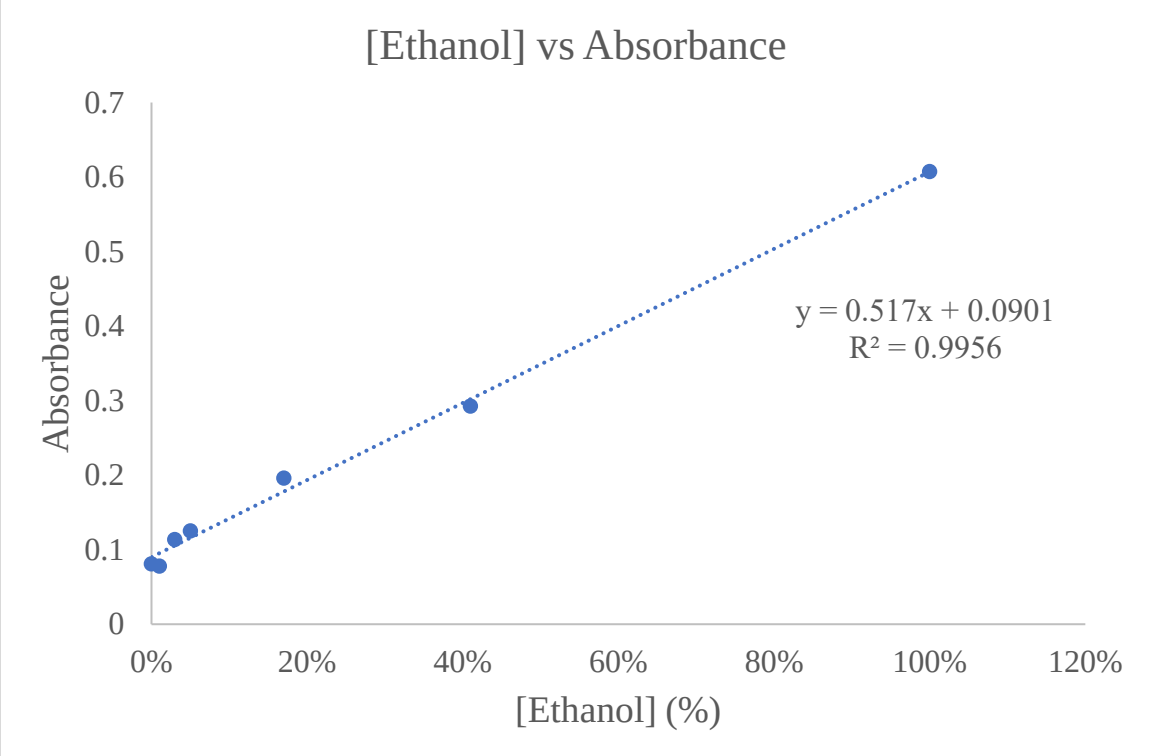

Trials	0%	1%	3%	5%	17%	41%	100%
1	2.293	3.129	4.439	5.792	6.366	12.054	21.151
2	2.082	5.347	3.545	3.399	7.426	10.054	21.405
3	2.049	3.924	5.767	5.065	9.492	12.941	30.937
4	0.528	4.629	7.22	10.61	8.811	14.441	32.25
5	4.184	7.289	6.488	3.944	8.706	15.615	33.147
Average	2.2272	4.8636	5.4918	5.762	8.1602	13.021	27.778
SD	0.9455	2.08	1.0245	0.924	1.17	1.7805	5.998

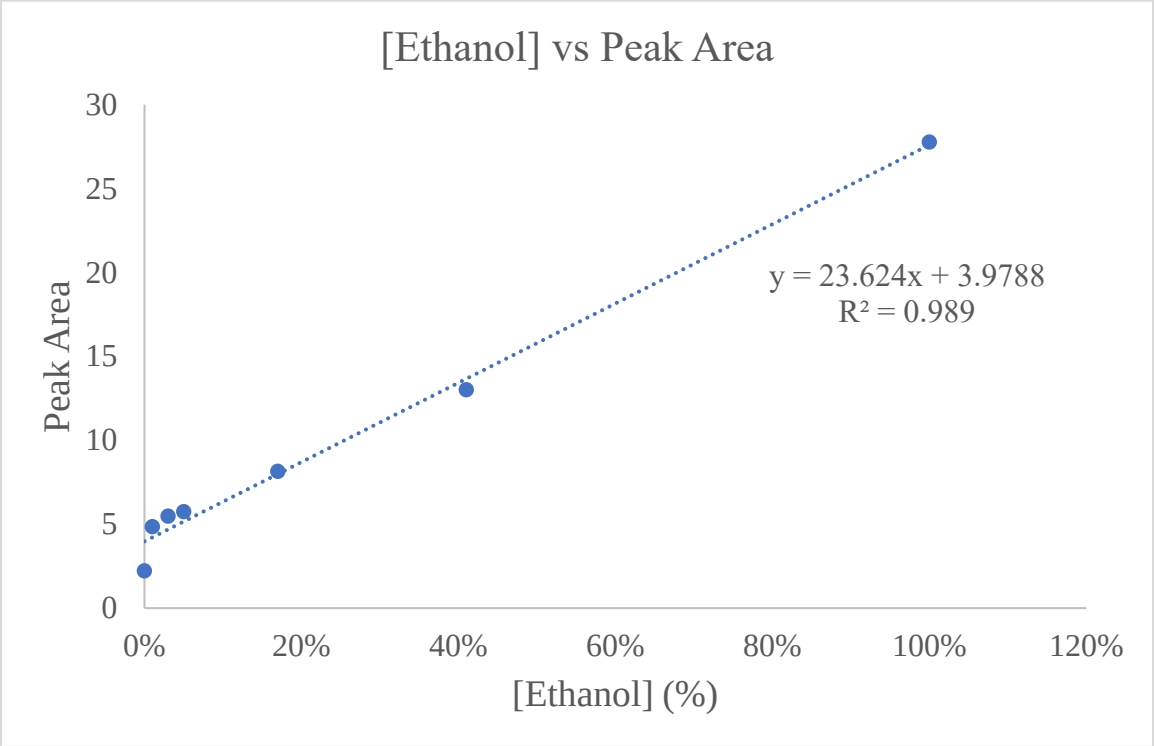

An acetone analysis was performed using the Ge flow cell. Below is the IR spectrum comparing acetone to D.I. water using a D.I. water background. The acetone signal can be seen at $\tilde{\upsilon}$ ~1696 cm^{-1}.

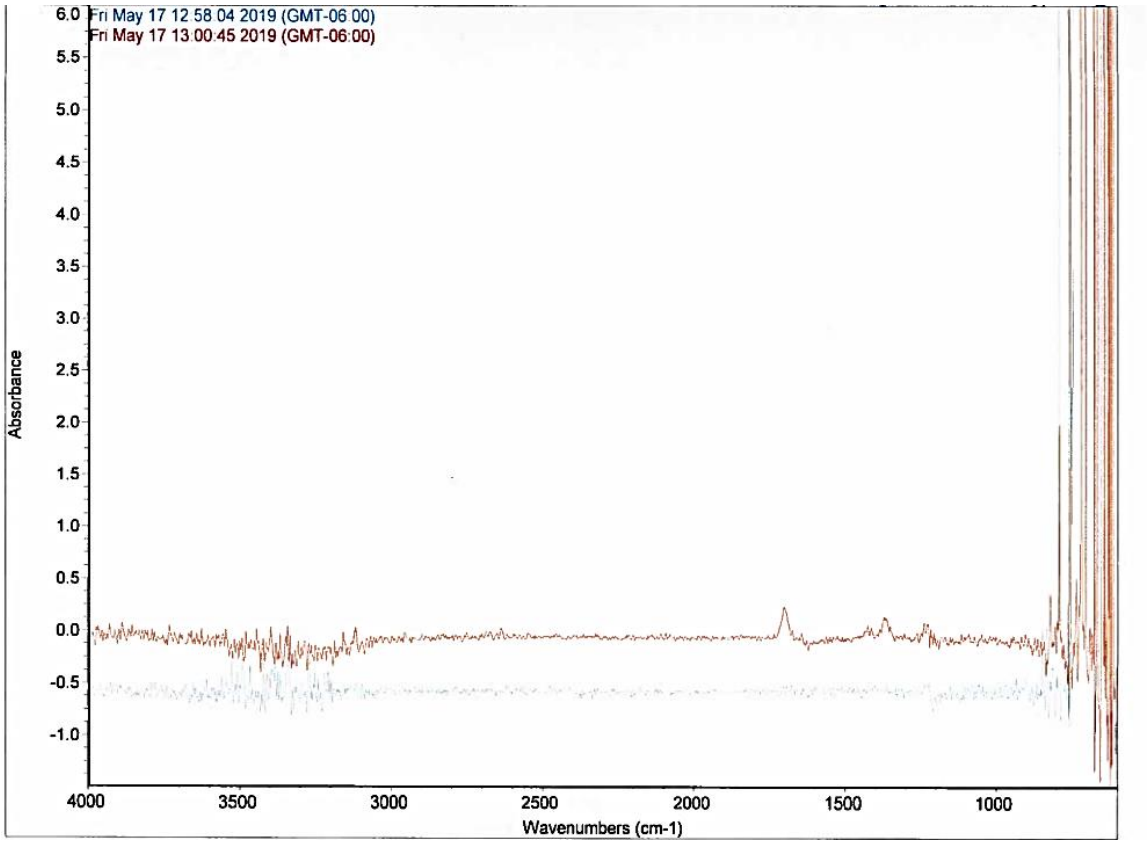

iS50 FTIR

Tonic water (Fevertree®) was analyzed using the iS50 FTIR. The water was chilled and poured onto the ZnSe sample cell. Below is the IR spectrum of three trials superimposed onto one another at $\tilde{\upsilon}$ ~2342.8 cm^{-1}. Trial 1 of 1.

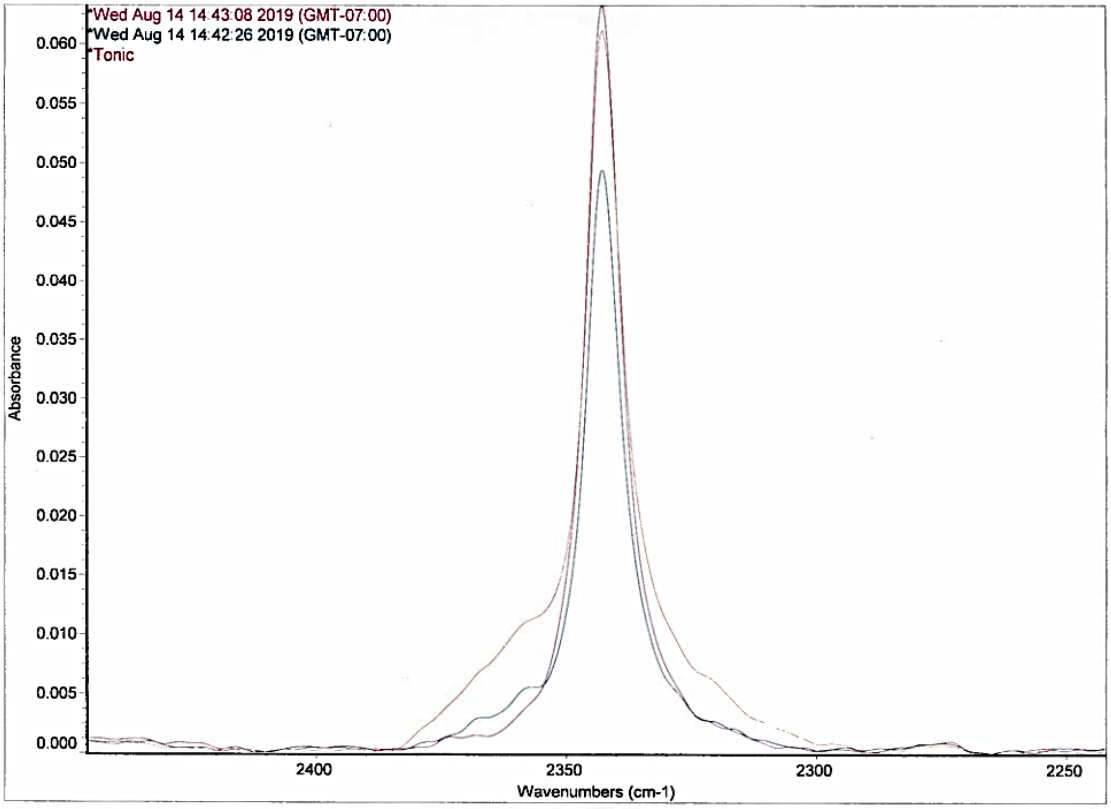

Diacetyl was also analyzed using the iS50 FTIR. The IR spectrum can be seen in the results section, below is a table of the data collected from trial 1 of 1. The plots below are for each wavenumber observed for this analyte, such as $\tilde{\upsilon}$ = 1717.5 cm^{-1}, $\tilde{\upsilon}$ = 1636.3 cm^{-1}, $\tilde{\upsilon}$ = 1045.8 cm^{-1}, and $\tilde{\upsilon}$ = 1122.9 cm^{-1}.

Diacetyl					
%	Absorbance	%	Absorbance	%	Absorbance
1	0.353	1	1.307	1	0.385
2	0.370	2	1.304	2	0.384
5	0.400	5	1.290	5	0.384
10	0.559	10	1.21	10	0.608
$\tilde{\upsilon}$ = 1717.542		$\tilde{\upsilon}$ = 1636.374		$\tilde{\upsilon}$ = 1045.875	
%	Absorbance	%	Absorbance		
1	0.350	1	0.376		
2	0.358	2	0.396		
5	0.374	5	0.430		
10	0.462	10	0.610		
$\tilde{\upsilon}$ = 1359.387		$\tilde{\upsilon}$ = 1122.985			

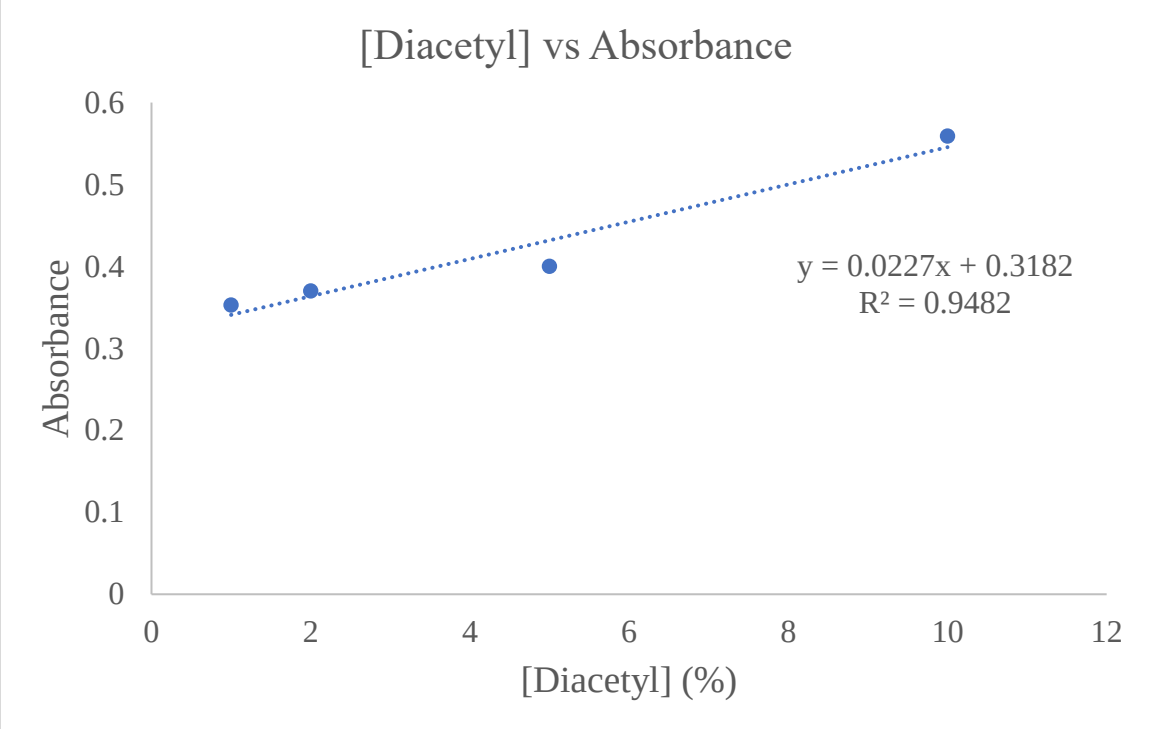

$\tilde{\upsilon}$ = 1717.5 cm^{-1}

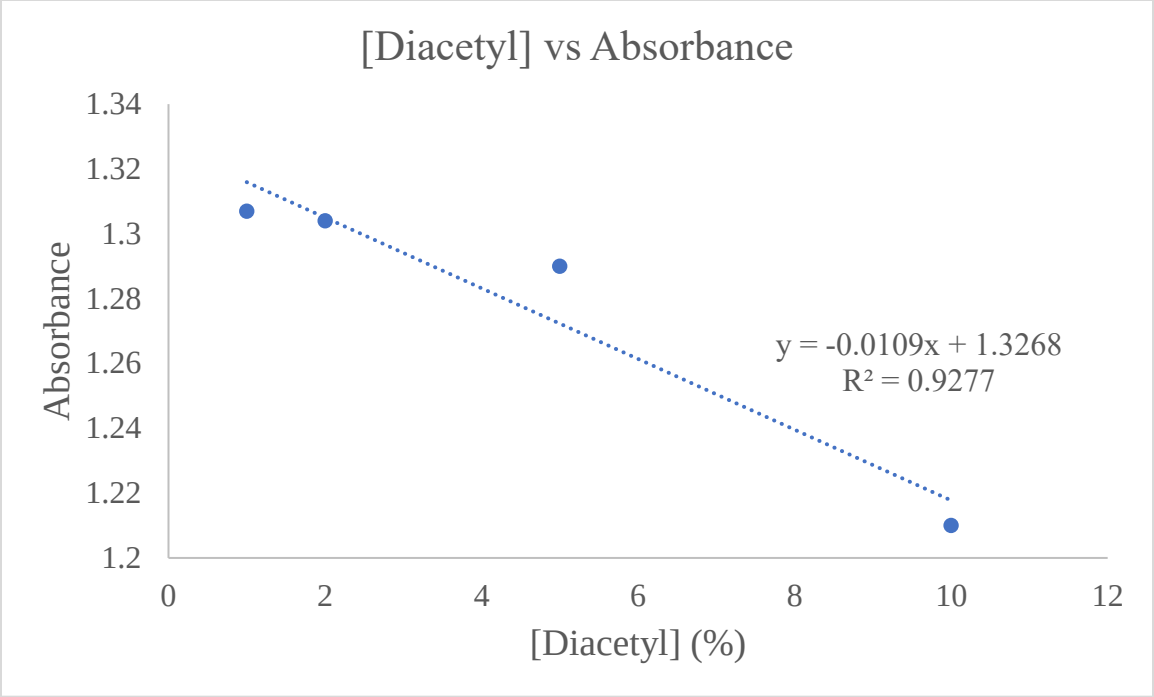

$\tilde{\upsilon}$ = 1636.3 cm^{-1}

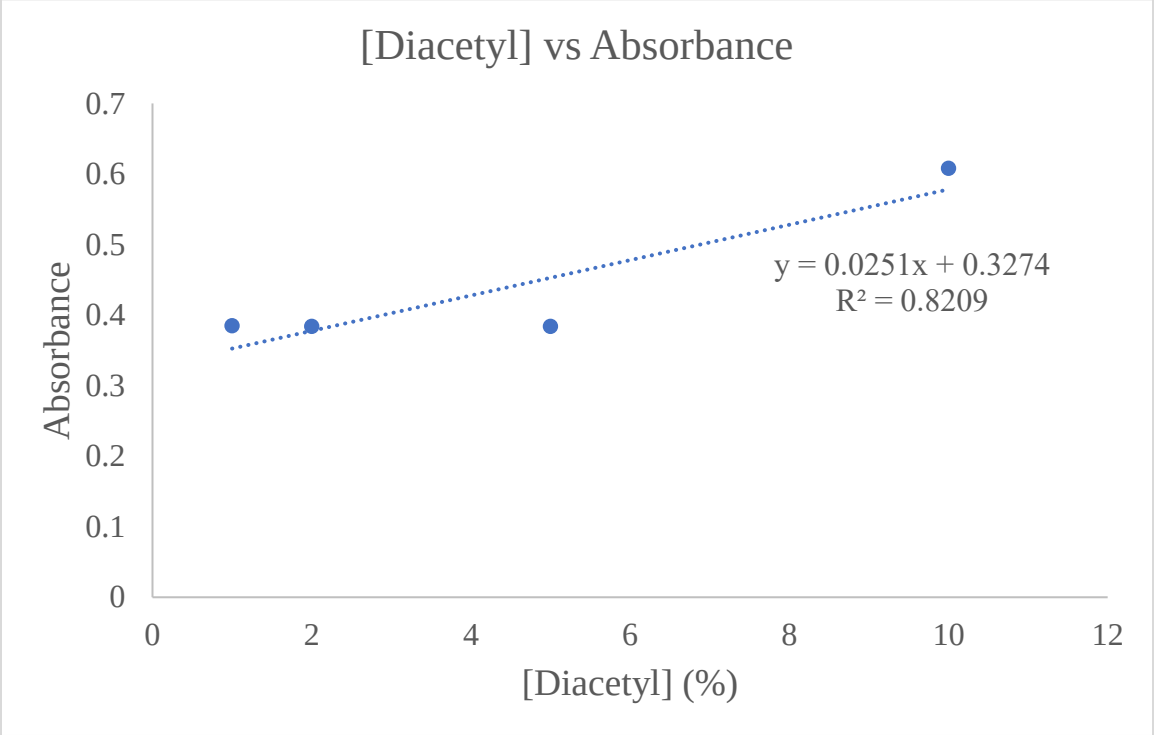

$\tilde{\upsilon}$ = 1045.8 cm^{-1}

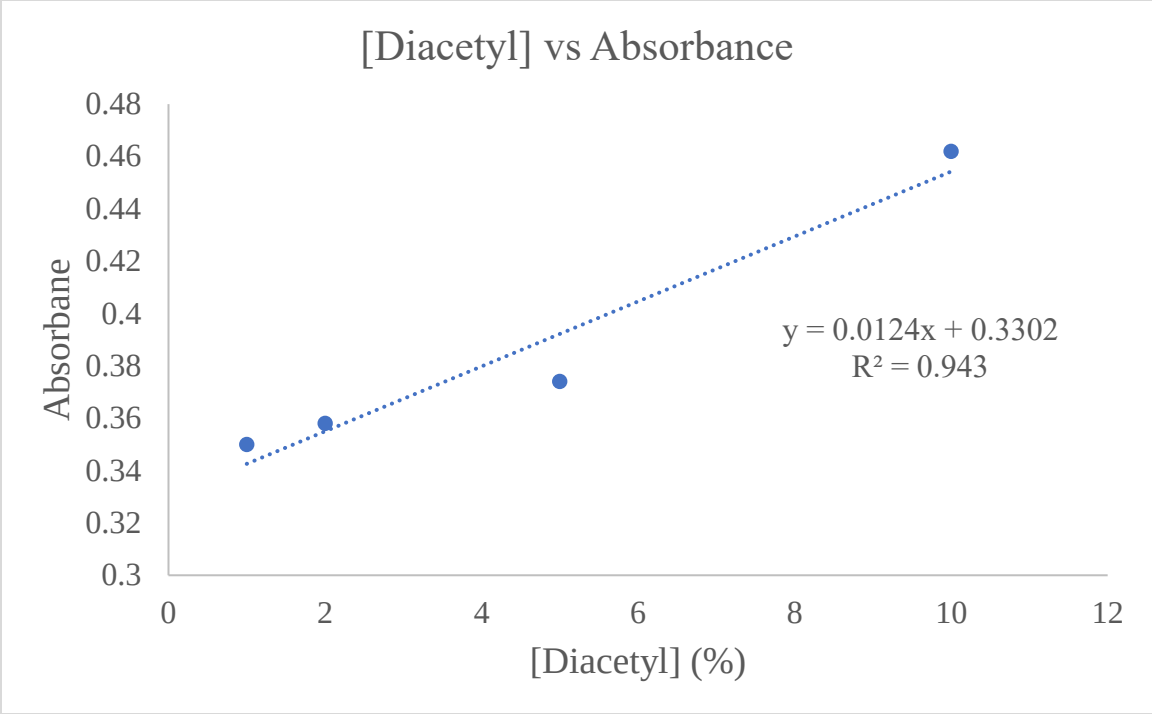

$\tilde{\upsilon}$ = 1359.3 cm^{-1}

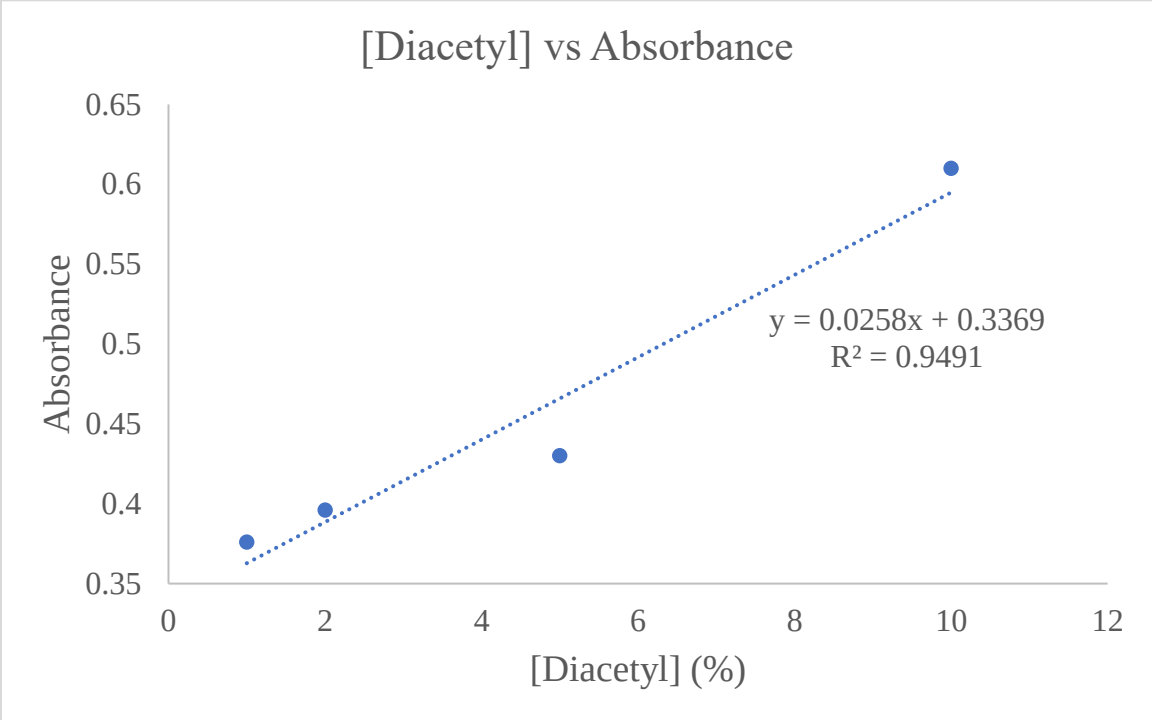

$\tilde{\upsilon}$ = 1122.9 cm^{-1}

Gas Collection Analysis

A bubble analysis was performed to determine if the reaction of ethyl acetoacetate was producing CO_2. Below is a table showing the results from one of the trials at 70 ℃, exhibiting the stair-step effect due to the bubbles sticking to the glass transportation tube.

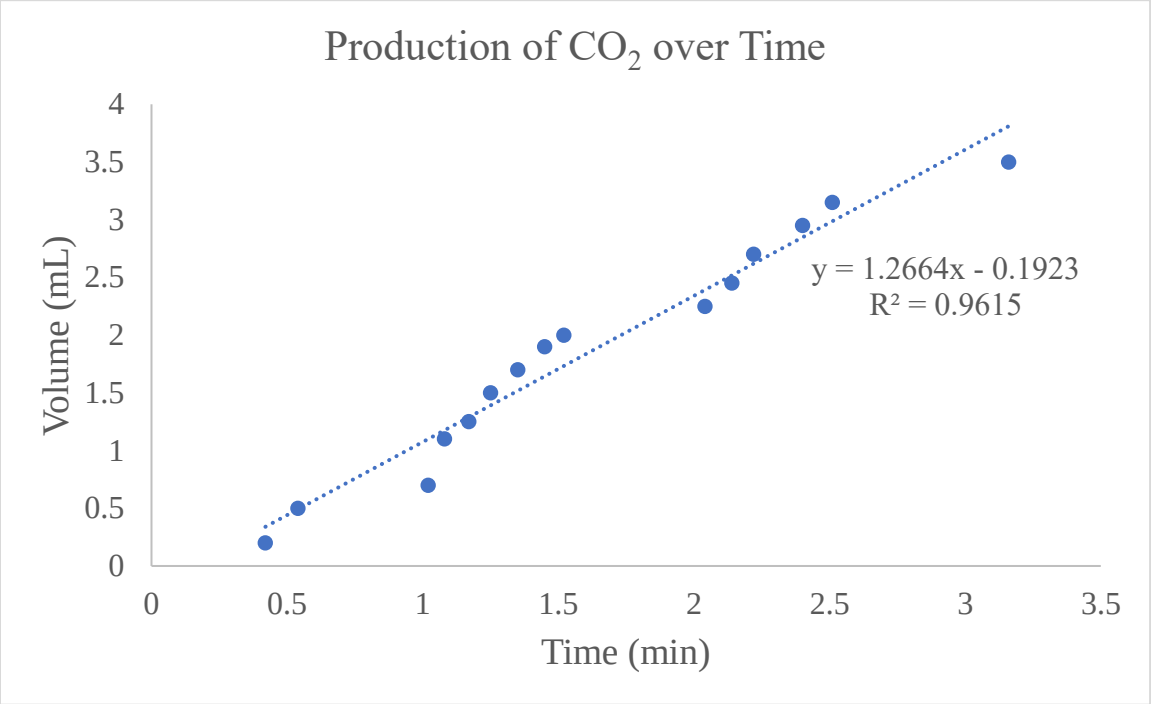

Image of the water trap used in the N_2 purge of the IR system.